66–10,415

COWLEY, Thomas Gladman, 1938–

A SPECTROSCOPIC STUDY OF THE PREMIXED, FUEL–RICH OXYACETYLENE FLAME.

Iowa State University of Science and Technology
Ph.D., 1966
Chemistry, analytical

University Microfilms, Inc., Ann Arbor, Michigan

A SPECTROSCOPIC STUDY OF THE PREMIXED, FUEL-RICH OXYACETYLENE FLAME

by

Thomas Gladman Cowley

A Dissertation Submitted to the
Graduate Faculty in Partial Fulfillment of
The Requirements for the Degree of
DOCTOR OF PHILOSOPHY

Major Subject: Analytical Chemistry

Approved:

Signature was redacted for privacy.

In Charge of Major Work

Signature was redacted for privacy.

Head of Major Department

Signature was redacted for privacy.

Dean of Graduate College

Iowa State University
Of Science and Technology
Ames, Iowa

1966

TABLE OF CONTENTS

I. INTRODUCTION

Analytical flame spectroscopy is rooted well back in the 18th century. However, according to Herrmann and Alkemade (1, p. 6), neither the early workers (e.g. Geoffroy, 1732; Melvill, 1753; Marggraff, 1758) nor their contemporaries realized the scientific import of their various observations. The work of Talbot (2) represents the earliest use of flames as an excitation medium. Studies of the emission of Li, Na, and K from the flame earned Talbot the credit of founding qualitative flame analysis. However, general acceptance of the flame as an excitation source for qualitative studies did not come until 1860 and 1861 when Bunsen and Kirchhoff (3-6) reported the discovery of cesium and rubidium.

Janssen (7) first suggested the use of flames for quantitative analysis in 1870. Three years later Champion, Pellet and Grenier (8) successfully applied Janssen's suggestions to the determination of sodium. Despite this early start the real impetus was given to flame spectroscopy through the comprehensive studies of Lundegardh (9-18) in the period between 1928 and 1938. Since then flame spectroscopy has enjoyed a steady increase in popularity. Gilbert (19) in 1964 noted that the literature of flame spectroscopy ran to nearly 5,000

publications and that this number was increasing at the rate of about one paper per day.

The popularity of flame spectroscopy is not surprising in light of the many advantages the method has over other spectrochemical techniques. The principal advantages result from the stability and reproducibility of the flame as an excitation source. The stable nature permits use of sequential photoelectric readout techniques which greatly reduce the time necessary for a given analysis. Reproducibility of the flame conditions coupled with control over sample introduction give flame spectroscopy precision that is difficult to match by any other spectrographic method (20, p. 3). Compared to electrical discharges the flame is a low energy source and therefore produces relatively simple atomic spectra. This lack of complexity reduces spectral line interference and aids line identification. Further, the flame is the least expensive of the commonly used spectrographic sources.

Despite many advantages, flame spectroscopy has been subject to a number of serious limitations. Prior to 1962 one major problem was that many elements could not be analyzed by flame techniques. In 1959, Gilbert (21) reported that only 39 elements emitted intense line spectra. Consequently, there was some fear that flame spectroscopy would enter a period of

decline and ultimately give way to the rapidly advancing competitive methods (19). However, during the past five years, interest in flames as sources has been renewed. The focal point of this new interest was the realization that chemical environment in the flame plays a major role in the production of free atoms and their subsequent excitation.

Early observation of environmental effects in flames can be traced to Piette (22) who in 1928 described the reducing properties of what he called the "gray zone" of an oxy-acetylene welding torch. In 1947 Alkeseeva and Mandel'shtam (23) proposed the formation of metal oxides and hydroxides as the cause of intensity variations observed in different cones of a premixed, air-acetylene flame for the elements As, Bi, Cd, and Sn. Mavrodineanu's (24, p. 200) suggestion that metals forming monoxides would produce free atoms in a reducing flame was born out by Knutson (25) who reported an enhancement in the emission of magnesium upon increasing the fuel-to-oxygen ratio of an air-acetylene flame. The advent of atomic absorption spectroscopy in the middle 1950's brought with it similar reports of enhancements based on the control of chemical environment in the flame. Thus, Allan (26, 27) found improved sensitivities for Mg, Sn, Cr, and Ru in an

incandescent air-acetylene flame as did David (28) for Mo and Gatehouse and Willis (29) for Sn. The most spectacular demonstration of the potential of environmental control was achieved by Fassel, Curry, and Kniseley (30) when they showed that a fuel-rich oxyacetylene flame produced intense atomic spectra of most of the lanthanide elements. In a later publication, Fassel, Myers, and Kniseley (31) added V, Nb, Ti, Mo, and Re to the list of elements yielding strong line spectra in fuel-rich oxyacetylene flames. More recently Mossotti and Fassel (32, 33) have shown that the lanthanides as well as V, Ti, Nb, Sc, Y, and Re show similarly enhanced atomic absorption spectra.

The observation that both atomic emission and absorption spectra of many elements are strongly enhanced in fuel-rich oxyacetylene flames has led to two important changes in analytical flame spectroscopy. Most obvious is the increase in the number of elements determinable. However, it is the second change that may prove more valuable. The fuel-rich phenomenon attracted attention to the fundamental processes that occur in flames and offered the prospect that further improvement in analytical sensitivities can be achieved through the proper manipulation of the chemical environment of the flame.

From the analytical standpoint the processes of primary importance are those related to the production of free atoms from solvated metal ions. These processes, whatever they may be, take place within the influence of the flame itself. Unfortunately, the flame is an extremely complex chemical system which is not clearly understood. The addition of a solution carrying foreign materials to the flame greatly compounds the problems.

Among the numerous difficulties involved in the study of fuel-rich oxyacetylene flames is the problem of flame structure. The early studies of Fassel et al. (30-33) were done using total consumption burners of the Beckman type. Beckman burners are of the surface mixing type wherein the fuel and oxidant come together coincident with ignition. The flames produced when such burners are operated fuel-rich are highly turbulent and yield a great deal of both spectral and audible noise. The audible noise is merely an inconvenience. However, the spectral noise severely limits the sensitivity of emission studies. In 1963, a premixed oxyacetylene burner was described by Kniseley, D'Silva, and Fassel (34) that possessed a number of unique features. Three of these features make the flame produced by the premixed burner worthy of careful study. First, there is a significant reduction in the background

noise. Second, when compared to the fuel-rich Beckman flame, the premixed flame produces marked enhancements in the detection limits of many elements (35). Third, the premixed burner produces a flame structure more favorable for study than does the Beckman type burner.

Comparison of the two flames (see Figure 1) reveals a number of marked differences, the most striking of which is the development of a third zone, the interconal zone, in the premixed flame. The presence of an interconal zone has been noted before. It is in fact the "gray zone", to which Piette (22) refers. Gaydon (36, p. 12) points out that the formation of three zones is common to many premixed hydrocarbon flames. However, the Kniseley flame, as the premixed oxyacetylene flame has come to be called, appears to be the only three zone oxyacetylene flame to which a sample solution may be added.

The enhancements seen in the Kniseley flame occur predominately in the interconal zone (35). This fact fosters the suspicion that the processes leading to enhancement may be localized within one flame region. A study of this region should then produce information relevant to an explanation of the enhancement processes. Further, the reasons for the formation of the interconal zone are as yet unknown. Information on the composition of the interconal zone coupled with

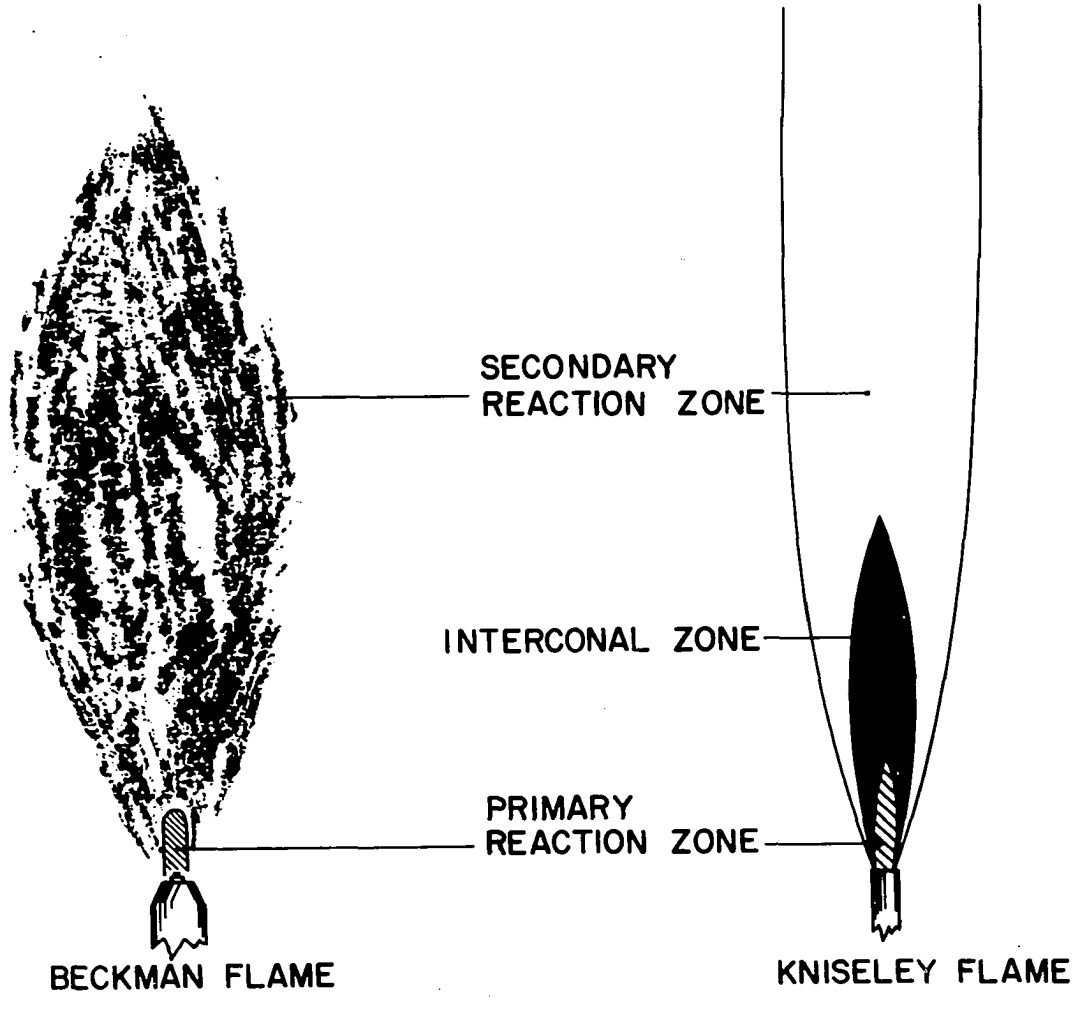

Figure 1. Schematic comparison of the structure of the Beckman and Kniseley flames

similar data on the other two zones should aid in finding an explanation. Therefore, one of the major purposes of this work is to investigate the composition of the three zones of the Kniseley flame with particular emphasis being placed on the interconal zone.

To date, the studies made with the fuel-rich premixed oxyacetylene flame have all been done using the original Kniseley design. It is entirely possible that further improvements can be made simply by changing some physical parameters of the burner. A second purpose of this work, therefore, is to make a study of the physical properties of the Kniseley burner.

This thesis describes work on both the fuel-rich premixed oxyacetylene flame and the burner[a] that produces the flame. The intention is two-fold, to gain information that will provide theoretical background and to exploit the information for the purpose of analytical utility.

---

[a]The term premixed burner will be used throughout this thesis to denote burners in which the fuel and oxidant are intimately mixed prior to ignition.

II. APPARATUS AND PROCEDURES

A. Introduction

One of the desirable features of flame spectroscopy is that often the apparatus required is quite simple. In principle, there are but four essential parts: the flame; some means of wavelength selection; a detector; and a system that will indicate or record the detector output. An investigator building a flame system has considerable latitude in his selection of the individual components. His choice will be largely dictated by the nature of the problem and the availability of the desired equipment. A common system would employ a monochromator for dispersing the flame radiation and a photomultiplier, amplifier, and recorder to detect and measure the intensity of the radiation.

Since this study encompassed several problems, a fairly large number of components were used, some of which found application in only one phase of the work. Each experimental arrangement is described in some detail. In addition, a number of the operations common throughout the work are discussed.

B. Flames and Burners

The term "flame" is applied to a broad class of combustion reactions. Fristrom and Westenberg (37, p. 4) define a flame as "a combustion reaction which can propagate subsonically through space". The emphasis is on spatial propagation since it is this property that distinguishes flames from other combustion reactions. Gaydon and Wolfhard (36, p. 1) list four general properties commonly associated with flames. These are: highly exothermic gas phase reactions; rapid temperature rise; some form of oxidation; and the emission of visible radiation. Such considerations encompass a great number of combustion systems. However, for the purpose of analytical spectroscopy only stationary flames need be considered.

Stationary flames are generally classified as either diffusion or premixed flames. In the former, the fuel and oxidant are kept separate until they enter the combustion region. The combustion reactions then occur at the diffusion interface. Properties of such flames are dependent upon the rate of diffusion as well as the specific nature of the fuel and oxidant. The most familiar example of a diffusion flame is the burning of a match. In the case of premixed flames,

the fuel and oxidant are intimately mixed prior to ignition. Generally, the gases are directed into some form of a tube where the mixing occurs. A flame is sustained at the tip of the tube by balancing the rate of gas flow against the burning velocity. If the flow rate is greatly in excess of the burning velocity, the flame will blow-off the burner. If the opposite occurs, the flame will propagate back down the burner tube and result in what is known as "flashback". The properties of the premixed flame are governed to a large extent by the kinetics of the combustion reactions. The flame produced by the familiar Bunsen burner is an example of a premixed flame.

During the past decade the Beckman integral-aspirator burner (38) has enjoyed great popularity among analytical spectroscopists. Figure 2 shows the principal features of this burner. The construction is entirely of brass except for the palladium capillary. A sample solution may be introduced into the flame because of a reduced pressure at the tip of the palladium capillary. This pressure reduction is one result of the high exit velocities of oxygen. Fuel is provided through the outer jacket.

Beckman burners have a number of desirable features that account for their wide acceptance. Since the gases do not

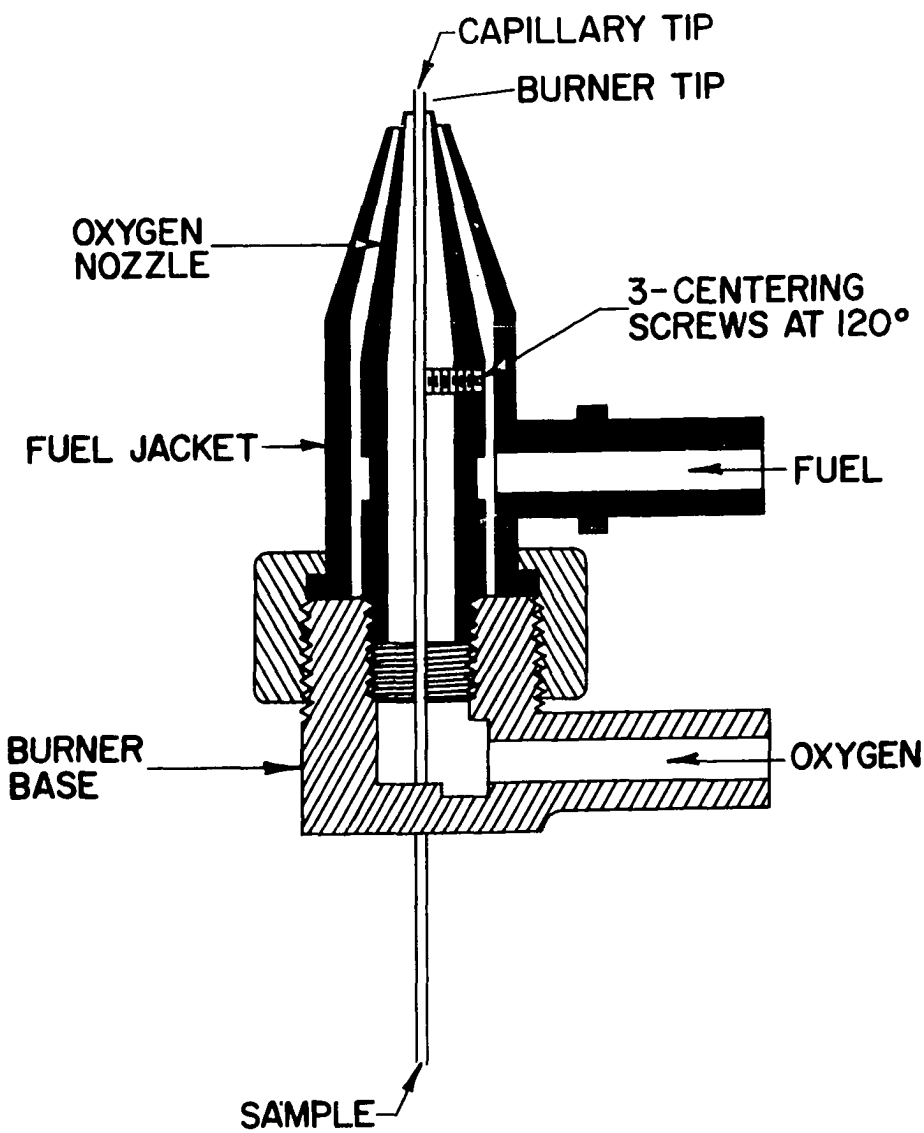

Figure 2. Cross-sectional drawing of the Beckman integral-aspirator burner

come together until they are ignited, gas mixtures that would be difficult to handle otherwise can be burned on them. The burner is small and rugged in construction and produces flames that are easily controlled. Relatively little sample is consumed, from 0.5 to 1.5 milliliters per minute normally, so small volumes of sample may be analyzed. Also, the burner is nearly free of cross contamination effects.

The Beckman burner suffers from three disadvantages that make it unsuitable for fundamental studies. First, the rate of sample introduction is directly controlled by the flow of oxygen. Second, the flame is not classified as either of the diffusion type or premixed type but rather somewhere in between. The gases are ignited at the point of their meeting, as in the diffusion flame, but the high exit velocities cause a significant amount of premixing. The combination of turbulance, due to high gas velocities, and diffusion produce a flame with no well defined zones. As a consequence the flame does not lend itself well to systematic study. The third disadvantage is related to the second. The turbulent nature of the Beckman flame produces a great deal of background noise. Frequently, this noise is the limiting factor in an emission study.

The major disadvantages of the Beckman burner are overcome by the design of Kniseley et al. (34, 35). The principal feature of this burner (Figure 3) is a premixing channel into which the oxygen, acetylene and the nebulized solution from the Beckman burner are directed. This channel performs two functions; the gases are intimately mixed prior to ignition and the flow pattern is made more laminar. The resulting flame is clearly classified as being of the premixed type.

The premixed flame offers several important advantages over the Beckman type. The three, well-defined zones formed when the premixed flame is operated fuel-rich offer a flame structure that is more favorable for study. Further, spectral noise and background are substantially reduced. The background emission from the fuel-rich Kniseley flame and the fuel-rich Beckman flame are compared in Figure 4. For the Kniseley flame only the interconal zone was observed, whereas for the Beckman flame observations were made in the flame region that produced maximum line emission. While both flames exhibited the fuel-rich phenomenon, the reduced background of the Kniseley flame permitted the establishment of lower detection limits for many metals (35).

The major disadvantages of the premixed burner have been previously described (34, 35). Burner performance is

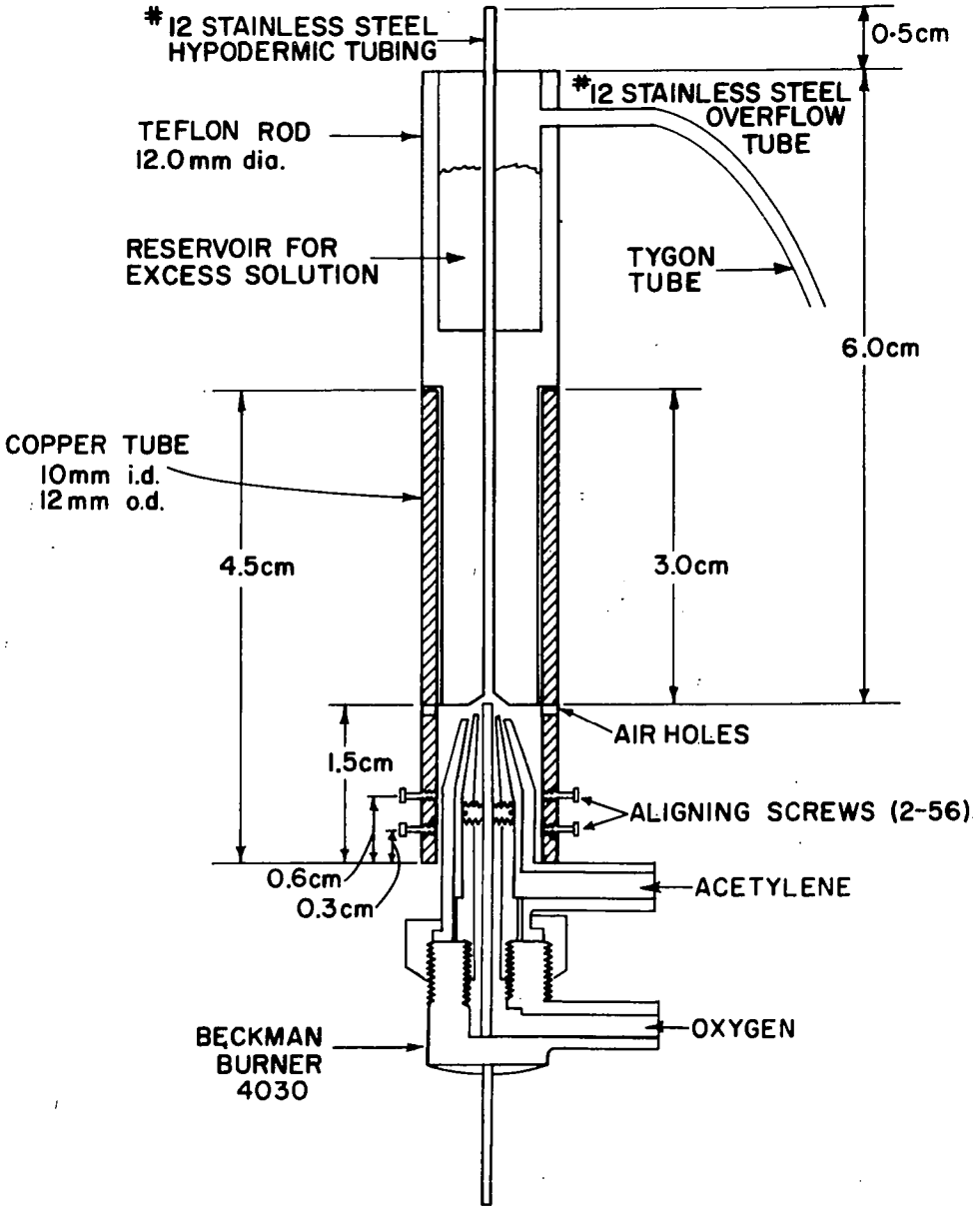

Figure 3. Cross-sectional drawing of the Kniseley burner

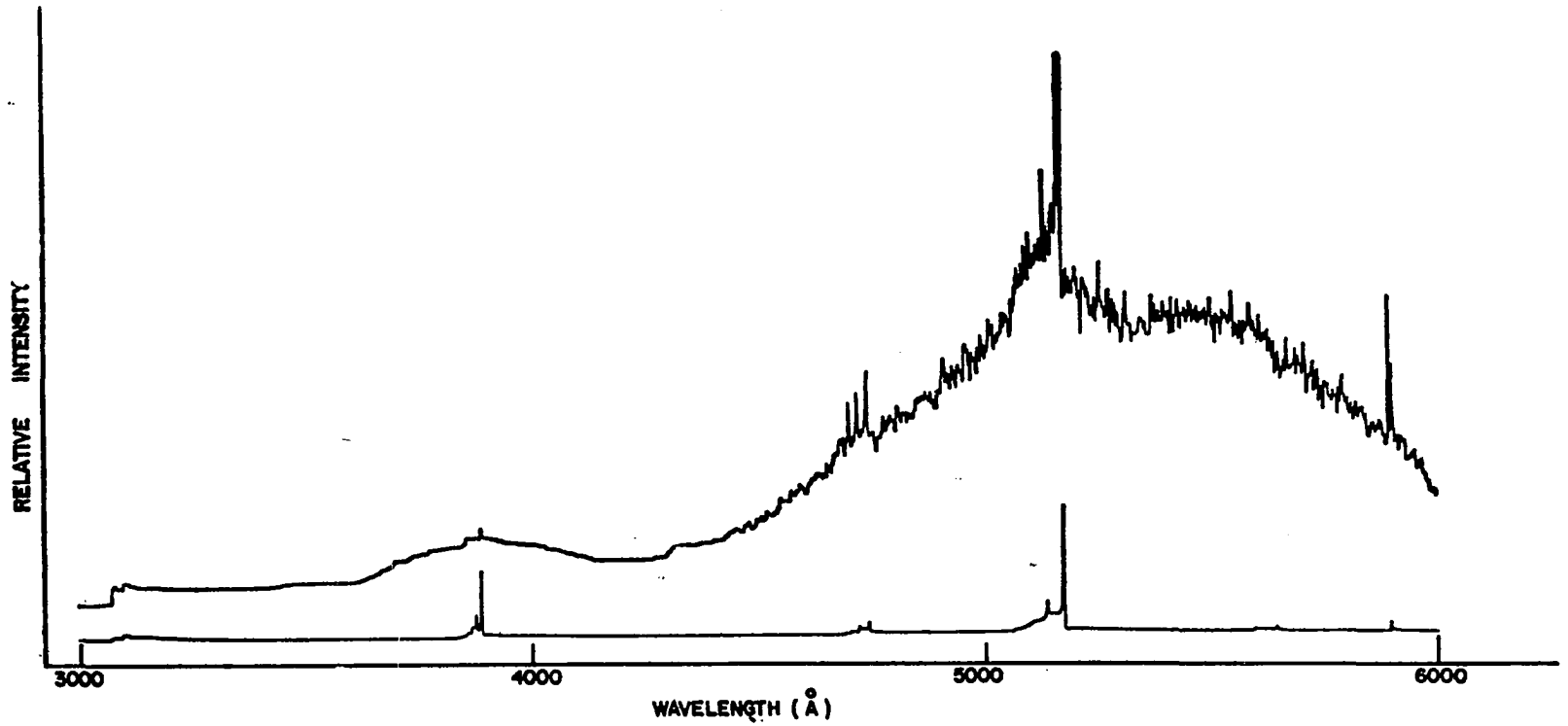

Figure 4. Comparison of background emission from Beckman burner (upper curve) and Kniseley burner (lower curve) when both are operated under fuel-rich conditions

sensitive to the proper alignment and this alignment is difficult to achieve. Unlike the Beckman burner, the premixed burner must be used with an organic solvent. Further, since spillover of the excess solvent provides cooling for the premixing tube, nebulization must be maintained whenever the flame is burning. A Beckman burner provides sample nebulization. Consequently, the oxygen flow rate still controls the rate of sample introduction, unless a positive feed mechanism is used.

A number of materials have been used for the premixing channel. The original design (34) employed a drilled carbon rod. However, the porous nature of graphite gave rise to cross-contamination. The use of a Teflon barrel with a stainless steel insert (35) eliminated the cross-contamination effect but resulted in a much less rugged burner. Golightly (39) replaced the steel tube with a pyrex glass tube and achieved adequate performance. Mossotti (40) designed a Teflon clip-on system that eliminated the alignment process. The major disadvantage of the design was that each clip-on had to be custom built for a specific Beckman burner.

A number of studies in this work required a burner that was free of cross-contamination and offered a degree of ruggedness that was comparable to that of the carbon chimney

type burner. Boron nitride was found to be a material that could provide both of these features. Figure 5 shows the premixed burner with a boron nitride premixing chamber. The chimney design is similar to the original carbon chimney except that the tip is tapered to avoid the accumulation of excess solvent near the flame.

In operation, the boron nitride premixing chamber was shown to possess a number of advantages. The burner can withstand higher tip temperature than can the steel chimney type. The tip is predominantly heated by radiation from the primary reaction zone. The favorable heat capacity and high reflectivity of boron nitride combine to minimize heating from this source. As a consequence, the burner may be operated without solvent nebulization and the flame may be made fuel-lean without adverse effects. The non-porous nature of boron nitride eliminates cross-contamination. Experiments with saturated ethanolic NaCl solutions showed that a 10 second washout period would free the chimney of residual sample. Finally, boron nitride is easily machined and therefore reduces fabrication problems.

There are two disadvantages to the use of boron nitride. It is more costly than other chimney materials. Also, it has

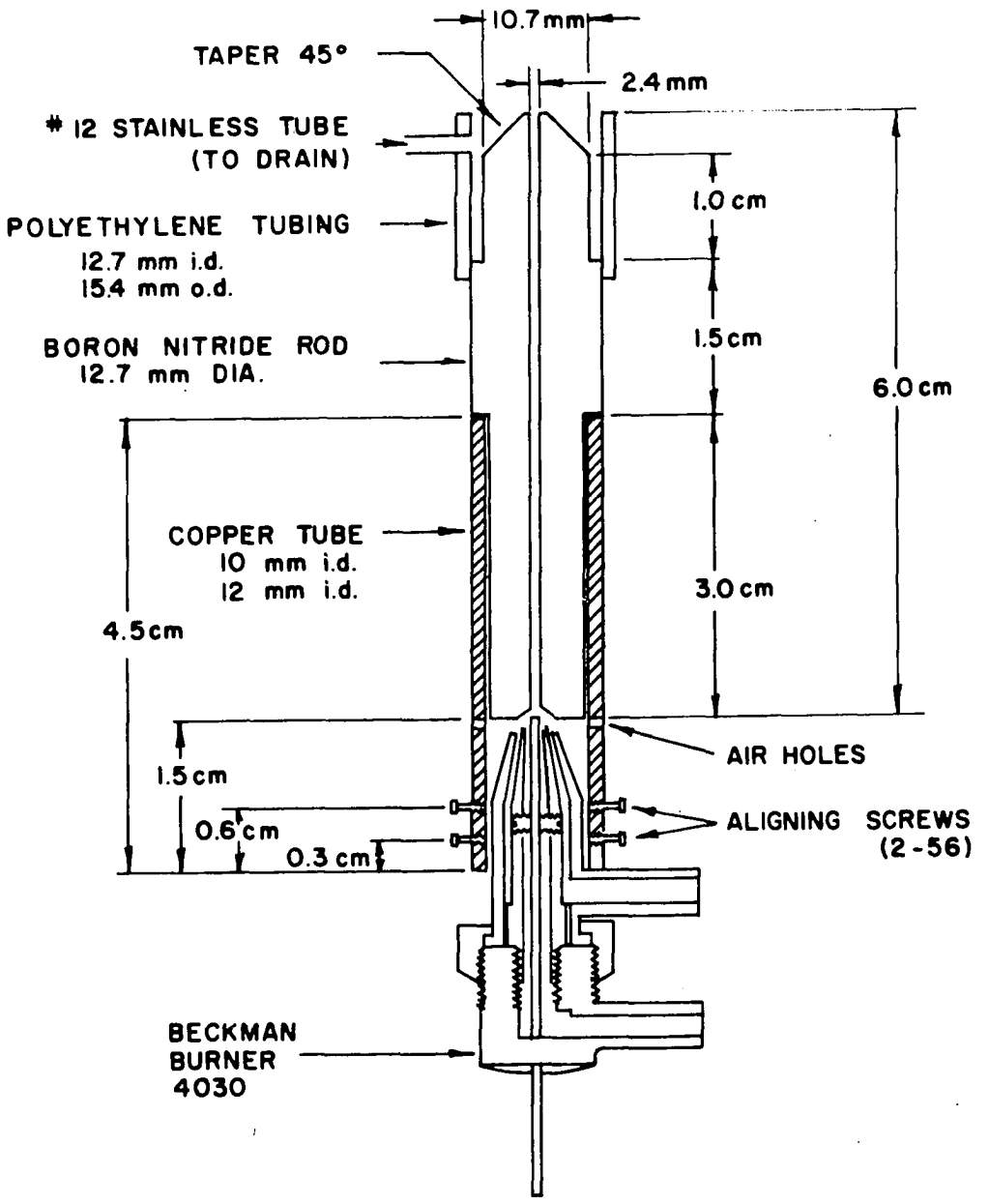

Figure 5. Cross-sectional drawing of Kniseley burner with a boron nitride premixing chamber

been suggested that boron nitride is slightly hygroscopic (41, p. 184). However, boron nitride chimneys have been used for long periods with no apparent difficulty due to hydrolysis.

One characteristic of the Kniseley burner is the presence of air holes at the base of the premixing channel. These holes are essential to the operation of the burner, since without them the burner will invariably flashback. However, a problem is presented in that an uncontrolled volume of air may enter the gas column via the holes. Two burner designs were used in this study that permitted control over the volume of air entering the burner. The first (Figure 6) is a Kniseley burner that has been provided with a sleeve. Gas entering the single port is easily controlled and monitored. The second design (Figure 7) allows control over input simply by controlling the volume of air entering through the holes in the sealing ring. This design also features a tapered premixing channel.

The principle of the tapered premixing channel is discussed by Fiorino (42) who successfully applied the concept to maintain adequate gas velocity near the walls of the premixed oxyacetylene slot burner which was specifically designed for atomic absorption studies. In the burner shown in Figure 7, the tapered portion was fabricated from boron nitride principally because of the relative ease with which

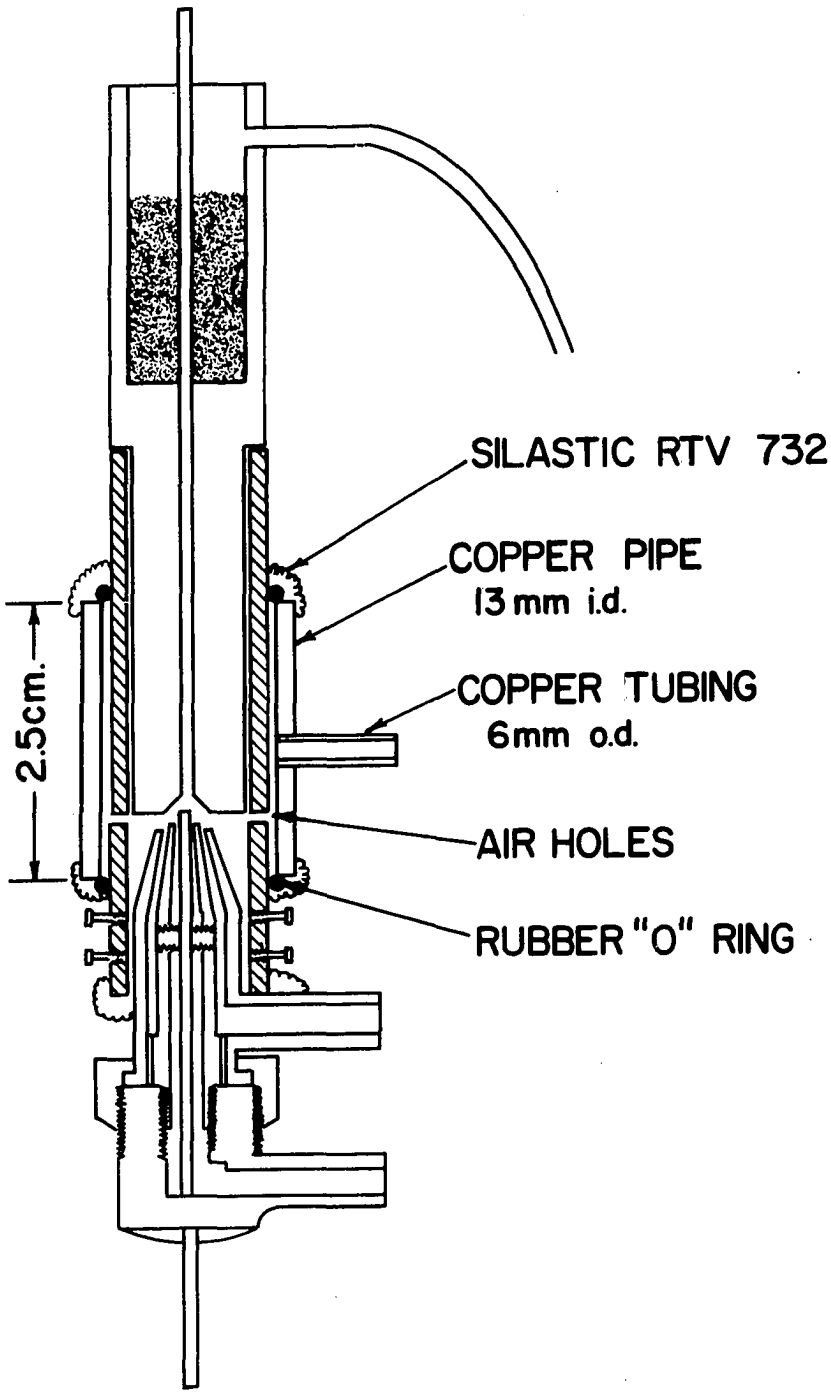

Figure 6. Cross-sectional drawing of a Kniseley burner with gas sleeve

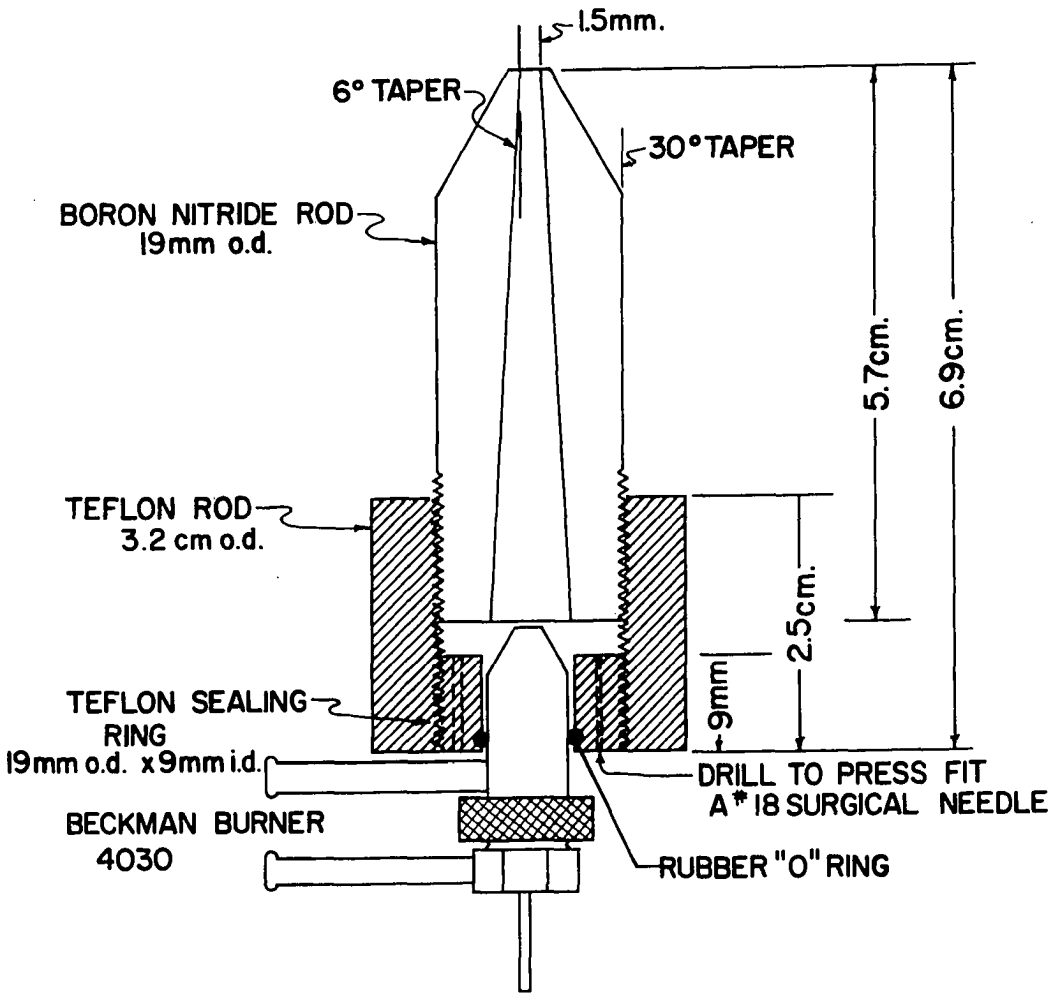

Figure 7. Cross-sectional drawing of the Kniseley burner with a tapered chimney

boron nitride can be machined.

In its present form the tapered chimney Kniseley burner offers only two advantages over the conventional premixed burner. Since, the gases from the Beckman burner are essentially "funnelled" into the premixing chamber, little or no alignment is necessary. Also, oxyacetylene mixtures may be burned without including any atmospheric nitrogen. As a consequence, the effects of nitrogen, as well as other gases, upon the emission from the premixed flame may be studied.

C. Gas Regulation

The production of line spectra in a fuel-rich flame is very sensitive to the exact composition of the flame. Consequently, successful study of fuel-rich flames requires close control over the input of the oxygen and fuel. The system shown in Figure 8 was designed to provide both the control and monitoring capacity required. A constant pressure was preset and maintained through use of a low-flow regulator (Mason-Neilan Model 113) that was modified by the manufacturer to increase its flow capacity. The pressure range over which the regulator functioned was 2-20 psig, however, for the sake of convenience in calibration, an oxygen pressure of 15 psig and

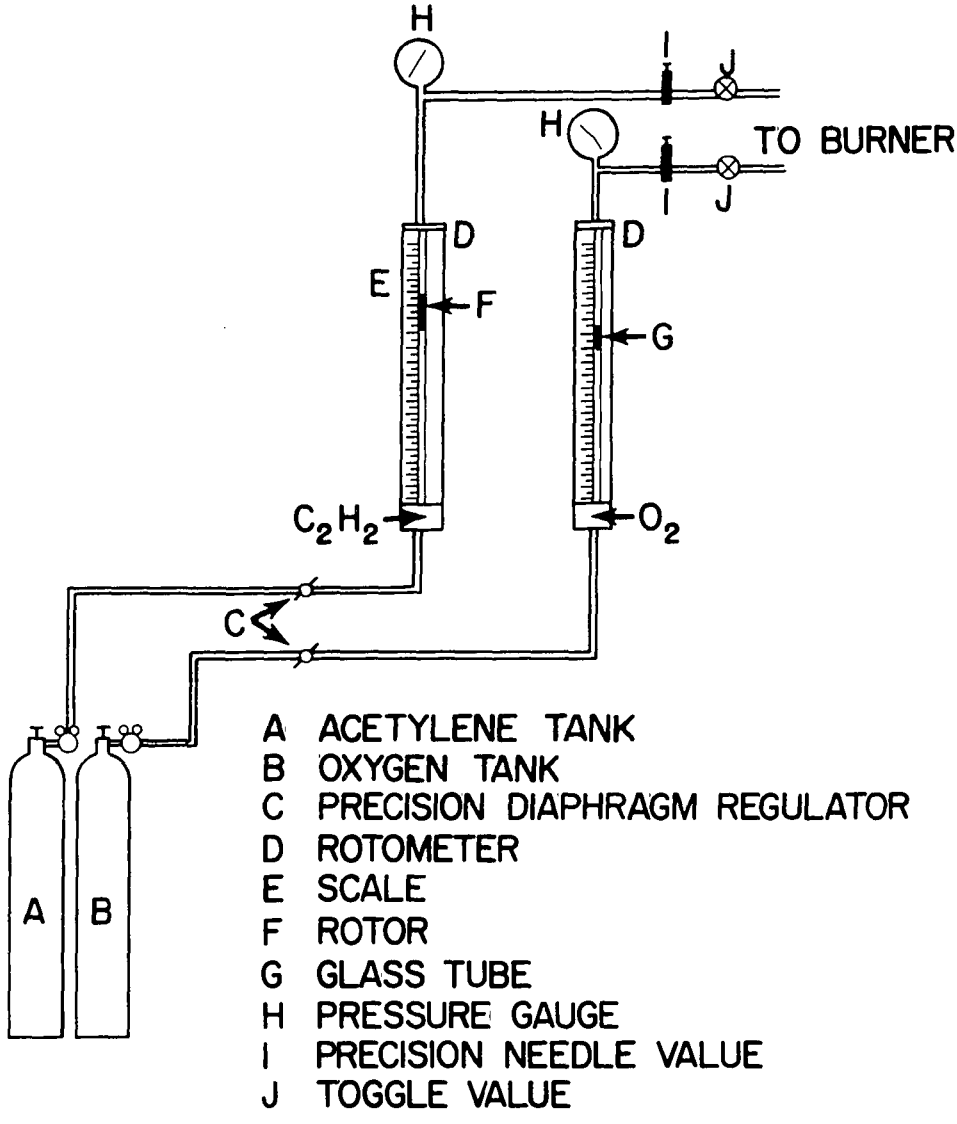

Figure 8. Equipment used to measure and regulate gas flows

an acetylene pressure of 3 psig were used throughout this study. The pressure of each gas was continuously monitored by Marshalltown pressure gauges (Marshalltown Manufacturing Inc., 0-30 psig scale, 3½ inch dial). Flow rates were established with the aid of high precision rotameters (Brooks Instrument Co., model FV 1110), 600 mm in length, capable of better than ¼ percent reproducibility, and providing ±1 percent instantaneous accuracy. Each rotameter was calibrated, at the desired pressure, with a precision wet test meter (Precision Scientific). A variable orifice was placed in each line in the form of a low-taper needle valve (Ideal Arrowsmith #51-4-23). The individual components were mounted in a portable, sixty-inch relay rack and connected with Dekoron "P" tubing (Samual Moore, Mantua, Ohio) having an outside diameter of ¼ inch. Swagelok connectors (Crawford Fitting Co.) were used throughout the gas delivery system with inlet and outlet connections being of the bulkhead type (Swagelok #400-QC-61).

Figure 6 shows only the fuel and oxygen system. However, in some instances a third gas was added through a system similar to the two described above.

D. Monochromators

One of the advantages of flame excitation is that usually the emitted atomic spectra are simple. This implies that a relatively simple dispersing device may be used and to a large extent this is true. However, there is a point of diminishing return. As will be pointed out later many flames produce considerable background in the form of band emission throughout the visible portion of the spectrum. Consequently, the selection of a dispersing device must be made with some caution. In most cases, the minimum requirement will be sufficient resolution to separate the atomic emission from the principle background features.

A Jarrell-Ash Model 82000, 0.5 meter Ebert, scanning monochromator was used in most of the investigations described in this thesis. Characteristics of this instrument are given in Table 1. During the later phases of these studies a 1.0 meter, Czerny-Turner, scanning monochromator (Jarrell-Ash Model #78-462) became available and some of the work was performed with this instrument. Characteristics of the 1.0 meter Czerny-Turner are listed in Table 2.

The 1.0 meter Czerny-Turner possesses several features that make it a more desirable research instrument than the

Table 1. Characteristics of the Jarrell-Ash Model 82000 Ebert scanning spectrometer

Feature	Specifications
Optical arrangement	0.5 meter Ebert grating mount arranged as described by Fastie (43). Effective aperture ratio f/8.6.
Grating	Plane, replica grating, 1180 grooves/mm over a 52 x 52 mm ruled area, on a blank 58 mm square. Blazed for 5000 Å.
Dispersion	Reciprocal linear dispersion at exit slit is 16 Å/mm in first order.
Slits	Fixed-slit housing for a series of slits mounted on interchangeable slides.
Scanning action	Automatic scan speeds of 500, 250, 125, 50, 20, 10, 5, and 2 Å/min. are available with manual override. Wavelength counter accuracy is ± 2 with ± 0.5 Å reproducibility.

Table 2. Characteristics of the Jarrell-Ash Model 78-462 Czerny-Turner scanning spectrometer

Feature	Specifications
Optical arrangement	1.0 meter Czerny-Turner grating mount arranged as described by Czerny and Turner (44). Effective aperture ratio f/8.7.
Mirrors Collimating beam Exit beam	Replica, 1.0 meter focal length 152.4 cm diameter, slabbed 203.2 cm diameter
Grating	Plane, replica grating, 1180 grooves/mm over a 102 x 102 mm ruled area, on a 113 x 105 mm blank.
Dispersion	Reciprocal linear dispersion at exit slit is 8.2 Å/mm in first order.
Slits	Fixed slit housing for a series of slits mounted on interchangeable slides.
Scanning action	Automatic linear scanning drive housing speeds of 2500, 1250, 500, 250, 125, 50, 25, 12.5, 5.0, 2.5, 1.25 and 0.5 Å/min., all with manual override. Wavelength counter accuracy ± 1 Å.

0.5 meter Ebert. The most obvious advantage is an increase of two in the reciprocal linear dispersion without a corresponding decrease in speed. A second advantage is the ability to use either photographic or photoelectric read-out. With the Polaroid attachment, a photographic survey of a 700 Å portion of the spectrum can be obtained within less than one minute. Such a photograph may then be used to select a portion of the spectrum to study in more detail with the photoelectric read-out system. In addition, the Czerny-Turner possesses a number of design improvements that make its operation more convenient than that of the 0.5 meter Ebert.

E. External Optics and Spatial Resolution

The isolation of a desired area in the flame is a problem frequently encountered in flame spectroscopy. A review of the literature reveals numerous solutions (45-53), all of which proved successful in the particular study for which they were designed. Unfortunately, each study and each experimental arrangement presents a slightly different solution to the spatial resolution problem.

For this work it was desirable to provide good spatial resolution coupled with the ability to rapidly change the flame

position. The basic optical system employed a spherical quartz lens (11.0 cm focal length, 3.5 cm diameter) to establish a one-to-one object-to-image ratio between the flame and the slit. The image was diaphragmed at the slit, generally to a height of one-millimeter. Flame positioning was affected through use of an inexpensive microscope stage mount (Lafayette Universal Mechanical Stage, Model F-613, Lafayette Radio Electronics Corp.), to which the burner was attached (Figure 9). Two crossed verniers provided accurate and reproducible flame positioning. In most cases, a 25 micron entrance slit was used, thereby permitting an area of about 0.025 mm^2 to be viewed when the image was diaphragmed to 1 mm.

The selection of a reference point presented a problem. Since flame dimensions vary as a function of the fuel-to-oxidant ratio, the use of the burner tip as a reference point did not permit intercomparison between flames. However, if the tip of the primary reaction zone was used such comparisons were possible. A mark was made on the face of the monochromator near the slit opening. The image of the tip of the primary reaction zone was then moved into coincidence with this mark and the positions of the verniers noted. Since the magnification of the optical system was known, this operation served to

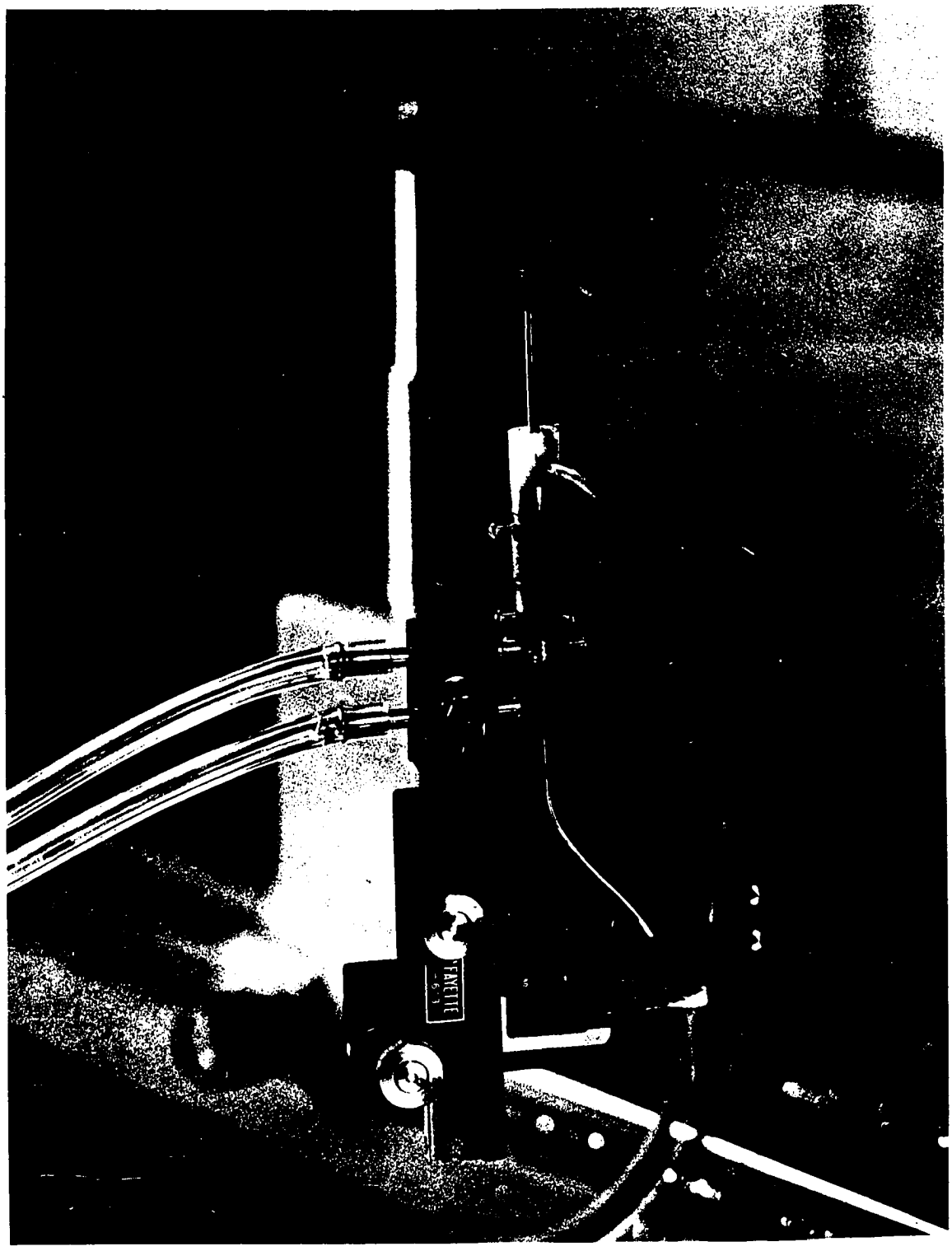

Figure 9. Photograph of mechanism used for flame positioning

calibrate a position scale for a given set of flame conditions. Frequently, throughout the work, reverse optics were employed to insure the integrity of the positioning system.

F. Detectors

In principle, any photosensitive device may be used as a detector in flame photometry providing it has sufficient response in the spectral region of interest and possesses enough sensitivity for a given application. The preferred detector, especially for weak light intensities, is the photomultiplier (20, p. 84). Since research applications are frequently quite broad and since, in general, highly sensitive photomultipliers are expensive, considerable care should go into their selection.

The first consideration must be the wavelength dependency of the response. Each type of photosensitive surface shows a different characteristic response as a function of wavelength. In selecting a photomultiplier, the most desirable response features would be high sensitivity over a very broad wavelength region. While such photomultipliers are available, they usually cannot be used because they possess high dark current and high noise.

For the purposes of this study, the requirements of the photomultiplier were: good photosensitivity in the region 2000 Å to 8000 Å; low dark current; and low noise. To satisfy these requirements, it was necessary to use two photomultipliers. Table 3 lists the typical characteristics of the tubes employed as listed by the manufacturer. Dean (20, p. 86) points out that tube parameters may vary considerably among individual tubes and frequently a "selected" tube will outperform a "typical" one.

G. Electronics

The electronic systems used for this study were of modular construction. This facilitated rapid conversion of systems and allowed a great deal of flexibility in obtaining the proper instrumentation for a specific task. During the course of the work a number of substitutions were made for individual components; however, the overall structure and response of the electronic system remained the same.

The primary requirements of the system were long term stability and low noise. The components described below and assembled as shown in Figure 10 were found to satisfy these requirements.

Table 3. Description of photomultipliers

Feature	EMI 6255B	EMI 9558Q
Cathode diameter (mm)	44	44
Number of dynodes	13	11
Cathode dark current at 23°C (amps)	6×10^{-15}	1.5×10^{-15}
Cathode type	SbCsO on fused quartz window	SbNaKCs on fused quartz window
Spectral response type	S-13	S-20
Wavelength of maximum quantum efficiency (Å)	4000	4000
Approximate useful sensitivity range (Å)	1650-6500	1650-8500
Average photosensitivity (microamps/lumen)	70	140
Average overall sensitivity at 1400 volts (amps/lumen)	2000	200

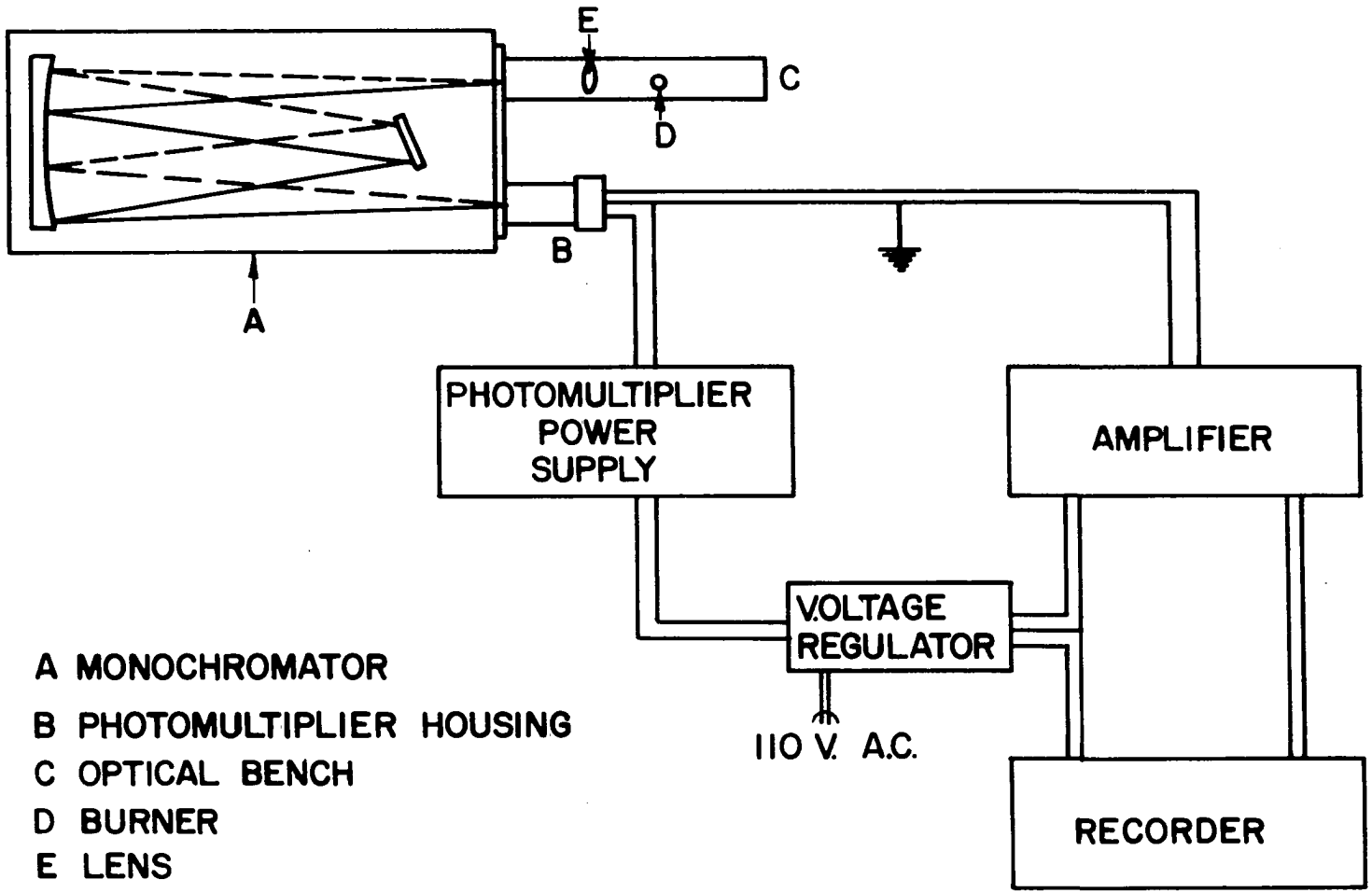

Figure 10. Block diagram of arrangement of components used for emission studies

Dynode voltage was supplied to the photomultiplier by a NJE (New Jersey Electronics Corporation) model S-325-RM power supply. This supply was capable of supplying any voltage from 500 to 2500 volts at currents from 0 to 10 milliamperes.

The photomultiplier output was amplified with a Leeds and Northrup 9836-B micro-microammeter. The 9836-B combined AC amplification with overall DC feedback to achieve an accuracy of $\pm$0.5 percent. The amplifier gain was adjustable over eleven equally spaced ranges from 2×10^{-6} to 10^{-9} amperes. Response times of the 9836-B were normally less than 1.5 seconds, however, the amplifier output was provided with an additional damping control by introducing a variable R-C network in the output line.

The amplifier output was sufficient to drive a Leeds and Northrup Speedomax G, Model S millivolt recorder. Modification of this recorder provided: a continuously adjustable zero from -50 to +50 millivolts; a continuously adjustable range from 1 to 50 millivolts; and a response time of one second. A one inch per minute chart speed was used throughout the study.

Line voltage regulation for all electronic components was accomplished with a Stabiline (Superior Electric Company) automatic voltage regulator (Model 1E5101). This regulator

maintained an output voltage of 115 volts rms $\pm$0.1 percent over an input range of 95-135 volts.

At various points in the study a Keithley (Keithley Instruments) Model 410 micro-microammeter was substituted for the Leeds and Northrup 9836-B and the Speedomax G recorder was replaced with a Bristol (The Bristol Company) Model 590, wide strip, two pen, Dynamaster recorder. Since the essential characteristics of the two "substitutes" were comparable to their original counterparts, the electronic system was effectively unaltered by the substitution.

H. Atomic Absorption System

The measurement of atomic absorption spectra presents a different type of problem than does the measurement of emission spectra. In the latter a small signal must be amplified whereas in the former the difference between two large signals must be determined. Further, when a flame is used to provide free metal vapor, the atomic absorption system must incorporate some means of discriminating between flame emission and flame absorption. Frequently, this discrimination is accomplished with either a single or double beam AC system (54).

Figure 11 shows schematically the system used in this study while Table 4 describes the individual components in

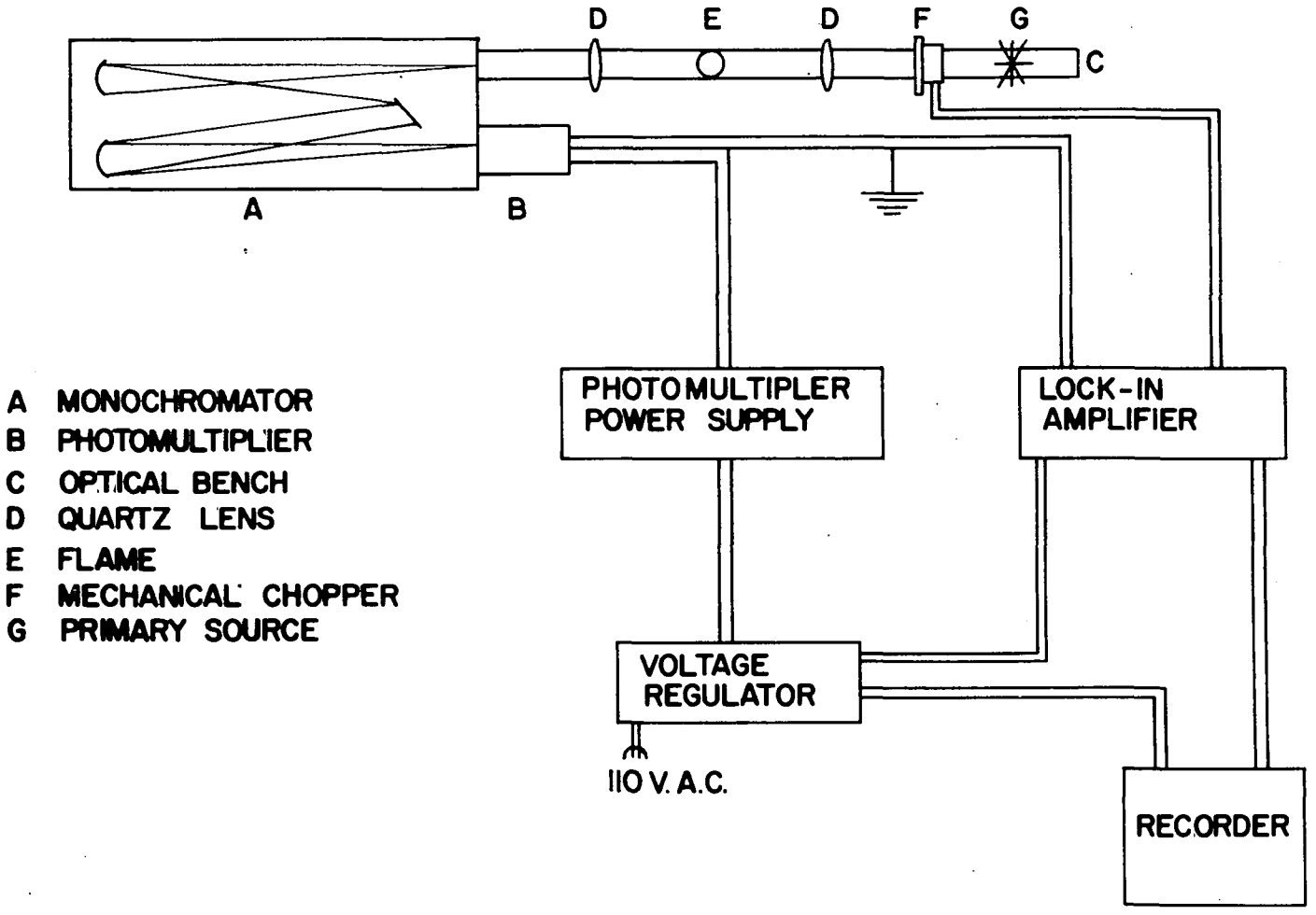

Figure 11. Block diagram of arrangement of components used for absorption studies

Table 4. Description of components of the atomic absorption system

Feature	Specification
Monochromator	1.0 meter Czerny-Turner scanning spectrometer.
Amplifier	Princeton (Princeton Applied Research Corporation) Model HR-8, precision lock-in amplifier (55).
Chopper	Princeton (Princeton Applied Research Corporation) Model BZ-1, mechanical light chopper (56). Internally generated signal used as reference for lock-in amplifier.
Primary sources	Xenon arc lamp, 150 watt, 7.5 amp, Hanovia 901C-1, (2500 Å - 3700 Å). Tungsten filament lamp, 625 watt, 118 volt, Sylvania type DXL (3600 Å - 6000 Å). Hollow cathode tubes.
Lenses	Two, spherical quartz lenses (12.5 cm focal length, 4.5 cm diameter). Arranged to provide a 1-to-1 image of the primary source at the flame and a 1-to-1 image of the flame at the slit.
Other	All other components were the same as those previously described.

more detail. The system was used as shown in making atomic absorption measurements. However, conversion to an emission measuring system was easily effected by moving the chopper to between the flame and the monochromator.

I. Infusion Pump

As previously mentioned, one disadvantage of the Beckman burner is that the sample consumption rate depends upon the oxygen flow rate. However, this situation may be relieved through use of a positive feed mechanism. Positive feed was achieved for some phases of this study with a Harvard (Harvard Apparatus Co., Inc.) Infusion/Withdrawal Pump, Model 600-900. This device provides sample at a uniform rate by driving a hypodermic syringe with a synchronous motor. Any of 72 infusion rates, between 0.00079 and 38.2 cc/min., may be selected through the proper combination of syringe size and motor speeds.

J. Solutions

In general the metals whose spectra were examined in this study were selected because they represent a group of elements

rather than because of an interest in the specific metal itself. As a consequence, few dissolution problems were encountered. Metals that were difficult to place in solution were simply not selected. Since Curry (57) reported that perchlorate - absolute ethanol was the most useful anion-solvent combination, an attempt was made to use such solutions as much as possible. In those few cases where a perchlorate solution was not possible, chloride solutions were used.

The preparation of perchlorate solutions of most metals has been discussed previously (30, 39, 57). Generally an aqueous solution that contained perchloric acid was boiled to near dryness and the resulting slurry redissolved in absolute ethanol. Since perchloric acid and ethanol have the potential of forming an explosive compound when heated together (58), care was taken to insure that the slurry was cooled to room temperature prior to dissolution.

K. Optimization of Emission

The most convenient index of the composition of a fuel-rich flame is a value known as the fuel-ratio (moles O_2/moles fuel). Since in the Kniseley burner the gases are expanded to atmospheric pressure before burning, the volume ratios may be

assumed equal to the molar ratios. Thus, a fuel-ratio of 1.5 is calculated for the stoichiometric combustion of acetylene in oxygen if the following reaction is assumed.

$$C_2H_2 + 1.5O_2 \rightarrow 2CO + H_2O$$

This reaction must be considered only approximate since numerous products other than CO and H_2O are produced (36, pp. 283-301). However, since the reaction is the best single statement of the overall stoichiometry, the value 1.5 was selected as a reference point. Fuel-ratios in excess of 1.5 denote a lean flame while fuel-ratios below this value indicate a flame burning fuel-rich.

In most cases, the fuel-ratio is determined by measuring the input volumes of oxygen and acetylene. As a consequence, a specific value does not account for either the oxygen added to the flame due to air entrainment or the oxygen consumed by the burning of the organic solvent. Therefore, comparison of fuel-ratios must be undertaken with a great deal of caution. Methods for gaining more meaningful fuel-ratio data will be discussed in a later section.

The production of metallic line emission is dependent upon the fuel-ratio. Figure 12 shows this dependency for

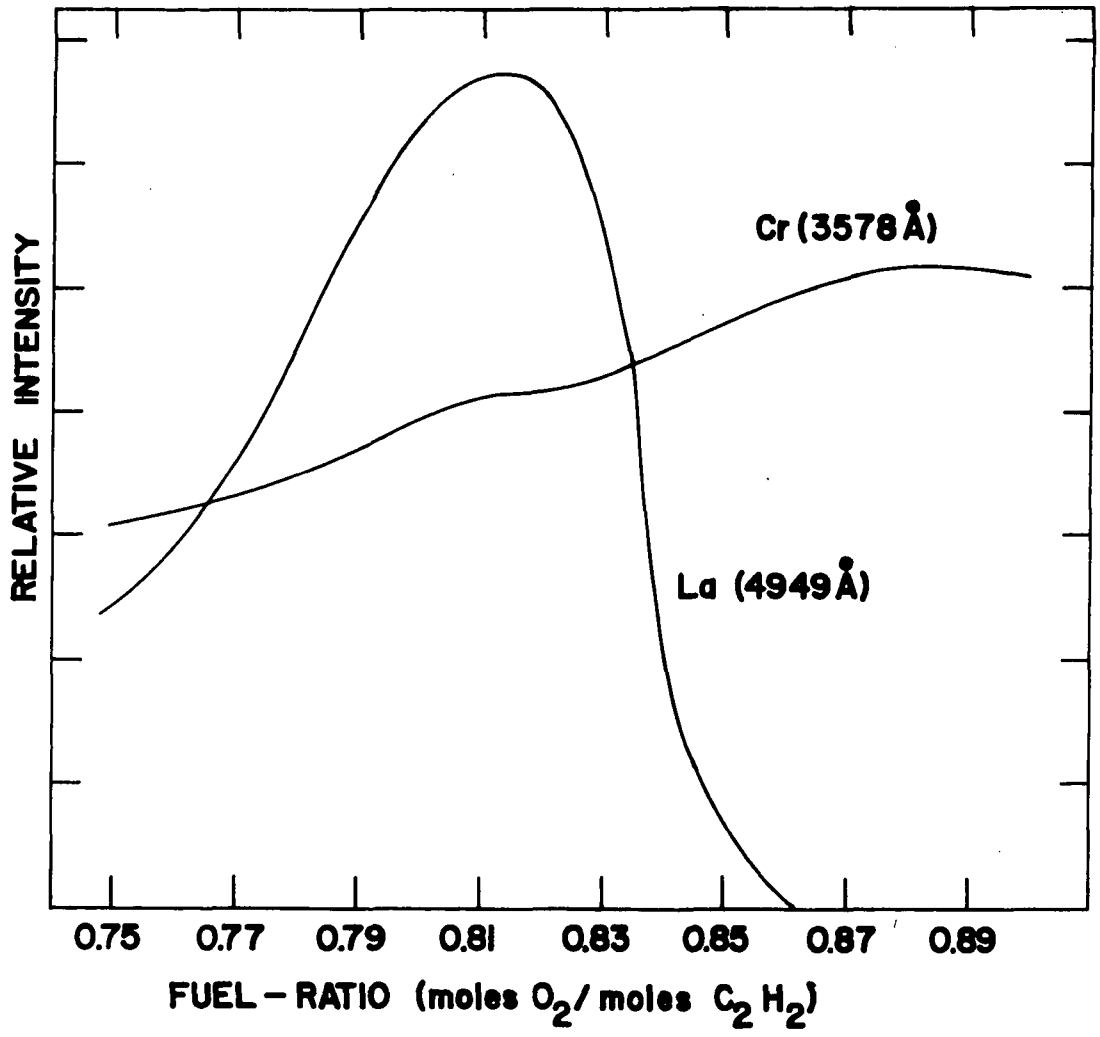

Figure 12. Effect of fuel-ratio on the emission intensity of Cr and La

chromium and lanthanum. As can be seen from the figure, not all metals show their maximum emission at the same fuel-ratio value. Consequently, it is necessary to prepare a plot similar to Figure 12 for each metal before any serious study begins. Fortunately, it is not very time consuming to gain such information. A convenient line of the metal spectrum is selected and repeatedly scanned as the fuel-ratio is changed. It is important that only the acetylene flow rate be changed in varying the fuel-ratio since changes in the oxygen flow rate also change the rate of sample consumption. This effect may be minimized, but not eliminated, through use of a positive feed mechanism.

III. A STUDY OF FLAME PROFILES

A. Introduction

The atomic line emission from a flame is influenced by many factors related to chemical environment and temperature (20, p. 26). Since both the temperature and environment vary as a function of horizontal and vertical position, corresponding changes in the intensity of atomic line emission would be expected. The recent literature contains numerous papers (48, 49, 59-63) describing the variations in metallic emission as a function of height in the flame. The most comprehensive of these are two papers by Buell (48, 49) which list the spatial location of maximum emission when 41 elements in naptha solution were nebulized into the oxy-hydrogen flame. Gibson, Grossman, and Cooke (61) employed both emission and absorption profiles of sodium and calcium to study the effect of organic solvents on the emission from an oxyacetylene flame. Rann and Hambly (64) employed atomic absorption to study the distribution of atoms throughout the flame. In this study, as in that of Gibson et al. (61) profiles were made both vertically and horizontally.

Changes are also observed in the background radiation as various portions of the flame are observed. This background consists primarily of molecular emission superimposed on continuum radiation. Background greatly influences the ultimate limit of detection since it affects the observed signal-to-noise ratio. In the case where the line of interest lies within a molecular band system, the background variation due to band components degrades the signal-to-noise ratio thus leading to poor detection limits. A stable continuous background does not greatly influence detection limits when photoelectric readout systems are used unless the background level becomes so high that the noise level of the photoemissive detector is affected. Unfortunately, in hydrocarbon flames, operated under fuel-rich conditions, normal changes in flame conditions cause substantial changes in both the level of the continua and the intensity of the molecular emission. These changes influence the signal-to-noise ratio.

Thus, studies of spatial variation, i.e., emission profiles, for both lines and background are of importance to the analytical spectroscopist. Emission profiles, coupled with a knowledge of the wavelength dependency of the background, aid in the selection of those parameters that afford

the optimum signal-to-noise ratio for a given element. Failure to obtain the optimum ratio can result in serious losses in the analytical utility of a flame method. Gibson, Grossman, and Cooke (61) have attributed many of the discrepancies found in the literature to inadequate height profile information and the subsequent failure to achieve this optimum condition.

Of equal importance is the fact that intercomparison of the profiles of various species permit the study of relationships between the flame environment and the enhancement of atomic emission. Further, such information may aid in explaining the mechanisms involved in the combustion process itself.

While the emission profiles of many metals have received attention, little has been done toward the corresponding studies of variation in the emission of molecular species. Buell (49) reports the points of maximum emission for 27 molecules. However, only six of these can be considered as part of the flame background. Molecular absorption studies, which would yield vital information on ground state concentrations, appear to be nearly non-existent. According to the literature (36, p. 154), the major flame species do not show significant absorption under normal pressures. However, Fiorino (42) has

recently observed the absorption of C_2 in a long path oxyacetylene flame. Hopefully, his observations will lead to more extensive studies using absorption techniques.

The work of Marr (65, 66) appears to be the most comprehensive single study of the flame from an oxyacetylene welding torch. In many respects his work is analogous to that of this study. However, since the welding torch does not provide for the addition of a sample solution, Marr's investigations were necessarily limited to the so-called "natural flame species".

To date there have been no reported studies of the variation of either atomic or molecular emission in the Kniseley flame. However, the appearance of three distinct zones already indicates that considerable variation does exist. The work described in this section elucidates the nature of the changes in emission and an attempt is made to explain why they occur.

B. Experimental

The spectral region 3000 Å to 6000 Å was selected for study for three reasons. First, the ability to perceive zones in the flame indicates that variation in the background

emission occurs at least in part within the visible portion of the spectra. Second, most metals produce atomic emission in this interval. Third, the region was easily accessible to existing instrumentation.

The work was divided into two distinct phases. The first was of the nature of a survey of the overall emission characteristics of the flame. Since this phase involved a number of scans of the entire 3000 Å - 6000 Å wavelength interval, the term complete wavelength scan is used to distinguish the survey work from the more detailed second phase. In the second phase, individual lines and band heads were selected and their variation in emission as a function of both vertical and horizontal positions were studied. The term "profiles" refers to this second phase of the study. Summaries of the experimental conditions for the long scans and the profiles are presented in Table 5 and 6 respectively.

The spectra of Cr, Gd, and La were recorded for the complete wavelength scans. For each of these elements six scans were made, three with a fuel-rich flame and three with a leaner flame. The fuel-ratio used for the fuel-rich flame was that ratio that produced optimum line emission for lanthanum. The same ratio was used for all three elements. Gadolinium

Table 5. Experimental conditions for complete wavelength scans

Component	Description
Monochromator	0.5 meter Ebert
Burner	Kniseley burner with stainless steel premixing channel.
Slits	0.025 mm for both entrance and exit slits; entrance slit diaphragmed to 10 mm.
Detector	EMI 6255B photomultiplier. Applied voltage 1250 volts.
Amplifier	Keithley, Model 410, micro-microammeter.
Amplifier gain	Variable, adjusted to provide near full scale deflection for the most intense component.
Recorder	Bristol, Model 590, two pen, Dynamaster recorder.
Solutions	La; 1000 μg/ml in ethanol Gd; 1000 μg/ml in ethanol Cr; 500 μg/ml in ethanol
Wavelength scan rate	125 Å per minute

Table 6. Experimental conditions for profiling the flame species

Component	Description
Monochromator	0.5 meter Ebert
Burner	Kniseley burner with stainless steel premixing channel.
Slits	0.025 mm for both entrance and exit slits. Entrance slit diaphragmed to 1 mm.
Detector	EMI 6255B photomultiplier except EMI 9558Q used for ScO.
Amplifier	Leeds and Northrup 9836-B micro-microammeter.
Amplifier gain	Variable, adjusted to provide the most convenient scale for each specie profiled.
Recorder	Leeds and Northrup Speedomax G, Model S millivolt recorder.
Solutions	La; 1000 μg/ml in ethanol V ; 1000 μg/ml in ethanol Sc; 1000 μg/ml in ethanol Cr; 500 μg/ml in ethanol
Wavelength scan rate for vertical profiles	10 Å per minute.
Flame scan rate for horizontal profiles	6.9 mm per minute.

produces its maximum emission at the same fuel-ratio as does lanthanum. However, as can be seen in Figure 12, chromium yields maximum line intensity in a significantly leaner flame. The reasons for this will be discussed later as will be the effect of using non-optimum conditions for the long scans of chromium. For each element, three scans were made of the fuel-rich flame, one in each of the three flame zones.

The fuel-ratio for the leaner flame was selected in a somewhat arbitrary way. Starting with a fuel-rich flame, the oxygen flow was increased until the interconal zone just disappeared. Such a flame is considerably leaner than a fuel-rich flame. However, the fuel-ratio lies well on the rich side of the 1.5 value used to describe a stoichiometric mixture. As discussed previously, the value 1.5 does not account for either the alcohol consumed by the flame or the oxygen included via air diffusion. The Kniseley burner, employing a stainless steel premixing tube, cannot be operated for more than a few seconds under stoichiometric conditions. The tip of the tube rapidly overheats and flashback occurs. As with the fuel-rich flame, three scans were made for each element. Since only two flame zones were present, the three scans were made in the same flame positions as were used for the fuel-rich flame.

The lines and band heads selected for the more detailed profile work are listed in Table 7. The metal lines and bands were selected on the basis of minimal background in all three flame zones. This selection criterion yielded lines that were not necessarily the most sensitive lines available. However, since relatively concentrated solutions were employed, sensitivity was not a problem.

As was the case for the complete wavelength scans, the fuel-ratio employed was that ratio that produced maximum lanthanum line emission. The same ratio produced the optimum emission for scandium and vanadium but not for chromium. The natural flame species were profiled with alcohol being nebulized and with the same fuel-ratio as was used for the metallic species.

Vertical profiling was done as follows. The line or band head was selected and the wavelength drive of the monochromator brought to a position that was within a few Angstrom units of the desired wavelength. A vertical position was then set on the vernier scale. The line or band head was scanned six times at a drive of 10 Å per minute. A new vertical position was selected and the scanning process repeated.

Horizontal profiling was accomplished with the aid of a 1 rpm synchronous motor. This motor was connected to the

Table 7. Wavelengths and excitation energies of the lines and band heads used for profile studies.

Species	Line or band head (Å)	Excitation energy (eV)	Reference
La	5791.34	2.651	67
	5177.31	2.827	67
V	4408.20	3.087	67
	4379.24	3.131	67
	3182.98	3.932	67
Cr	3593.49	3.449	67
	3578.69	3.463	67
ScO	6036.2	2.052	68, p. 397
LaO	4418.2	2.805	68, p. 400
C_2	5165.2	2.478	69
C_3	4050	3.06	68, p. 350
CH	3871.3	3.013	69
CN	3883.4	3.198	68, p. 348
	3871.4	3.209	69
OH	3063.6	4.022	69

horizontal vernier drive knob with an 18-inch section of flexible cable. Such an arrangement permitted the flame to be driven horizontally at a uniform rate of 6.9 millimeters per minute. Since the flame was continuously moved, the emission profile could not be obtained by scanning the line or band head. Consequently, the following approach was adopted. With the flame positioned such that the region of maximum emission was being sampled, the monochromator was manually driven to the point where the selected line or band head showed maximum emission. A vertical position was selected and the flame image moved across the slit by driving the flame with the synchronous motor. At least two horizontal scans were made for every vertical position selected.

The vertical and horizontal profiles employed different techniques because of the difference in spatial resolution requirements. Spatial resolution depends upon two factors. The size of the flame element being sampled and the ability to locate exactly where in the flame the element is being selected. In the vertical direction the element size is 1 millimeter and since the vernier on the flame racking mechanism is accurate to 0.1 millimeter, the relative error in position is 10% of the element size. However, in the horizontal direction a 0.1 mm variation represents a 300% error

with respect to the 0.025 mm element. In order to reduce this error a highly sophisticated racking mechanism would be needed. This need was eliminated by adopting the continuous scanning technique.

Since the fuel-rich oxyacetylene flame produces considerable background radiation, the background intensity had to be subtracted from the line or band intensity if meaningful profiles were to be obtained. This was particularly true in the lower portions of the flame. The background was most easily handled in the cases where a metal line or metal monoxide band head was being studied. Here it was only necessary to replace the metal solution with pure alcohol and re-scan. In the case of the natural flame species however, this procedure was not possible. To obtain the background for these species, the monochromator was manually adjusted until a minimum emission signal was obtained with the wavelength setting no more than ± 3 Å from the band head under study. The horizontal scanning procedure was then repeated.

The technique employed to obtain the atomic absorption profiles were similar to those used for the emission profiles. When a continuum was used as the primary source, as for scandium, the line was scanned at each vertical position and

the decrease in the continuum emission at the particular wavelength measured. The use of hollow cathode lamps, for vanadium and chromium, did not lend itself to scanning techniques. Therefore, the monochromator was manually adjusted until a particular line from the hollow cathode showed maximum emission. Atomic absorption measurements were made at each vertical position by comparing the intensity of this emission with and without the sample in the flame.

No molecular absorption profiles were made. However, C_2 absorption was measured in selected portions of the flame. A continuum was used as the primary source and the C_2 band head was scanned at a rate of 1.25 Å/min.

C. Results and Discussion

Figures 13, 14, and 15 are the results of the complete wavelength scans for the fuel-rich Kniseley flame. In addition to the various metallic species these figures show the principal spectral features in each of the three flame zones. The corresponding set of scans made for a leaner flame are not shown. The effect of reducing the acetylene flow to the point where the interconal zone disappears, essentially eliminates the emission characteristics of the interconal zone.

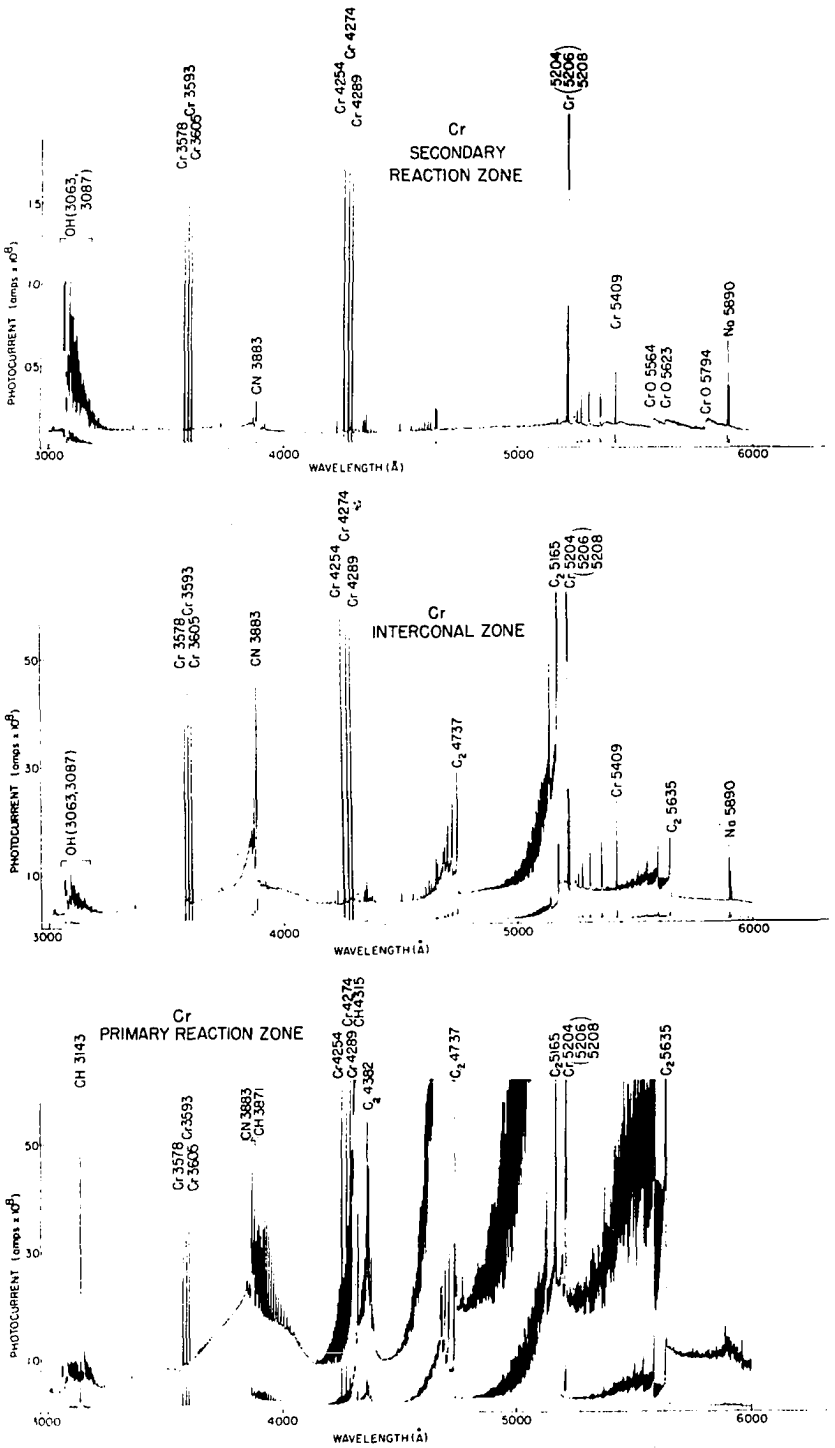

Figure 13. Emission spectra observed in three zones of a Kniseley flame containing an ethanolic Cr solution

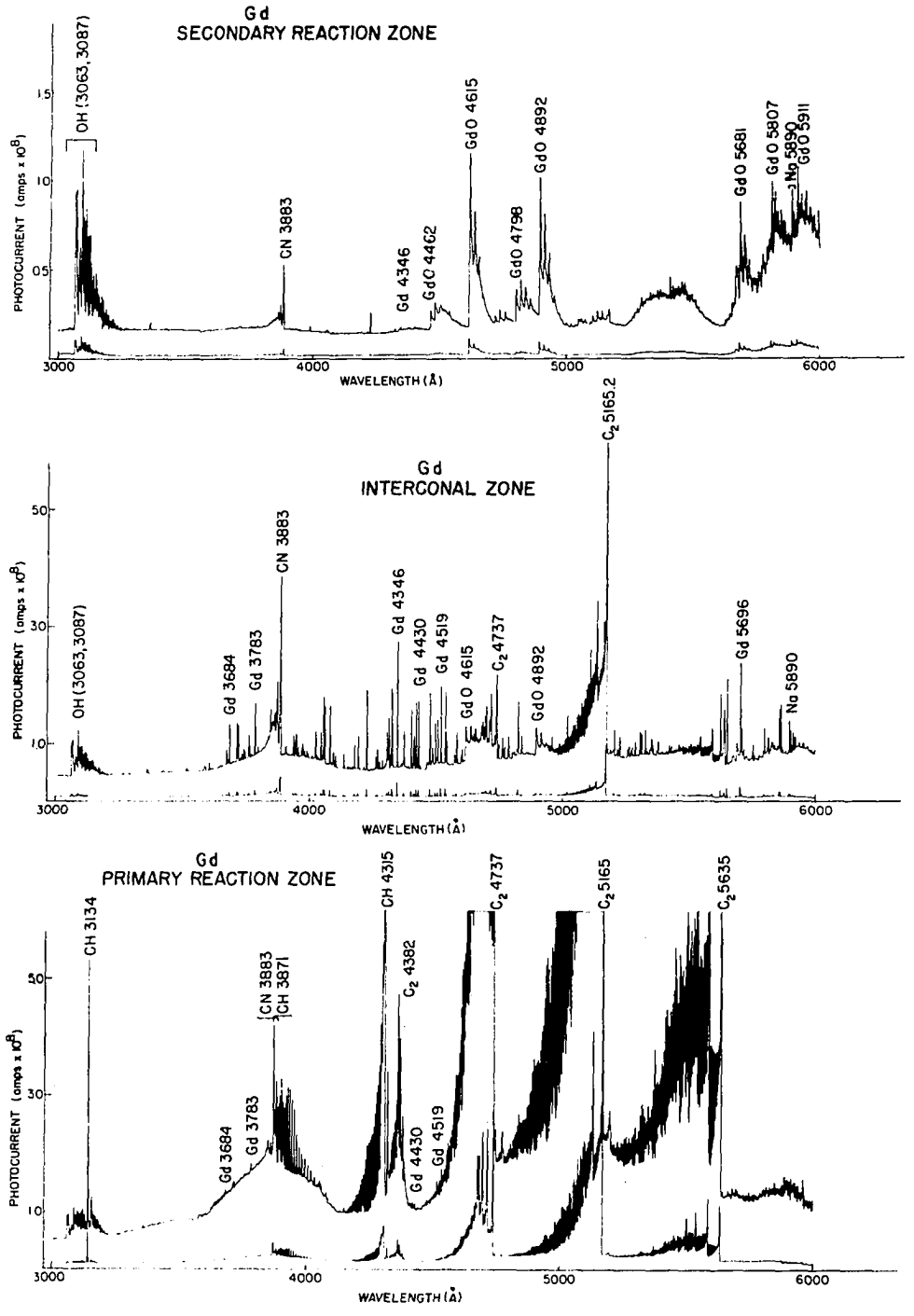

Figure 14. Emission spectra observed in three zones of a Kniseley flame containing an ethanolic Gd solution

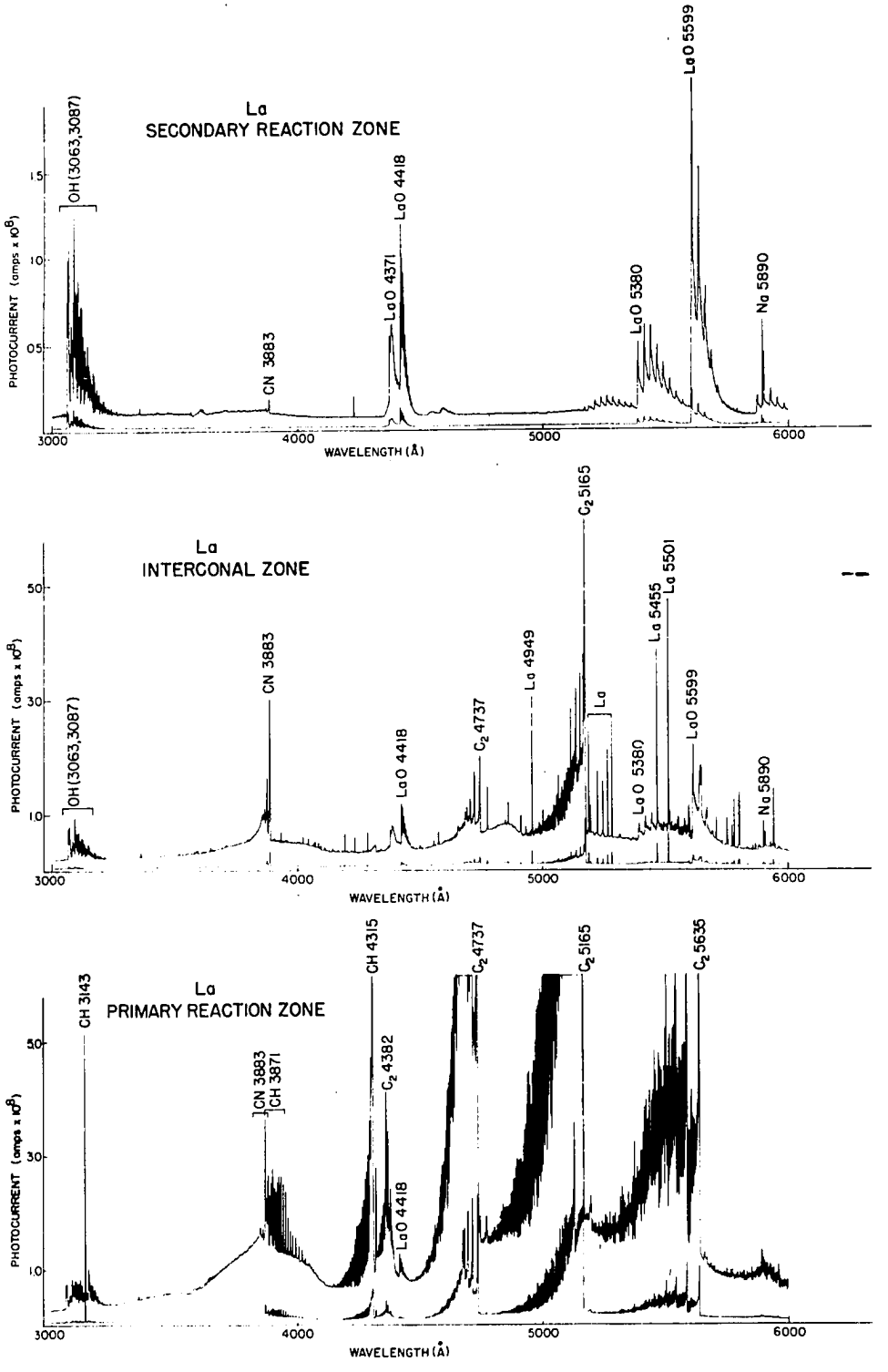

Figure 15. Emission spectra observed in a Kniseley flame containing an ethanolic La solution

Thus, in the leaner flame all three elements yield emission from the interconal region which appears to be the same as that of the secondary reaction zone.

Figures 16 and 17 show the vertical profiles of the natural flame species and the metallic species respectively. The intensity scales for these figures, as well as those for all of the other vertical profiles, has been adjusted so that the figures may conveniently be compared. Thus, while the intensity scale for a given curve is consistent no attempt should be made to compare the differences in intensity between curves. Each of the curves begins at the lowest point in the flame where an emission signal is discernible above the background. Since in all cases this signal is very small the curves essentially begin at zero on the intensity scale.

The horizontal profiles of the natural flame species and the metallic species are shown in Figures 18 and 19 respectively. As with the vertical profiles, the intensity scale is consistent for a given species but varies from one species to another. The scale at the bottom of Figures 18 and 19 is intended to give some idea of the physical breadth of the flame at various points along the vertical axis. It must be emphasized that this scale varies considerably from one burner

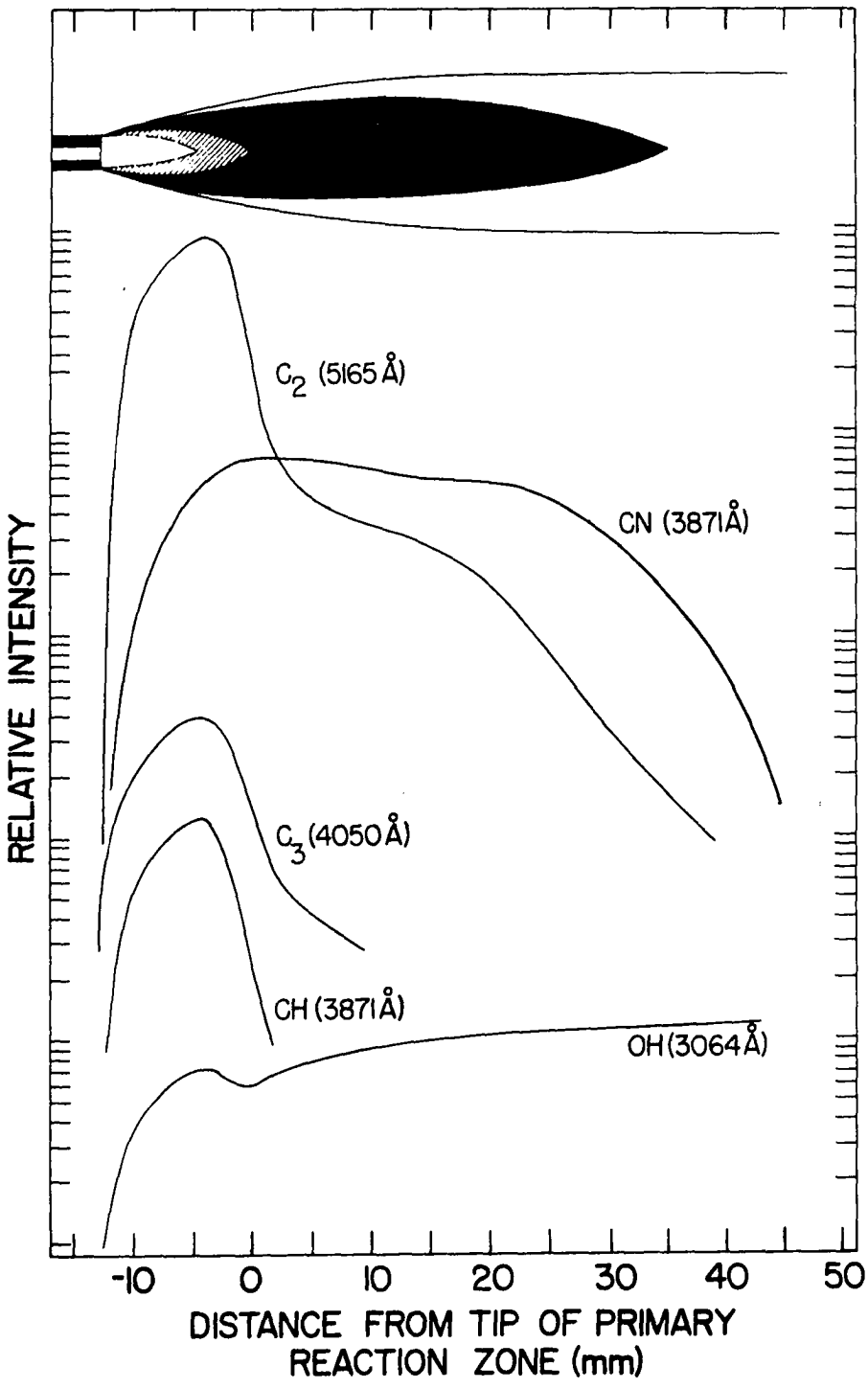

Figure 16. Vertical emission profiles of the natural flame species

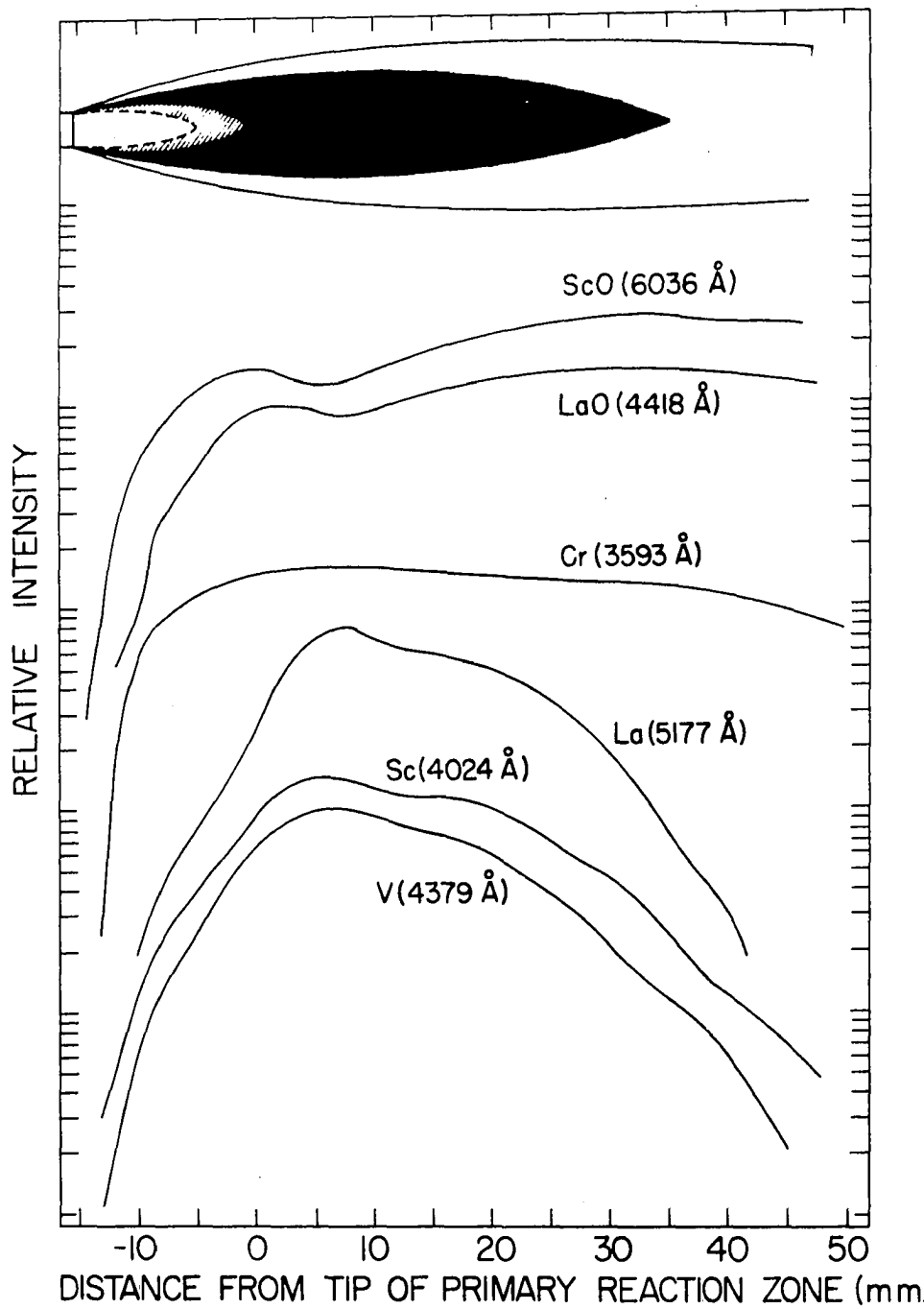

Figure 17. Vertical emission profiles of six metallic species .

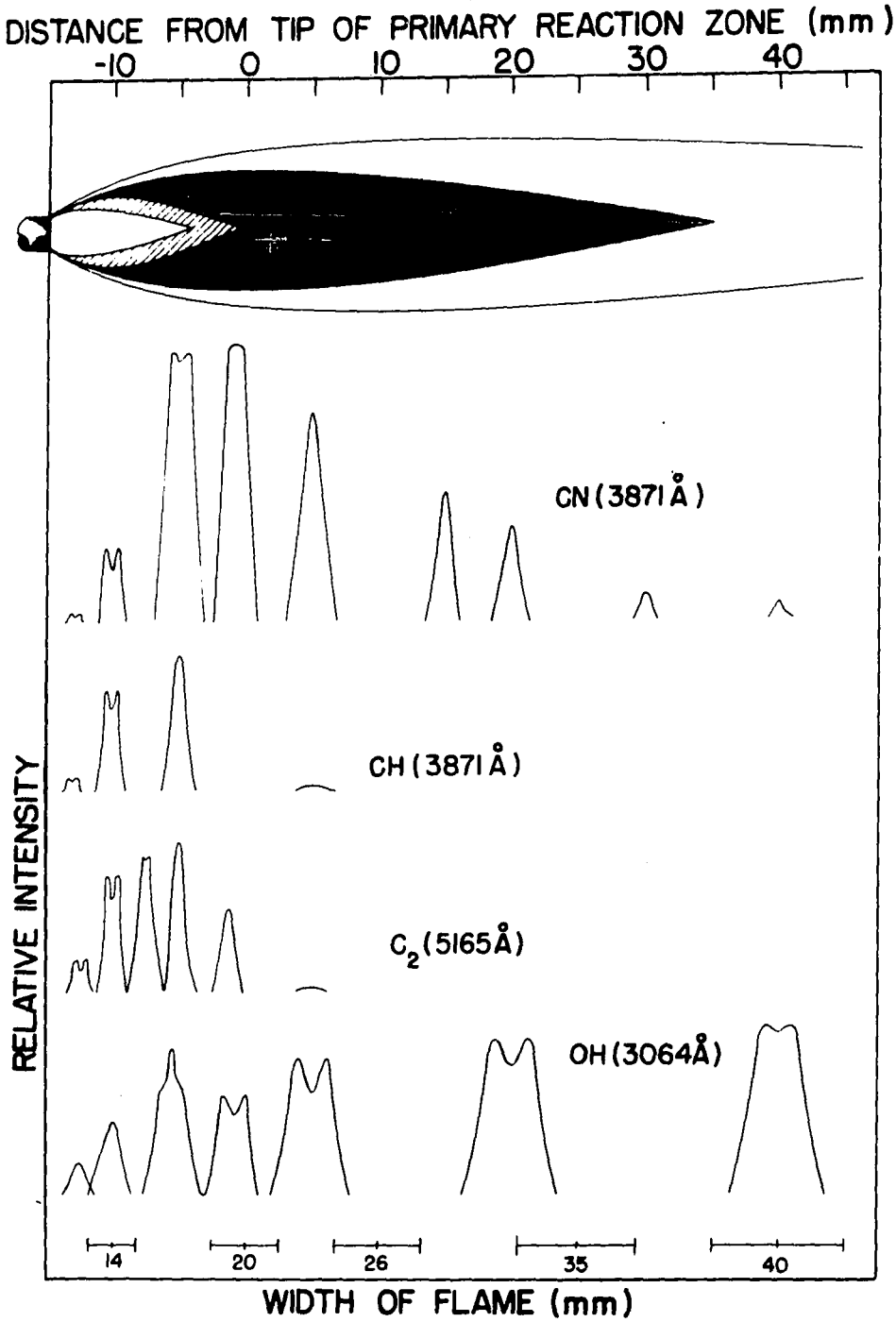

Figure 18. Horizontal emission profile of the natural flame species

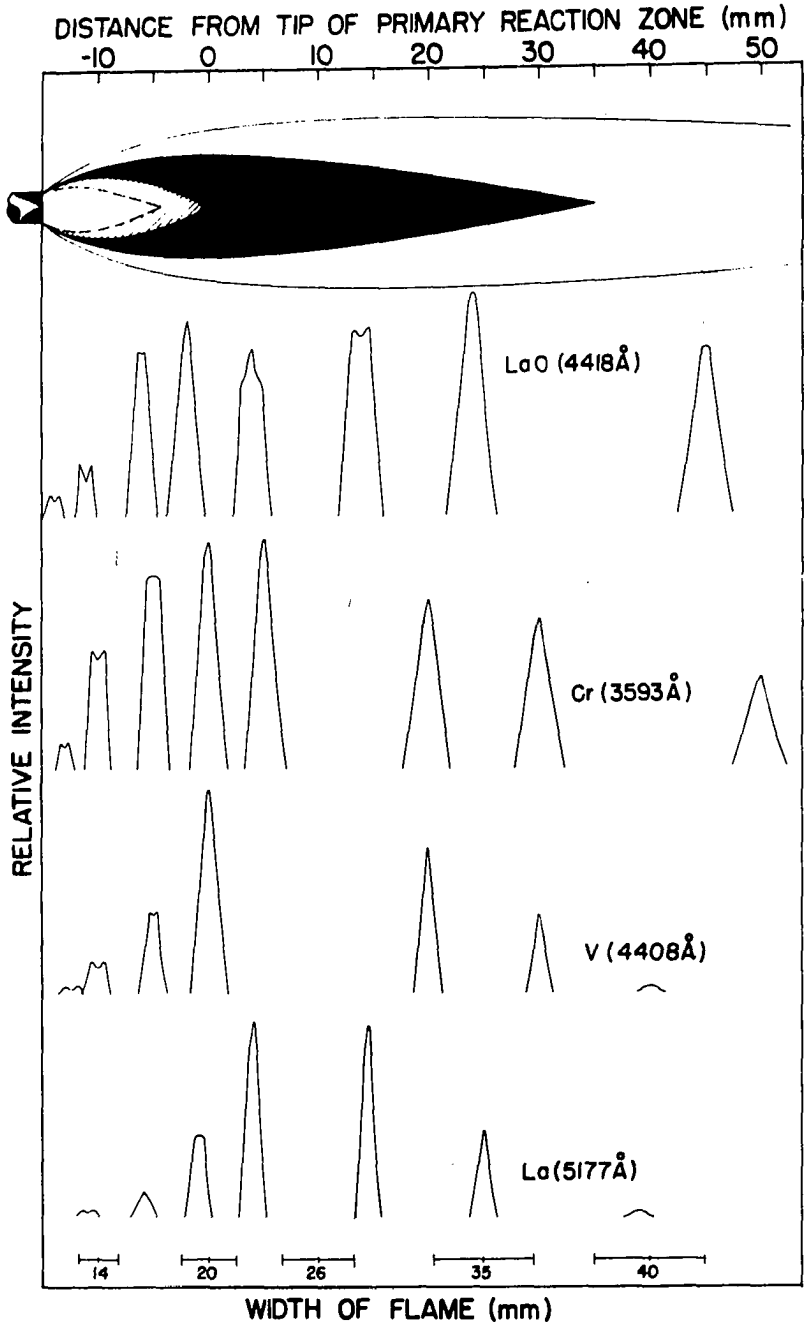

Figure 19. Horizontal emission profiles of four metallic species

to another as does the vertical extent of each of the three flame zones.

The atomic absorption profiles along the vertical flame axis for scandium, vanadium, and chromium are presented in Figure 20. Like the vertical profiles in emission, the three curves have been displaced to provide a more convenient display.

There are numerous problems associated with the interpretation of the profiles of the Kniseley flame. The first is caused by the geometry of the flame. Horizontal cross sections taken at various heights in the flame (see Figure 21) reveal the enveloping effect of the upper two flame zones. It should be noted that Figure 21 is merely an illustration and not a scale drawing. The degree to which one zone is enveloped by another varies as a function of the height in the flame. Thus, it is not possible to view emission from the primary reaction zone without having the radiation first pass through both the interconal zone and the secondary reaction zone. The secondary reaction zone provides similar envelopment for radiation from the interconal zone. Radiation originating from an outer zone cannot therefore be distinguished from the radiation of the enveloped zone on the basis of the vertical profile data alone.

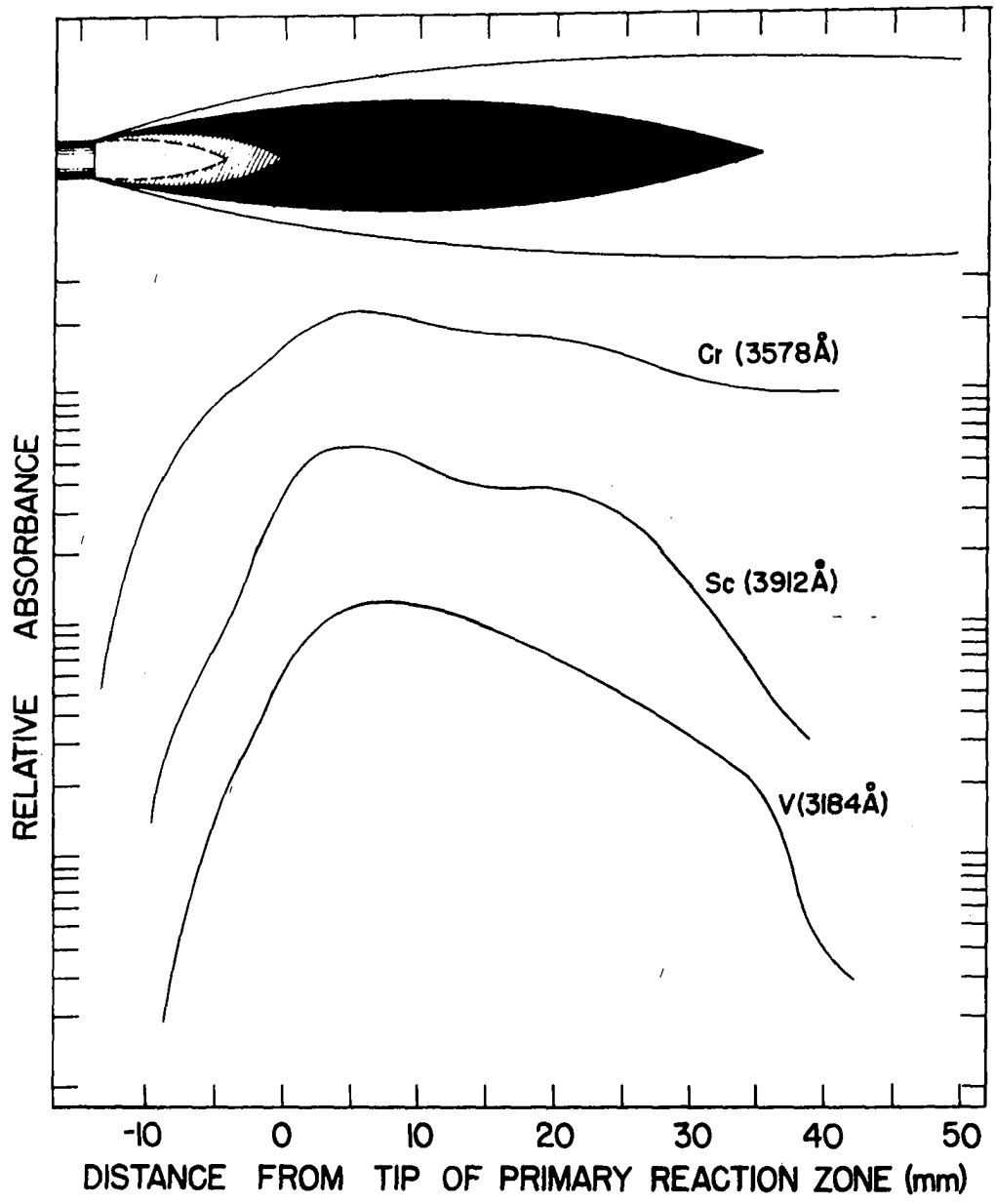

Figure 20. Vertical atomic absorption profiles for three metallic species

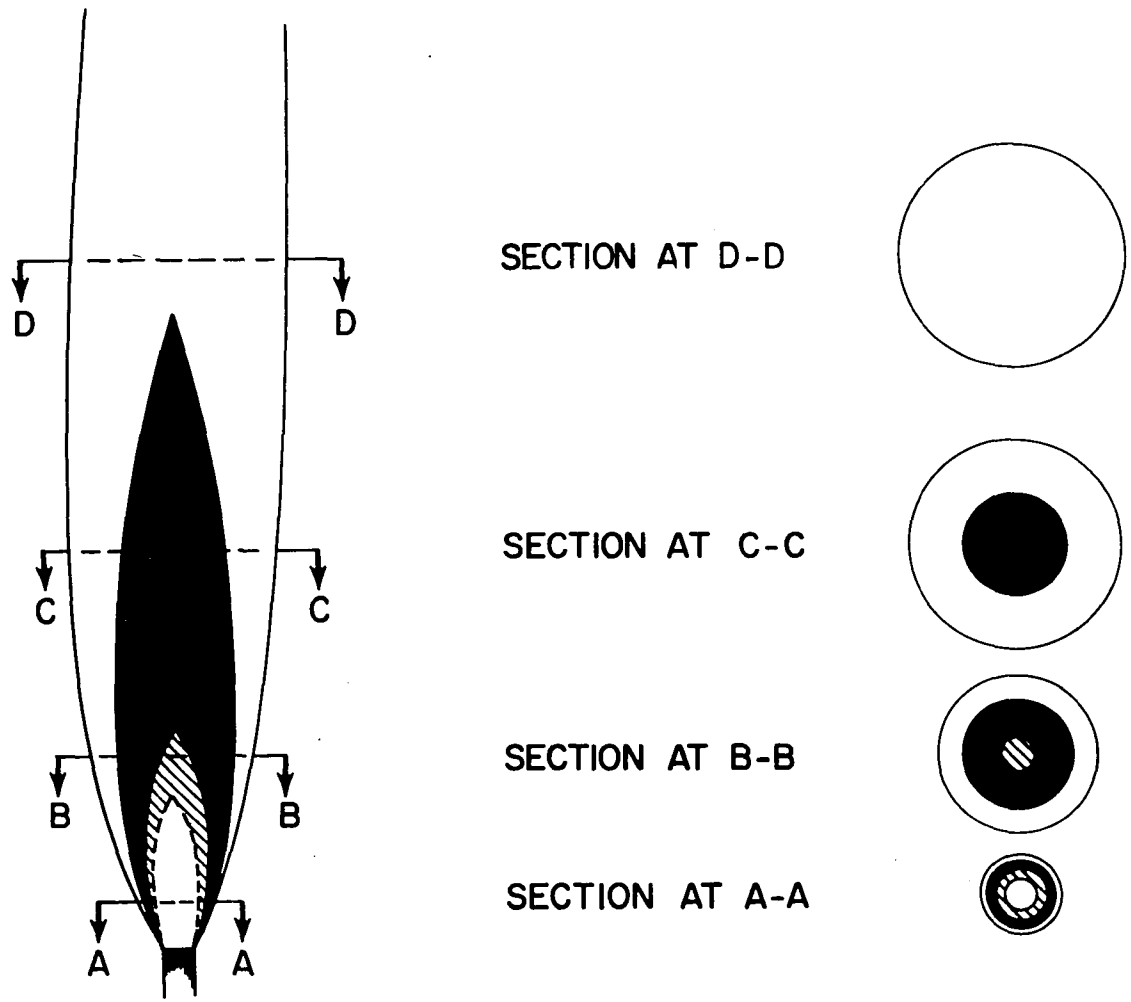

Figure 21. Cross-sections at various heights in the Kniseley flame

A second problem arises because the variation in emission intensity along the vertical axis does not necessarily indicate a corresponding variation in the concentration of the specie causing the emission. Thermal gradients exist in all flames and these gradients will produce intensity variation irrespective of the concentration of the emitting species. In flames, intensity changes due to concentration variation and changes due to temperature variation occur simultaneously. In the absence of exact temperature data, the quantitative interpretation of this superposition cannot be made. However, qualitative estimates are possible. The work of numerous investigators (61, 64, 68, pp. 32-37, 70, pp. 280-287, 71-73) indicates that the highest temperatures in premixed flames occur at a point immediately above the primary reaction zone. Consequently, the assumption that the point of maximum temperature in the Kniseley flame lies in the interconal zone, within 2 or 3 millimeters of the tip of the primary reaction zone, would seem fairly safe. The temperature would then be expected to: rise rapidly throughout the primary reaction zone; remain fairly constant through the interconal zone; and, then decrease through the secondary reaction zone.

Both the measurement of flame temperature and the measurement of intensity are further complicated by a phenomenon

known as chemiluminescence. This phenomenon arises when some of the energy released by a chemical reaction activates one of the reaction products to an excited state (68, p. 545). Unfortunately there is a tendency, in the literature, not to differentiate between true chemiluminescence and chemical reduction followed by thermal excitation (49). Consequently, some phenomenon are attributed to chemiluminescence that should not be. For the purposes of this discussion, the definition presented by Gaydon (74, p. 10) will be used and chemiluminescence will be strictly differentiated from other processes. Gaydon defines chemiluminescence as the formation of an abnormally high population of an excited state due directly to a chemical process.

Since chemiluminescence is, by definition, a non-equilibrium phenomenon, the effect would be expected in a flame region that does not exhibit equilibrium. Such a region is the primary reaction zone of the premixed flame. Further, since not all species exhibit chemiluminescence to the same degree, the determination of which profiles of the primary reaction zone reflect concentration changes and which profiles reflect chemiluminescence is not possible. The emission of C_2 and CH in the primary reaction zone is generally attributed to

chemiluminescence (74, p. 195). Here again the extent of the phenomenon is not known.

The vertical distance over which chemiluminescence might be expected in the Kniseley flame is somewhat in doubt. However, since the arguments of Mavrodineanu (68, p. 510) indicate that equilibrium is attained within a few millimeters of the primary reaction zone, the expectation would be that chemiluminescence ceases at the same point.

Interpretation is further complicated by dilution effects. Since air is entrained throughout the flame, all of the flame species experience some dilution. This dilution effect is manifested in the increased flame cross section at higher positions in the flame. Since presumably the various species distribute themselves throughout the cross section, an increase in cross section would reduce the number of atoms or molecules entering the solid angle of the spectrometer. A concentration gradient is also produced due to the nature of the aerosol flow. Since the aerosol is carried into the flame by the upward flow of the premixed gases, the aerosol droplets should tend to have a more or less vertical velocity vector. However, the rapid expansion of the gases in the primary reaction zone would serve to force some of the aerosol to the outside of the flame. Thus, low in the flame there should

exist a tendency for a high concentration of the aerosol near the flame center. This tendency should decrease in the upper portions of the flame and, coupled with an increase in flame dilution, should result in less intense emission. Unfortunately, these various processes occur simultaneously and since they cannot be studied independently only qualitative estimates as to the extent of each effect can be made.

Problems of interpretation, due to flame geometry may be solved, at least partially, by profiling the flame in the horizontal direction. This approach permits radiation from an enveloping zone to be viewed without the contribution from the shielded zone during at least a portion of the profile. Figure 22 shows schematically why this is so. If the flame is positioned so that the optical axis of the spectrometer is along line A, then the radiation entering the spectrometer will be a composite of the radiation from all three flame zones. If the optical axis is along line B, then radiation from the primary reaction zone is eliminated from the composite radiation and if the optical axis is along line C, then radiation from the secondary reaction zone alone reaches the monochromator. Comparison of different points along the horizontal profile should then permit an estimation of which of the three

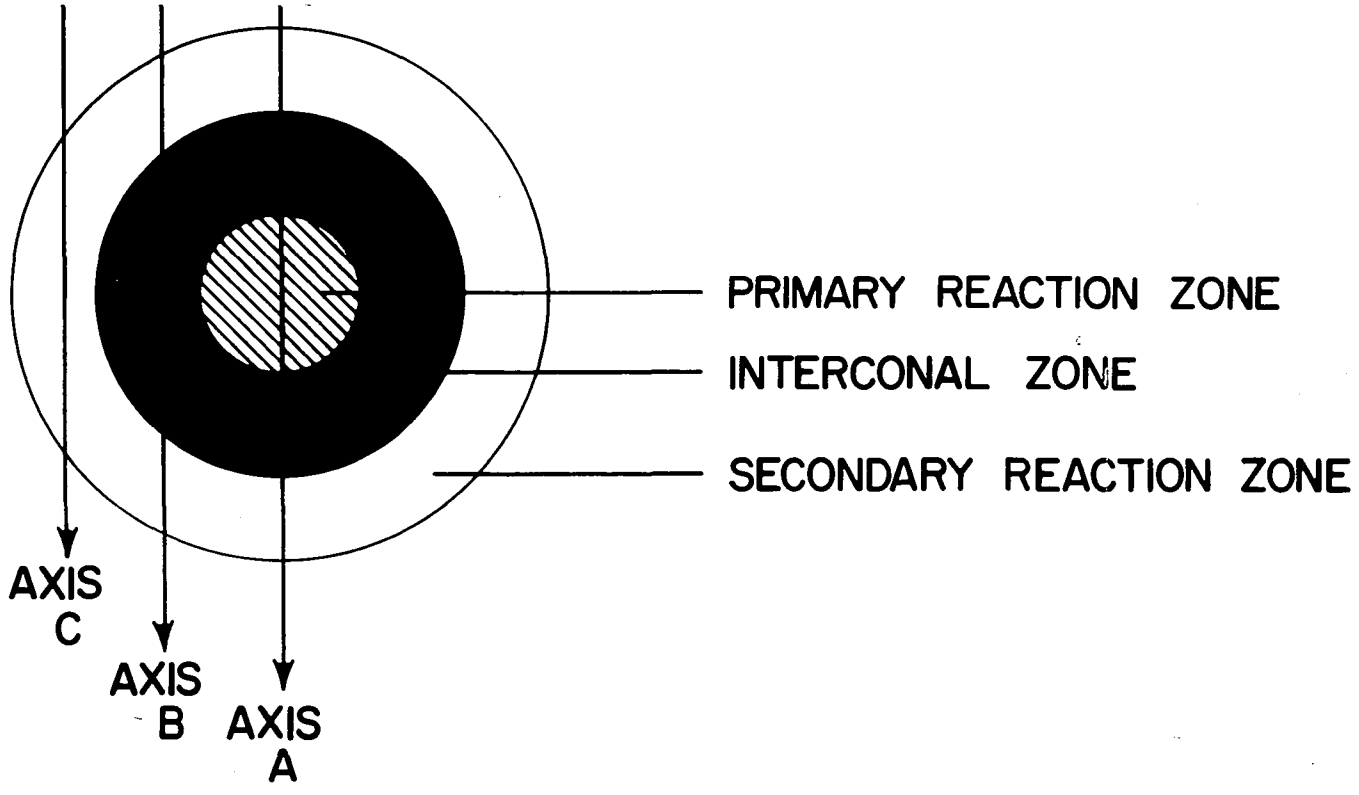

Figure 22. Illustration of the flame zones included along various optical axes

zones is responsible for the emission seen in the vertical profiles.

A feature common to most of the species, shown in Figures 18 and 19, is the winging effect seen in those horizontal profiles made near the base of the flame. The reason for this effect lies in the fact that the primary reaction zone is not homogeneous, but rather consists of two layers. Mavrodineanu (68, p. 20) terms these layers the preheating or preluminous zone and the reaction or luminous zone. Figure 23 is a photograph that shows the relative location of the two zones. Since the preheating zone produces no radiation in the visible portion of the spectrum, this region can be considered "hollow" with respect to those species that do emit visible radiation. The emitting species would thus form a ring around the hollow region. The term "hollow" as used here does not necessarily mean that the species is not present but rather that the emission from the species is reduced in the region. How such a situation affects the emission profile can be seen from Figure 24, which represents two homogenous emitting regions, one solid, the other a ring. If the picture is idealized such that the emission intensity is directly proportional to the depth of the region through which the optical axis is run, then the difference between the emission profiles

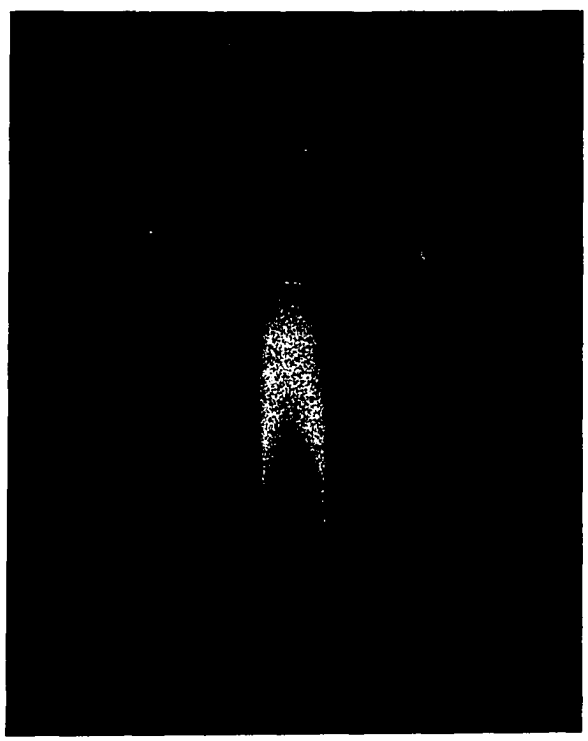

Figure 23. Photograph of the primary reaction zone of the Kniseley flame showing both the preheating and luminous zones

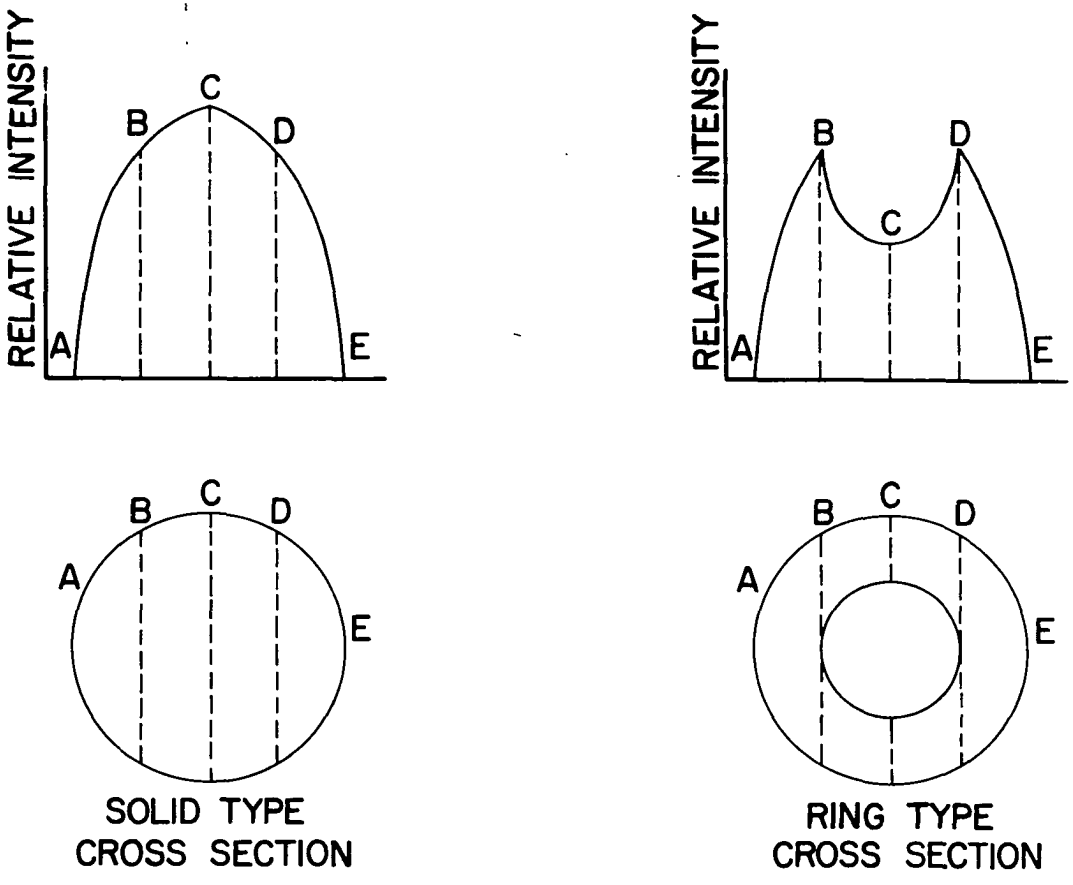

Figure 24. Schematic representation of variation in horizontal emission profiles due to changes in the flame cross-section

from two such regions becomes apparent. The solid region would produce a parabolic profile, since the maximum emission would occur when the optical axis was placed at the circle diameter (axis C) and the emission would decrease continuously to zero at the edge of the region (axis A and E). The ring-type region shows two maxima, one along axis B and the other along axis D. If the optical axis is placed along axis C, an emission minima occurs that is proportional to twice the ring thickness. Obviously such a naive picture is but an approximation. The conditions present in practice greatly distort such idealized profiles.

As was discussed for the vertical profiles, factors other than concentration changes can cause variation in emission for the horizontal profiles. The most obvious factor is the temperature gradient. In the horizontal planes, the flame temperature should show a rapid rise from near room temperature at the flame edge to a maximum at the flame center. Thus, all horizontal emission profiles must start and end at zero intensity. Further, dilution effects should be greatest near the edges of the flame while the distribution of aerosol should favor increased atom concentration near the flame center.

The problem of distinguishing between intensity variation caused by temperature gradients and variation due to concentration changes is greatly reduced by atomic absorption measurements. Since only the ground state concentration is determined, temperature effects are minimal with respect to the measurement. However, the production of free atoms may be influenced by the temperature. Inasmuch as the extent of this influence is unknown, atomic absorption profiles do not enjoy complete freedom from temperature dependence.

With the exception of the atomic carbon line at 2478.4 Å and a number of continua, the background emission of the oxy-acetylene flame consists entirely of bands. For the most part these bands do not differ from the bands found in other hydrocarbon flames (75). However, acetylene flames tend to produce more intensity largely because of higher flame temperatures (67, p. 329). Band emission from C_2, CH, C_3, CN, and OH are commonly found in the spectral region 3000 Å to 6000 Å.

The most prominent spectral feature of the primary reaction zone in most hydrocarbon flames is the C_2 emission. At present there are seven known band systems that are attributed to C_2. These are listed along with their transitions and excitation energies in Table 8. Of the seven, only five (the Mulliken, Fox-Herzberg, Deslandres-D'Azambuja, Swan and

Table 8. Band systems of C_2, CH, OH, and CN

Molecule	System	Wavelength of 0-0 band head or wavelength range (Å)	Excitation Energy (eV)[a]	References
C_2	Phillips	12,091	1.0251	(76)
	Deslandres-D'Azambaja	3,852.1	4.2447	(77)
	Mulliken	2,312.6	5.3592	(78, 79)
	Freymark	2,142.9	6.8109	(80)
	Ballik-Ramsay	17,657	0.7741	(81)
	Swan	5,165.2	2.4781	(82-85)
	Fox-Herzberg	2378-3000	5.0107	(86)
CH	Blue-violet	4,315	2.873	(87)
	Near ultraviolet	3,872	3.013	(87)
	Ultraviolet	3,144	3.941	(87)
OH	Ultraviolet	3,064	4.0175	(88)
	Schüler-Woeldike	4200-6000	8.4762	(89)
	Schüler-Michel	2248-2600	11.0862	(90)
CN	Red	10,960	1.130	(91)
	Violet	3,883.4	3.198	(92)

[a]Source of excitation energies: (68).

Phillips systems) have been seen in the air-acetylene flame (68, p. 341).

As would be expected, C_2 dominates the emission spectrum from the primary reaction zone of the Kniseley flame. Figures 13, 14, and 15 reveal that the Swan system provides most of the spectral features. The components of this system give rise to the characteristic color of the primary reaction zone. Since they extend from about 4300 Å to 5635 Å and show considerable intensity, the Swan bands render the primary reaction zone unsuitable for many analytical purposes.

The Deslandres-D'Azambuja system is much weaker than the Swan system and does not show up well in Figures 13, 14, and 15. However, the system is present in the Kniseley flame and the band head can be easily resolved at higher gain and slower scanning speeds. Since the origin of the system is located at 3852.1 Å, the CN band system interferes with many of the components.

In the interconal zone, the C_2 emission is greatly reduced from that of the primary reaction zone. However, the 5165 Å and 4737 Å heads still show considerable intensity. Observations in the secondary reaction zone revealed no C_2 emission.

The vertical profile of C_2 is shown in Figure 16. As would be expected C_2 emission is greatest in the primary reaction zone with the maximum occurring several millimeters below the tip of this zone. The decrease in emission is very rapid from the maximum to the tip of the primary reaction zone and then becomes gradual through the interconal zone. The observation that C_2 emission persists throughout the majority of the interconal zone is of particular interest. Horizontal profiles of C_2 (Figure 18) show similar results. However, since the sensitivities at which the horizontal profiles were determined were poorer than those used for the vertical profiles, the extension of C_2 emission into the interconal zone is not evident in Figure 18. A winging effect is clearly seen in the horizontal profiles of the lower portions of the flame.

The presence of C_2 in oxyacetylene flames is well established and considerable speculation has come forth in an attempt to explain how C_2 forms. The most attractive mechanism is the extraction of the two hydrogens from the acetylene molecule. This mechanism was originally discussed by Hsieh and Townsend (93) and was proposed to proceed via reactions of the form:

$$C_2H_2 + H \rightarrow C_2H + H_2 \qquad (a)$$

A second theory, proposed by Gaydon and Wolfhard (36, p. 199), suggested the formation of long chain hydrocarbons through some form of polymerization. These chains then broke up to yield smaller carbon fragments of which C_2 was but one. Both the pyrolysis, or extraction theory, and the polymerization theory were open to question in view of the work of Ferguson (94) who studied the effect of isotope dilution on the C_2 Swan bands. He concluded that few of the original carbon-carbon bonds of the fuel were found in the C_2 molecule, and that the acetylene was ruptured at the -C≡C- bond and then recombined to form C_2 via the reaction:

$$2\ CH \rightarrow C_2 + H_2 \qquad (b)$$

Goldfinger (95) suggested a modification of the above reaction that eliminated the necessity of numerous two-body collisions between identical radicals. Goldfinger proposed C_2 formation via the following scheme. First atomic carbon was produced by the reaction:

$$2\ CH \rightarrow C + CH_2 \qquad (c)$$

CH was then considered as a chain carrier that provided C_2 and other carbon species through reactions of the form:

$$C + CH \rightarrow C_2 + H \qquad (d)$$

$$C_x + CH \rightarrow C_{x+1} + H \qquad (e)$$

Herman, Hornbeck, and Laidler (96) proposed a complete set of reactions to describe the production of C_2, as well as the other molecular flame species. Their scheme, known as the peroxide mechanism is summarized in the following reactions:

$$C_2H_2 + O_2 \rightarrow H\text{-}C{\equiv}C\text{-} + HO_2 - \sim 60 \text{ kcal} \qquad (f)$$

$$H\text{-}C{\equiv}C\text{-} + O_2 \rightarrow H\text{-}C{\equiv}C\text{-}O\text{-}O\text{-}O + 50 \text{ kcal} \qquad (g)$$

$$H\text{-}C{\equiv}C\text{-}O\text{-}O\text{-} + C_2H_2 \rightarrow$$
$$H\text{-}C{\equiv}C\text{-}O\text{-}O\text{-}H + H\text{-}C{\equiv}C\text{-} - \sim 10 \text{ kcal} \qquad (h)$$

$$H\text{-}C{\equiv}C\text{-}O\text{-}O\text{-}H \rightarrow H\text{-}C{\equiv}C\text{-}O\text{-} + OH - \sim 30 \text{ kcal} \qquad (i)$$

$$H\text{-}C{\equiv}C\text{-}O\text{-} \rightarrow CH + CO - \sim 75 \text{ kcal} \qquad (j)$$

$$H\text{-}C{\equiv}C\text{-} + O_2 \rightarrow HO_2 + C_2 - \sim 120 \text{ kcal} \qquad (k)$$

$$2\ CH \rightarrow C_2 + H_2 + \sim 30 \text{ kcal} \qquad (l)$$

The same authors also suggested an additive mechanism which involved an initial attack by oxygen, as follows:

$$C_2H_2 + O_2 \rightarrow H\text{-}\overset{O\text{-}O}{\overset{|\ \ |}{C}}{=}C\text{-}H \rightarrow 2HCO + \sim 55 \text{ kcal} \qquad (m)$$

$$HCO \rightarrow H + CO - \sim 20 \text{ kcal} \qquad (n)$$

$$HCO + O_2 \rightarrow HO_2 + CO + \sim 40 \text{ kcal} \qquad (o)$$

$$CO + \tfrac{1}{2}O_2 \rightarrow CO_2 \text{ (via chain mechanisms)} \qquad (p)$$

The above reactions are known to occur at room temperatures and the energies given are those found when the reactions proceed at room temperature. The basic premise of both the peroxide and additive mechanisms is that the reactions occur in an analogous manner at the higher temperatures found in flames.

The various mechanisms discussed above should serve to demonstrate the complexity of the problems encountered in trying to find a satisfactory theory for the formation of the flame species. It would be naive to assume that a single mechanism can be found to completely explain flame processes. The evidence to date indicates that several competing processes are occurring simultaneously and that variations in the flame conditions can change the dominant mechanism from one scheme to another (65). However, any successful theory must be able to account for: the low ignition temperature of acetylene as compared to other hydrocarbon fuels; the wide range of composition over which acetylene is combustible;

and the extremely high burning velocity of oxyacetylene mixtures. Further, the overall process must be highly exothermic. Such requirements mean that the individual reactions contributing to the overall mechanism must be very rapid and few can be endothermic.

The behavior of C_2 in the Kniseley flame is quite important with respect to a number of subsequent discussions and should therefore be examined closely. In the lower portions of the flame the winging effect, seen in Figure 18, gives evidence of the hollow nature of the primary reaction zone. The fact that the preheating zone can be detected spectroscopically is trivial in itself since this zone is easily seen through a piece of dark glass. However, demonstration of the fact that a winging effect will be produced when an enveloped region yields less emission than the surrounding region is significant for some of the other flame species, notably OH. The relative decrease in the winging effect with increasing height in the flame indicates the transition from a ring-type zone to a solid zone and supports the conclusion that C_2 is not produced in the preheating zone by the thermal decomposition of acetylene. The rapid rise in C_2 emission can be attributed to the superposition of increasing C_2 concentration, increasing temperature, and chemiluminescence.

As discussed previously the relative contribution of each of these factors cannot be determined by emission profiles alone. However, some clarification results from examination of Figure 25 which shows a comparison between the emission and molecular absorption of C_2 in the interconal and primary reaction zones of the Kniseley flame. The emission of C_2 is seen to be about ten times less intense in the interconal zone than in the primary reaction zone while the corresponding decrease in absorption is only about a factor of two. Since C_2 emission from the primary reaction zone is known to be subject to chemiluminescence, a more accurate indication of the C_2 concentration is given by the absorption measurements. The observed decrease in absorption is expected on the basis of a shorter absorption path length in the interconal zone.

Table 9 shows that C_2 is a moderately stable molecule and as such will not undergo extensive thermal decomposition in the flame. However, the presence of oxygen would effectively lower the C_2 concentration by reacting to form CO. Thus, the presence of C_2 in the interconal zone reflects, a corresponding lack of oxygen. Further, the fact that C_2 exists in the interconal zone demonstrates that numerous other moderately stable carbon species, which do not exhibit emission spectra in the 3000 to 6000 Å region, may also be present. Thus, it may

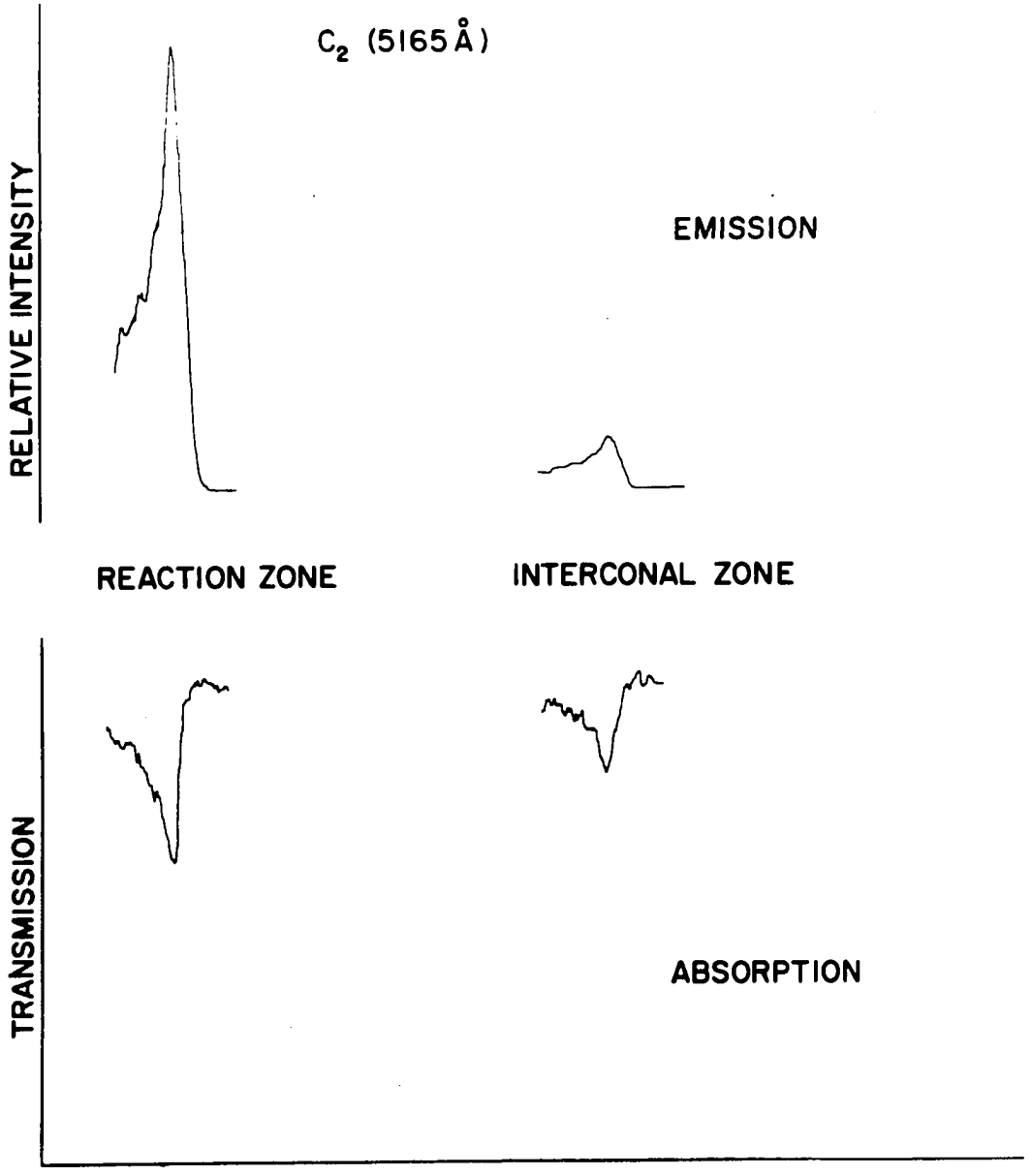

Figure 25. Comparison of emission and molecular absorption from two zones of the Kniseley flame

Table 9. Dissociation energies of some molecules encountered in this study

Molecule	Dissociation Energy (eV)	Reference
H_2	4.476	(97, p. 530)
OH	4.39 ± 0.01	(98)
CH	3.47	(99)
CN	7.55 ± 0.13	(100)
CO	11.09	(99)
C_2	6.25 ± 0.2	(101)
O_2	5.115	(99)
N_2	7.373	(97, p. 450)
ScO	6.9	(102)
LaO	8.4	(103)
GdO	7.0 ± 0.5	(104)
VO	6.4	(105)
CrO	4.38 ± 0.30	(106)

be reasonably assumed that the interconal zone is a region that is deficient in oxygen and relatively rich in carbon containing species.

There appear to be two sources for the C_2 seen in the interconal zone. The first is the combustion processes of the primary reaction zone. Thus, C_2 would be considered as a product, of the incomplete combustion of acetylene, which in the absence of sufficient oxygen sustains because of a favorable dissociation energy. The second possible source of C_2 is the excess acetylene. The work of Behrens (107) indicates that a considerable portion of the acetylene passes through the primary reaction zone essentially unreacted and then undergoes thermal decomposition. Since the thermal decomposition of acetylene should yield C_2, as well as other carbon species, the distribution of the excess acetylene throughout the interconal zone, prior to decomposition, would provide a source of C_2 within the zone itself. If acetylene dissociation were to occur more or less uniformly throughout the interconal zone, one would expect a more gradual reduction in the C_2 emission than is observed. However, since the interconal zone decreases in thickness very rapidly with flame height, there is a strong possibility that the observed decrease is a function of the flame geometry as well as the

removal of C_2 through chemical processes.

Three probable chemical processes are: the direct reaction of C_2 with oxygen; competition reactions between C_2 and oxygen bearing species such as OH; and the formation of other molecular species. The diffusion of air into the flame permits the direct reaction of atmospheric oxygen with the easily oxidized species of the interconal zone. The occurrence of these reactions is perceived visually as the reaction front of the interconal zone. The possibilities of C_2 entering competition reactions, as well as the formation of other molecular species will be discussed subsequently.

Like C_2, CH is a species common to all hydrocarbon flames. The CH spectrum consists of only three systems (see Table 8) and, as evidenced in Figures 13, 14, and 15, all three systems can be found in the primary reaction zone of the Kniseley flame. However, each system is at least partially interfered with by some other species. For the most part the individual components of the CH spectrum can be resolved from their interferences if slower scanning speeds are used.

The vertical profile of CH (see Figure 16) appears similar to that of C_2 in the primary reaction zone but the existence of CH more than a few millimeters beyond the primary reaction zone is not detected even under high gain.

The horizontal profiles (see Figure 18) show results similar to the vertical profiles. As expected a winging effect is observed in the lower portions of the flame.

The formation of CH via the peroxide mechanism has already been described. Two other possibilities are found in the literature. The first is the spontaneous break-up of acetylene into two CH molecules (66).

$$C_2H_2 \xrightarrow[\Delta]{} 2\ CH \qquad (q)$$

The second provides for CH through the reaction of C_2 with OH.

$$C_2 + OH \rightarrow CH + CO \qquad (r)$$

Such a reaction of course cannot be considered simultaneously with reactions such as (a, b, d, or e).

The rapid increase observed for CH in the primary reaction zone does not reflect a corresponding increase in the CH concentration. Like C_2, this species is expected to show considerable chemiluminescence in a non-equilibrium regions of the flame. The termination of CH emission in the interconal zone may at first be surprising since presumably there is little oxygen available to react with the species. However, as can be seen from Table 9 CH has a relatively low

dissociation energy and thus may be expected to dissociate via the simple reaction:

$$2\ CH \xrightarrow{\Delta} C_2 + H_2 \qquad (b)$$

This reaction offers yet another source of C_2 in the interconal zone and may be one cause of the slight leveling effect observed in the C_2 vertical profile a few millimeters above the tip of the primary reaction zone.

The presence of the molecule C_3 in flames has been reported by Kiess and Bass (108) as well as Marr and Nicholls (109). This species is of considerable astrophysical significance and consequently has received much attention (68, p. 351). The strongest bands occur at 4050 Å and 4072 Å. There are several heads reported to be in the 4050 Å region as well as an associated violet continuum.

In the Kniseley flame, the C_3 spectrum is greatly obscured by CH emission and thus cannot be distinguished in Figures 13, 14, and 15. Slower scan speeds reveal a number of components in the region around 4050 Å that clearly do not belong to the CH system. However, with the exception of the 4050 Å C_3 band head, these components appear too diffuse to make positive identifications. Fortunately, a positive

identification of the 4050 Å head has made possible the vertical profiling of C_3.

The profile of C_3 (Figure 16) appears quite similar to that of C_2. However, the extent to which C_3 emission persists in the interconal zone could not be studied because under high gain background from other band components near the 4050 Å C_3 band head became too high to permit the accurate determination of the band head intensity. The background under the C_3 band head also prohibited the determination of the horizontal profiles for C_3.

The formation of C_3 in fuel-rich flames has been discussed in considerable detail by Marr (66). The results of his study indicate that C_3 forms through reactions similar to reaction (e). Thus, C_3 formation would depend upon the presence of CH and the dissociation of CH beyond the tip of the primary reaction zone would mark the cessation of C_3 production. Like C_2, C_3 reacts easily with oxygen to form CO. Thus, the existence of C_3 in the lower portions of the interconal zone gives further evidence of a shortage of oxygen.

A fourth carbon containing species found in hydrocarbon flames is CN. The spectrum of this species is quite intense and well developed in hydrocarbon flames that are supported

with the oxides of nitrogen (74, p. 215). However, in air-acetylene or oxyacetylene the spectrum is neither particularly well developed nor very intense.

The CN spectrum consists of two well known systems, the violet and the red systems. Not all of the bands of these systems are seen in oxyacetylene flames. The strong components of the red system lie outside the 3000 Å to 6000 Å region and would not be seen in this study. However, the majority of the violet system should be seen. The strongest bands of the violet system have their heads at: 3883.4 Å, the (0,0) band; 4216.0 Å, the (0,1) band; and 3590.4 Å, the (1,0) band. These correspond to the sequence $\Delta v = 0$, $\Delta v = -1$, and $\Delta v = +1$ respectively and according to Pearse and Gaydon (69, p. 111) should have relative intensities of 10, 9, and 7.

The spectrum of CN from the Kniseley flame shows considerable variation from that which would be expected on the basis of the given relative intensities. The 3883.4 Å head is substantially stronger than that found with a Beckman flame (see Figure 4). However the $\Delta v = -1$ and $\Delta v = 1$ sequences do not appear at all in Figures 13, 14, and 15, and even under conditions of better resolution appears only weakly. The reasons for this apparent discrepancy in intensities has not

been explained. Durie (110) found similar anomalous intensity variation for CH and was able to explain this on the basis of selective excitation to a particular state. Such an explanation cannot be made here since population of the upper vibrational states is demonstrated by the existence of the $\Delta v = 0$ bands. A detailed study of the intensity variations in the CN spectrum from oxyacetylene flames might prove to be an interesting problem in itself.

The vertical profile of CN is shown in Figure 26 along with a similar profile obtained by Marr (66, p. 27). Comparison of the two profiles is of interest since an insight into the source of CN in the oxyacetylene flame is provided. Marr's studies were performed on an oxyacetylene welding torch. The primary source of nitrogen for such a device is through entrainment of atmospheric nitrogen. The Kniseley burner on the other hand provides nitrogen through the air ports in the burner base. Thus, nitrogen is supplied to the Kniseley flame from the very onset of the combustion. This results in the formation of CN in the primary reaction zone and accounts for the maximum occurring lower in the Kniseley flame than in the welding torch. Marr's study indicates that CN can be formed in the interconal zone. Consequently, a carbon containing species that has a dissociation energy

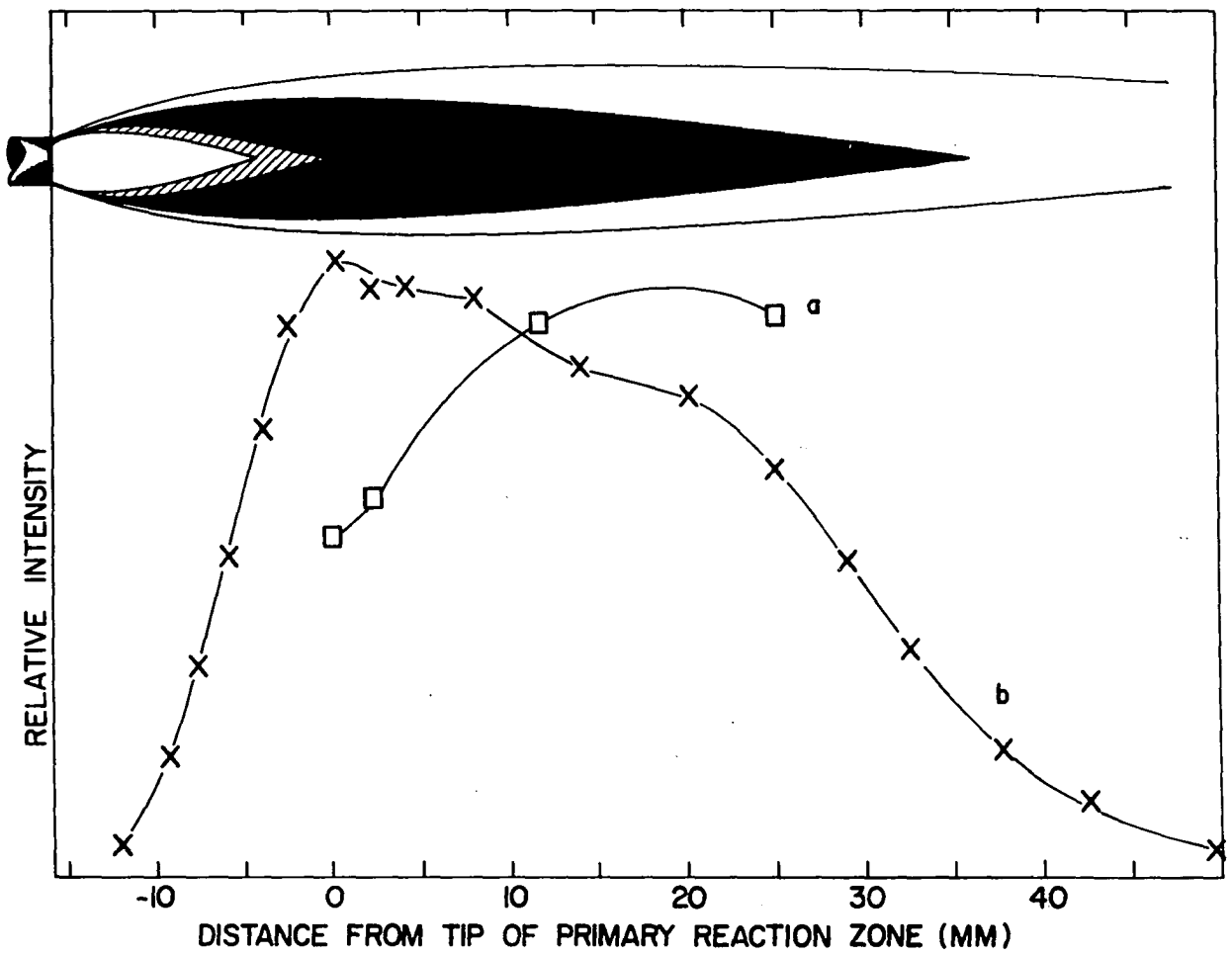

Figure 26.- Vertical emission profiles of the 3883 Å CN band head from Marr's (66) study (a) and from this study (b)

compatible with the formation of CN must be present in this zone. Comparison of the dissociation energies (Table 9) of the species that might be involved reveals that the carbon must come from a species other than CO. CH is eliminated because as seen in Figure 16, the existence of high concentrations of CH throughout the interconal zone is unlikely. Atomic carbon offers a possibility. However reactions of the form

$$C + N \rightarrow CN \qquad (s)$$

require a prior dissociation of N_2 and the necessary energy is not available. Thus, the most direct method and one which is consistent with the results of this work is:

$$C_2 + N_2 \rightarrow 2\ CN \qquad (t)$$

Here again there is the question as to whether or not the flame can provide sufficient energy to dissociate sufficient quantities of both C_2 and N_2. However, the need to dissociate the two molecules prior to reaction can be eliminated if an intermediate compound of the type $\begin{matrix} C=C \\ | \quad | \\ N=N \end{matrix}$ is postulated. Dissociation would then occur after the formation of the C-N bands. With the acceptance of such a mechanism, Marr's study indicates that the interconal zone contains sufficient C_2 to

favor CN formation and further that the interconal zone is not a reaction free zone. The results of the present study are consistent with the proposed mechanism in that they show C_2 in the interconal zone and that considerable C_2 is formed prior to the formation of CN. The peaking of the CN emission at the tip of the primary reaction zone indicates that more CN is produced in the primary reaction zone than in the interconal zone. However, since the temperature variation and the degree to which chemiluminescence affects the profile are not known, such a conclusion must be viewed with caution.

The favorable stability of CN (see Table 9) permits its existence in the flame until the oxygen concentration in the flame gases becomes high enough to remove CN through the formation of CO and N_2. Thus, the existence of substantial amounts of CN throughout the interconal zone adds to the evidence which indicates a low oxygen concentration in this zone.

The species OH is responsible for the remaining dominant features in the 3000 Å to 6000 Å region. This species has considerable importance to studies of kinetics in flames and consequently has received much attention (68, p. 339). Dieke and Crosswhite (111) have compiled an extensive report on OH.

Only one OH system is seen in flames. This lies in the ultraviolet and is well developed. Two other systems are known (89, 90) and are listed in Table 8. However, these have yet to be observed in flames. The region 3000 Å to 6000 Å yields only the $\Delta v = 0$ head at 3064 Å, which can be seen in *Figures* 13, 14, and 15. Not shown is the $\Delta v = +1$ head which appears quite clearly at 2811 Å. The remaining heads of the ultraviolet bands appear only weakly even under better resolving conditions.

The vertical profile of OH (Figure 16) shows two features that differ from those of the carbon containing species. The first is the dip near the interface between the primary reaction zone and the interconal zone. The second is the increase in emission in the upper regions of the flame.

The horizontal profiles of OH also differ from their counterparts for the carbon containing species. The most significant difference is the presence of a winging effect in the interconal zone rather than near the base of the flame.

There have been numerous suggestions pertaining to the formation of OH in flames. Reaction i has already been mentioned. In addition, Broida and Shuler (112) suggest reactions m, n, and o followed by:

$$HO_2 + CO \rightarrow OH + CO_2 \qquad (u)$$

Broida and Gaydon (113) concluded that OH is formed through the destruction of CH with oxygen via:

$$CH + O_2 \rightarrow CO + OH \qquad (v)$$

OH may also be formed by either of the reactions (112):

$$H + O_2 \rightarrow OH + O \qquad (w)$$

$$H_2 + O \rightarrow OH + H \qquad (x)$$

as well as the simple dissociation of water via the reaction:

$$H_2O \rightarrow OH + H \qquad (y)$$

Since OH is the only oxygen containing natural flame species profiled in this work, the interpretation of the two OH profiles is of considerable interest. Of prime importance is the observation of the winging effect in the interconal zone. By analogy with previous discussion such a dip implies a transition from a solid region to a ring-type region. Since the ring is formed around the interconal zone, the indication is that the interconal zone is hollow with respect to OH emission. In view of the evidence from the profiles of C_2,

C_3, and CN, this should not be too surprising. If the interconal zone is in fact deficient in oxygen and rich in carbon containing species, the dissociation energy of CO (Table 9) should favor the destruction of OH via reactions of the form:

$$OH + C \rightarrow CO + H \qquad (z)$$

The occurrence of such a reaction would of course render the interconal zone effectively free of OH emission. It should be noted that the point where the dip occurs corresponds to the same vertical flame position where the dip in the vertical profile occurs. The net result of the two profiles indicates that OH emission is fundamentally a secondary reaction zone phenomenon. Since the secondary reaction zone marks the completion of the combustion process, the production of OH should be continuous throughout the flame. Further, the emission profiles should reflect the OH production at least until the local temperature falls beneath that required for excitation. Figure 27 is an integrated emission profile prepared from the various horizontal profiles. This figure shows the required increase in OH emission. Presumably the relatively flat region between flame heights of -7 millimeters and 1 millimeter reflect a balance between the rate of OH production in

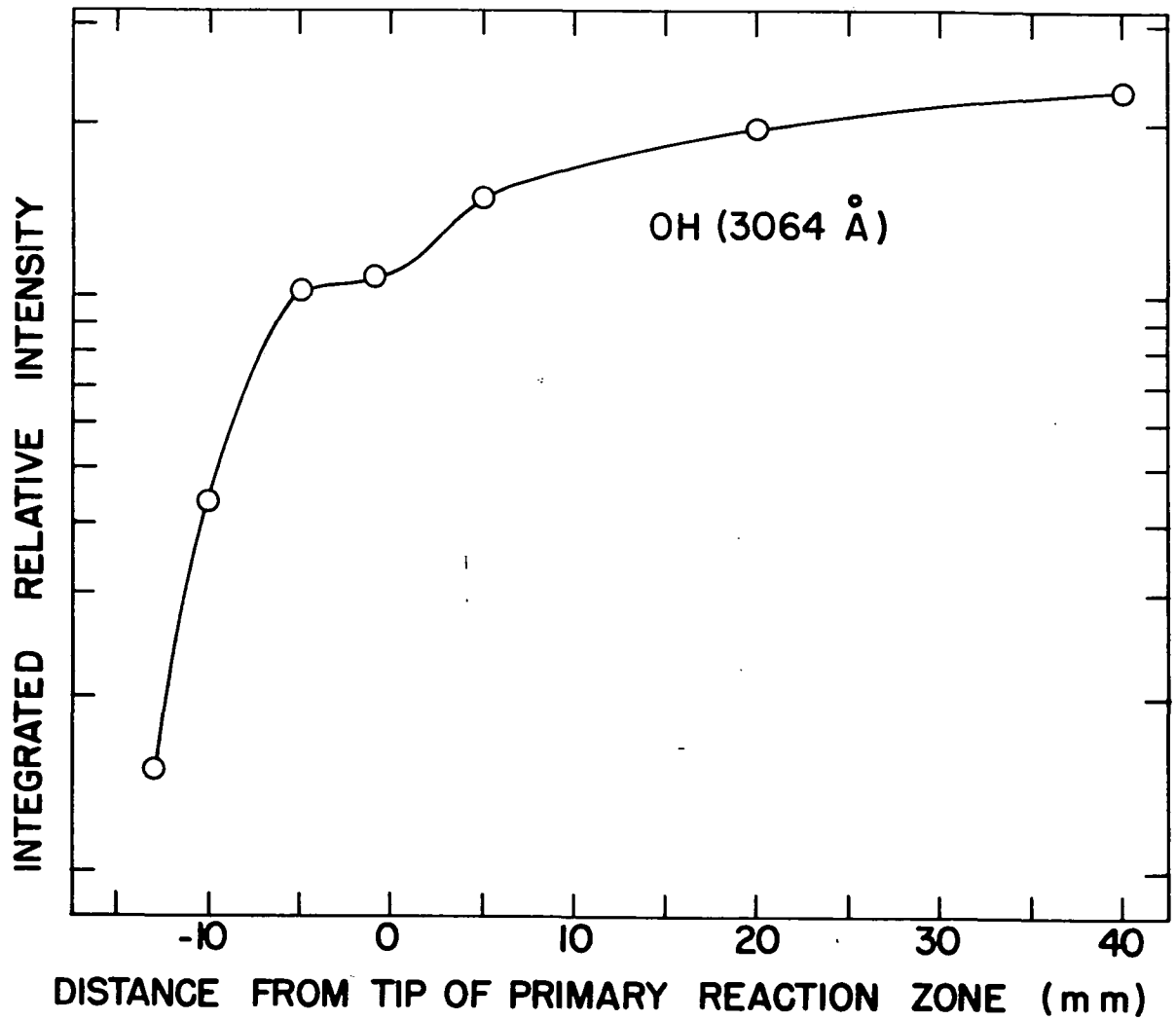

Figure 27. Integrated emission profile of OH

the secondary reaction zone and the destruction of OH in the interconal zone.

In addition to the species already mentioned there are a number of molecules that would be expected in the Kniseley flame but for which no emission was found. The major species are CO, CO_2, H_2O, and atomic carbon. Both CO_2 and H_2O would be expected to dissociate in all but the cooler outer portions of the flame. Further, since their most intense bands lie in the infrared, CO_2 and H_2O would not be detected with the instrumentation employed. However, both CO and atomic carbon produce emission between 2000 Å and 3000 Å. The "fourth positive" system of CO is reported to be easily seen in the primary reaction zone of the oxyacetylene flames (68, p. 349). Since CO is undoubtedly formed in the Kniseley flame, two possibilities must be considered. Either the spectrometer employed did not possess sufficient speed in the ultraviolet portion of the spectrum or the Kniseley flame does not provide sufficient energy to excite CO. The same possibilities exist for atomic carbon. However, there is also the somewhat doubtful possibility that little atomic carbon is formed in the Kniseley flame.

In addition to the band structure, there are a number of continua associated with the oxyacetylene flame. Gaydon (114)

describes an ultraviolet continuum extending from about 3000 Å to 5000 Å which he attributes to the reaction:

$$CO + O \rightarrow CO_2 + h\nu \qquad \text{(aa)}$$

Superimposed upon this continuum is the Phillips and Brewer (115) continuum which extends from 3500 Å to 4600 Å. Marr (66) suggests a reaction of the form

$$C + C_2 \rightarrow C_3 + h\nu \text{ (cont.)} \qquad \text{(bb)}$$

to be responsible for this radiation. Both continua appear in the primary reaction zone but the interconal zone exhibits only the ultraviolet continuum of Gaydon. Above 5000 Å, there exists a rather broad continuum that does not appear very strongly in Figures 13, 14, and 15. However, the Beckman flame produces the structure quite well (see Figure 4). This continuum is in all likelihood produced by the blackbody type radiation of solid carbon. Such radiation should increase to a maximum somewhere near 8000 Å. In Figure 4 the decrease in intensity near 6000 Å is due to a reduction in the sensitivity of the detector photocathode. Comparison of the blackbody emission of the Beckman and Kniseley flames indicates that there is less solid carbon formed in the Kniseley flame.

Visual inspection of the two flames supports this conclusion.

Since the scientific method requires the transition from the specific to the general, an explanation of the foregoing observations with respect to a generalized flame model would seem appropriate at this juncture. Admittedly this model will be born largely of conjecture. However, the following presentation at least qualitatively describes those processes essential to the fuel-rich phenomenon.

Premixing of the fuel, oxidant, and entrained air is accomplished as the gases rise through the premixing channel at a rise velocity compatible with the formation of a stationary flame. It should be noted that the rise velocity of the gases in the Kniseley burner are not as high as those velocities necessary to form a flame with an undiluted acetylene-oxygen mixture. The presence of a relatively large amount of nitrogen (68, p. 17) as well as the excess fuel (116) substantially reduce the burning velocity. Gases enter the combustion region by first passing through the preheating zone. This zone emits no visible radiation so it is doubtful if any reactions that would be classified as combustion reactions occur. There is the possibility that a limited amount of pyrolysis of the acetylene occurs but even this

is doubtful. The primary function of the preheating zone, as the name implies, is to preheat the gas mixture from room temperature to near the ignition temperature. The exact ignition temperature varies depending upon the composition of the gas mixture. Generally, the range of ignition temperature that can be expected in gas mixtures of the type used in the Kniseley burner may vary between 300° and 400°C (63, p. 15).

Upon reaching the ignition temperature the gas mixture begins the actual combustion process and forms the primary reaction zone. The reactions occurring in this zone are extremely fast and release a great deal of both thermal energy and radiation. Exactly what reactions occur is unknown. However, in the presence of the large excess of acetylene the major effect in the primary reaction zone will be the rapid and nearly complete removal of available oxygen from the gas mixture. Presumably, the majority of the oxygen will be in the form of CO. Further, the heat released when the CO forms provides sufficient energy to permit some of the endothermic reactions discussed previously to occur. In addition to CO, numerous other species are formed. For the sake of the model these species may be looked upon as debris from the reactions that deplete the oxygen supply. This debris then leaves the

primary reaction zone and enters the interconal zone. Consequently, the interconal zone of the fuel-rich flame, compared with that of a leaner flame, becomes a region relatively rich in carbon containing species but poor in oxygen. Further, since the interconal zone is fed directly from the primary reaction zone and is shielded from the surroundings by the secondary reaction zone, the temperature attained, particularly near the primary reaction zone is high.

Upon exiting the primary reaction zone, the debris mixture undergoes a series of reactions that provide the most stable composition. Thus, any oxygen containing species less stable than CO (see Table 5) reacts with the carbon-containing species to form CO. Species that are not thermally stable dissociate. CH is one of these and should dissociate via the simple reaction

$$2\ CH \xrightarrow[\Delta]{} C_2 + H_2 \qquad (b)$$

The more stable species, such as CN and C_2, should not be dissociated to a large extent and, along with a considerable amount of CO, become the principal molecules in the interconal zone.

The mixture of flame species, producing the interconal zone, is destroyed upon encountering the oxygen provided

through air diffusion. In the presence of sufficient oxygen the carbon-containing species as well as the hydrogen will be completely oxidized and the flame will assume the characteristics of the secondary reaction zone. The rate at which air enters the interconal zone is unknown, however Marr's (66) CN profile indicates that some air is available within a few millimeters of the primary reaction zone. The atmospheric oxygen will of course begin to deplete the carbon species while the nitrogen will both deplete C_2, through formation of CN, and serve to dilute the flame gases. The combustion of the carbon-containing specie with atmospheric oxygen occurs at the flame front that is perceived as the outer boundary of the interconal zone. Since more air will become available higher in the flame, there should be both a lowering of the flame temperature and a decrease in the reducing properties of the interconal zone as a function of flame height.

The above model is consistent with the observed profiles. Thus, the increase in emission of C_2 and CH in the primary reaction zone is due to a superposition of a concentration gradient and chemiluminescence. After the maximum, CH emission terminates because of the relative instability of

the molecule, while C_2 emission sustains because of both sufficient stability and because C_2 is produced from the acetylene that has passed into the interconal zone. The decrease in C_2 emission as a function of higher flame position reflects the depletion of C_2 through reactions with atmospheric oxygen and nitrogen. Like C_2 and CH, CN is formed in the primary reaction zone from the nitrogen that enters through the air-ports at the base of the premixing channel. The species persists through the interconal zone because of the favorable stability of CN coupled with the formation of additional CN from the C_2 found in the interconal zone. The profiles of OH show that OH emission is predominately a secondary reaction zone phenomenon. The OH, produced in the primary reaction zone, is destroyed in the interconal zone due to the inability of hydrogen to successfully compete with carbon for the oxygen.

The foregoing model is intended to provide a description of the physical environment in which various metallic species will exist in the flame. Attention now will be turned to the behavior of a number of specific metallic species.

Metals are introduced into the flame in the form of solutions. Consequently, there are numerous processes that

must occur to provide the transition from metal in solution to metal as free atoms. Dean (20, p. 31) attempts to catalogue these processes as occurring through a number of distinct steps which are incorporated by Gibson, Grossman, and Cooke (61) into the following scheme:

solution feed → nebulization → evaporation →
precipitation of salt → decomposition of salt →
formation of metal vapor → excitation process →
excited metal → emission

While such processes undoubtedly occur, there is reason to doubt that they will occur in an orderly stepwise fashion. Since the nebulized solution is carried into the flame by the premixed gases, the metal enters at a rate comparable to the rise velocity of the gases. The work of Gibson et al. (61) indicates that the nebulized droplets pass through a Beckman flame in a matter of a few milliseconds. If this figure is assumed to be approximately true for the Kniseley flame, a particle will pass from the base of the flame through the primary reaction zone in less than 1 millisecond. This rapid transit opens some questions as to whether or not a stepwise system, such as that proposed by Dean, has time to occur.

A more likely process would be one in which all of the physical transformations occur nearly simultaneously. The following is proposed as such a process.

The aerosol droplets enter the flame through the pre-heating zone. In this region, the solvent begins to evaporate. However, since the rise time is so short the droplets arrive at the primary reaction zone with little loss due to evaporation. The droplets now pass into the primary reaction zone where they encounter a sudden temperature change of about 2000°C. This causes the processes of evaporation, dehydration and volatization to occur essentially simultaneously and with considerable violence. The net effect is an explosion-like destruction of the individual aerosol droplets. Since this occurs within a highly reactive environment, the destruction of the aerosol droplets may be further aided by chemical reactions such as combustion of the solvent. The metal species that until the explosion were in the form of the solvated ions, now distribute into three forms: metal atoms (M); metal monoxides (MO); and other metal containing molecules (MX). The species designated as MX represents a large number of compounds that might form in the flame, such as the metal polyoxides, metal salts, metal

hydrides and carbides, and polymeric forms of the metal itself. While the existence of all of the above forms of MX is not being conceded, the designation MX is intended to represent all metal containing species in the flame except metal atoms and metal monoxides. The relative amounts of M, MO and MX, formed by the explosion, depend to a large extent upon the nature of the metal. Thus, metals possessing a high monoxide dissociation energy would tend to form a greater proportion of MO, while metals that have a particularly stable molecular form would tend to produce a high proportion of MX. Metals that have neither a sufficiently stable monoxide, at flame temperatures, nor a stable form of MX would tend to form a high proportion of free metal atoms. This does not mean that one form of metal species is produced exclusively for a given element. All metals will form all three species to some extent. However, the relative proportions will be different for different metals.

The relative proportion of the three species may change, after the explosion, by a redistribution based on the following competing equilibria.

(cc)

Since the explosion products depart from the primary reaction zone very rapidly, complete equilibrium between the three species in the primary reaction zone is doubtful. However, in the interconal zone an equilibrium may be established. The equilibrium point for a given metal will be dictated by the local flame temperature and the flame environment. As the metallic species travel upward through the interconal zone they will encounter varying temperatures and environments. As a consequence, the equilibrium point will vary as a function of flame position as will the appearance of atomic emission.

Examination of the metallic profiles should clarify how the above processes operate for specific metals. The following discussion deals largely with the MO to M conversion, seemingly to the neglect of MX. There are several reasons for this. The specific nature of MX for the elements studied is not known and therefore no actual data on the MX distribution was obtained. Also, for many metals the same properties, i.e. - electronegativity, atomic size, etc., that lead to stable monoxides will also produce stable forms of MX. Thus, the behavior of MO should represent the behavior of MX to some degree. Throughout the following discussion, the reader should remain cognizant of the fact that MX can form either

MO or M and that both of these species can be destroyed through the formation of MX.

Comparison of Figures 13, 14, and 15 reveals the apparent variation of metallic emission in the fuel-rich Kniseley flame as a function of the dissociation energies of the metal monoxides. Curry (57) points out that the degree of enhancement due to the fuel-rich phenomenon seems to increase with increasing monoxide dissociation energies. If this is true and if the processes involved in the phenomenon are indeed exclusive properties of the interconal zone, then there should be a corresponding tendency for the fuel-rich phenomenon to be exhibited only in the intercone as metals having higher monoxide dissociation energies are studied. The three figures reveal that this is the case. Lanthanum, having the highest D_o, (see Table 9) produces line emission only in the intercone while gadolinium, having a moderate D_o, shows line emission in all three zones with the interconal zone providing the major portions. Chromium has a D_o sufficiently low that CrO will be easily dissociated by the flame. Chromium line emission shows no zone dependency. It should be noted, in comparing Figures 13, 14, and 15, that the photocurrent scale is not the same for all three zones. Comparison of the monoxide band emission

is difficult, since the flame background in the primary reaction zone does not permit a valid estimation of the intensities. However, it does not appear that the line emission, in the interconal zone, is provided at the expense of the monoxide band emission.

The vertical profiles of the line emission of four elements are shown in Figure 17. Comparison of these profiles reveal that the three elements having monoxide dissociation energies in excess of about 6 eV (Table 9) show similar behavior while chromium, having a relatively low D_o, shows an apparently unrelated behavior. There appears to be a tendency for the maximum emission to occur higher in the flame as a function of higher D_o. Thus, Cr exhibits its maximum emission at 6 millimeters while V, Sc, and La produce their maximum emission at 7, 7 and 8 millimeters respectively. There also seems to be some tendency for the emission profile to be broader with decreasing D_o. Thus, La shows a more localized emission profile than does Sc, etc.

Since chromium was not profiled under optimum conditions, there was a question as to whether or not the spatial variation in emission was being altered significantly by the fuel-ratio. Consequently, a second chromium profile was made

using a leaner flame which provided optimum chromium emission. The result (Figure 28) shows that only minor variations occur. Since these can be explained on the basis of a higher temperature for the leaner flame and changes in the flame shape, the chromium data shown in Figure 17 was considered to be adequate for qualitative comparisons.

Vertical profiles ScO and LaO are also shown in Figure 17. Like OH, these two species show a definite dip in their emission profiles just above the tip of the primary reaction zone. The point at which this dip occurs seems to vary as a function of the dissociation energy of the molecule. Apparently, the greater the dissociation energy, the higher in the flame will the dip occur. Further, the maximum line emission for both La and Sc occurs at the same point in the flame as does the dip for the corresponding monoxide profile. This last observation seems to point directly to a process whereby free atoms are produced by reduction of the monoxide. This conclusion does not agree with the results of the long scan study. However, since better spatial resolution was employed in this second phase of the study more value can be put on the profile data.

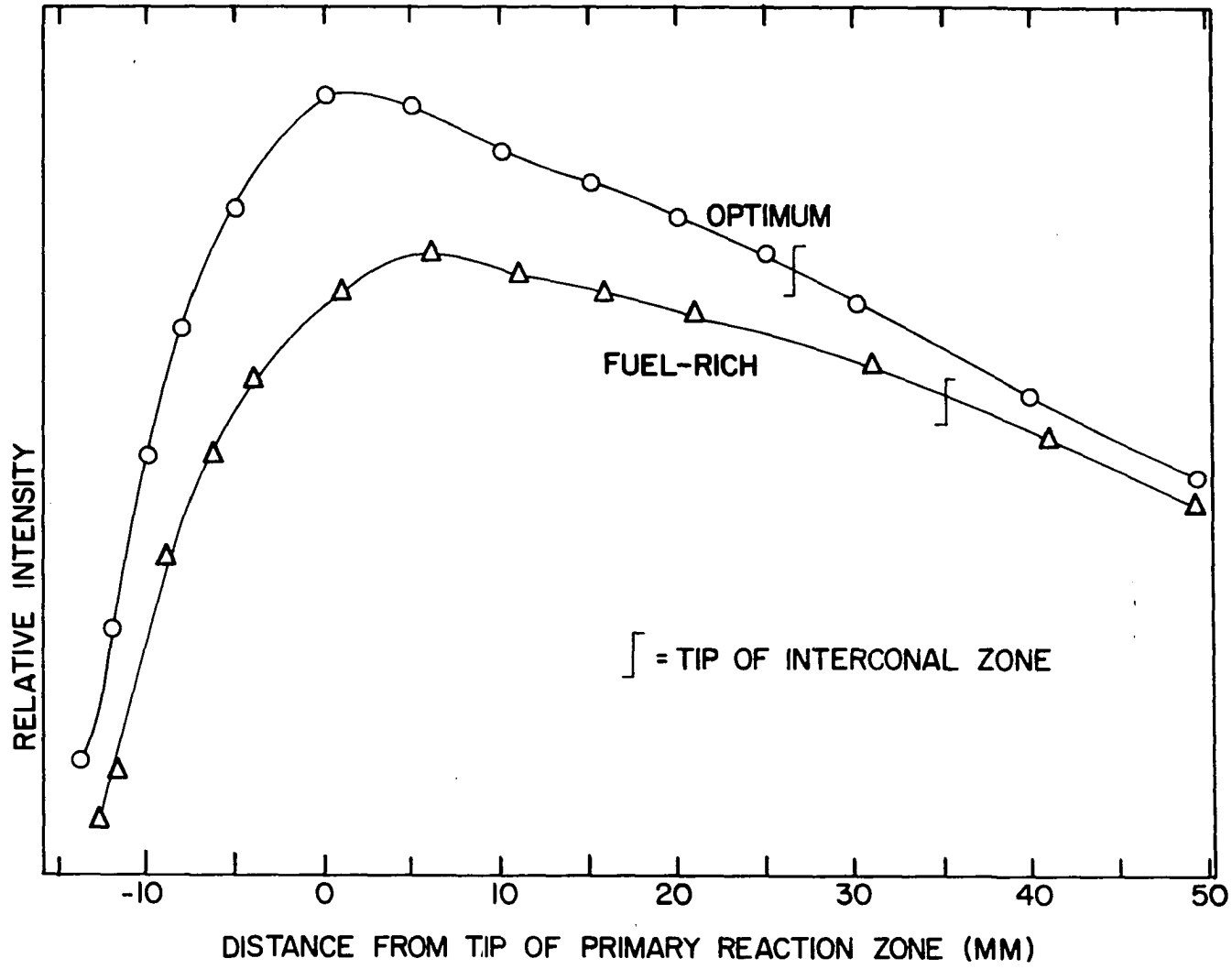

Figure 28. Vertical emission profiles of CN (3883 Å) at two different fuel-ratios

The horizontal profiles (Figure 19) show two features that should be mentioned. First, the tendency for metal emission to become localized as a function of increasing monoxide dissociation energy is again seen in the fact that the lanthanum profiles are more narrow than those of either chromium or vanadium. Second, the horizontal profiles of LaO clearly show a winging effect in the interconal zone. This observation is foreshadowed by the dip seen in the vertical profile of LaO and the analogous experience with OH.

In order to gain an insight into the fuel-rich phenomenon, it is now necessary to explain the observed behavior of the metallic species with respect to the conclusions drawn from the study of the natural flame species. Obviously, the prerequisite to atomic emission is the production of free atoms. Therefore, this discussion will be directed toward explaining how the fuel-rich flame may produce free atoms. Again the reader is cautioned that while MO is specifically discussed, similar arguments apply to MX type specie.

Free atoms are most directly obtained as a product of the decomposition of the aerosol. The flame should form some free atoms of most metals in this manner. However, in order for an appreciable amount of free atoms to be formed, the

dissociation energies of the various possible molecular forms of the metal must be lower than the energy available in the flame.

Numerous elements possess monoxide dissociation energies sufficiently low that the flame energy will prevent the formation of a stable monoxide molecule. These elements are represented in this study by chromium. The explosion of aerosol droplets containing chromium will result in a high percentage of chromium atoms and relatively few CrO or CrX molecules. The fuel-rich flame therefore does little to increase the chromium free atom concentration and in fact hinders optimum chromium emission by possessing a lower flame temperature than does a leaner flame. The fact that the fuel-rich flame is not particularly useful in enhancing chromium emission is further demonstrated by the lack of any zone dependency. Chromium shows substantial line emission in both the interconal zone and the secondary reaction zone.

The elements that possess monoxide dissociation above the available energy of the flame cannot produce free atoms by such a direct route as chromium. These elements are represented by lanthanum. The explosion of an aerosol droplet containing lanthanum will tend to produce largely LaO and LaX.

Free lanthanum may form but only in low concentration. Thus, in the absence of some further process no lanthanum line emission would result. From the profile data of lanthanum, it is obvious that the interconal zone does provide some other mechanisms. At least two, based on the reducing character of the interconal zone, are possible.

The first is a reduction of the monoxide by the carbon containing species whereby carbon enters into competition, with the metal, for the oxygen and forces reactions of the form

$$MO + C \rightarrow CO + M \qquad (dd)$$

toward the right thereby providing free atoms. The success of this process depends upon a sufficiently high concentration of carbon or carbon containing species. While data on carbon itself was not obtained in this study the profiles of other carbon containing species indicate that the interconal zone is capable of supporting such a mechanism. The exact point in the interconal zone where the maximum extent of monoxide reduction occurs varies from one element to the next. Thus, the ScO profiles show a minimum slightly lower in the intercone than does LaO. This is because ScO, having a lower monoxide

dissociation energy than LaO, is more easily reduced. Once the free atoms are formed, the excitation process is essentially thermal. Free atoms, that are produced through monoxide reduction, will be destroyed when they encounter a sufficient oxygen concentration. This oxygen is provided by air diffusion. The rate of disappearance of free atoms will depend, again, upon the monoxide dissociation energies as well as the rate of oxidation of the carbon species. Elements such as lanthanum, will reform monoxides in the presence of higher carbon concentrations than will elements having lower monoxide dissociation energies. Thus, the La metal emission will cease lower in the flame than will emission from Sc and V.

The second mechanism makes use of the fact that the interconal zone is a region containing little oxygen. Thus, the equilibrium between the metal monoxide and free metal

$$MO \rightleftarrows M + O \qquad \text{(ee)}$$

is shifted far to the right. Gilbert (117, p. 205) has done some simple calculations on such equilibria and concluded that extensive dissociation will occur for any monoxide not having a dissociation energy in excess of 8.0-8.5 eV. Thus, most metal monoxides will provide free metal atoms in the

fuel-rich flame. As was the case with the chemical reduction mechanism, the exact point in the flame where the greatest production of free atoms occurs depends upon the specific monoxide molecule with a more stable monoxide producing a maximum higher in the flame.

There is little doubt that the temperature of the oxy-acetylene flame aids in shifting the above equilibrium since the fuel-rich air-acetylene flame, which is cooler, does not show the same degree of enhancement. However, the possibility of higher temperature alone being responsible for an increase in free atom production is doubtful from two standpoints. First, for many monoxides the temperature of the oxyacetylene flame is not high enough to cause extensive dissociation. Second, the enhancement in emission for elements such as lanthanum is not seen in the hotter, stoichiometric oxy-acetylene flame.

From the data presented in this work, it is not possible to determine which of the two processes leading to free atoms dominates. Doubtless, both occur to some extent. This work provides ample evidence for a deficiency of oxygen in the interconal zone and thus support for the monoxide dissociation mechanism. In the absence of data on carbon, support for the

reduction mechanism is less substantial. However, the presence of considerable quantities of other carbon species makes the absence of atomic carbon unlikely.

As mentioned previously, one of the problems encountered with emission profiles is that emission is subject to temperature variation. Thus, from the emission profiles one cannot tell whether the free atoms are formed in the primary reaction zone and kept from reforming MO or if the free atoms are actually formed by one or both of the above processes acting in the interconal zone. The atomic absorption profiles (Figure 20) provide the answer. As is easily seen both the emission and absorption profiles, for a given element, show the same relative shape. Therefore, it can be concluded that the emission profiles are direct indications of variation in the concentration of metal atoms. Two other important conclusions can be formed through comparison of the emission and absorption profiles. The first is that, for the metals studied, chemiluminescence effects are negligible. Second, since the temperature dependent emission profile and the temperature independent absorption profile show the same rates of increase and decrease, for a given element, the temperature variation through the interconal zone must be quite small.

The results of the profile study with respect to the formation of free atoms may be summarized as follows. Metals will provide free atoms in flames as a function of existence of stable molecules of the metal. For some elements the thermal energy of the flame is sufficient to effectively inhibit compound formation while for other metals the flame must provide an environment conducive to the destruction of the metallic compounds. In a fuel-rich oxyacetylene flame, metals which form stable monoxides, or other stable compounds, will provide free atoms through a reduction of the monoxide or a favorable shift in the dissociation equilibrium in the carbon rich interconal zone. For a given element the extent of free atom production, the flame position at which maximum production occurs, and the rate at which the monoxide reforms are governed by the monoxide dissociation energy. Here again the monoxide is being used as an illustration. The various species of MX also provide free atoms in accordance with stability considerations. Metals that do not require the fuel-rich phenomenon will form free atoms in the primary reaction zone and will emit in accordance with the temperature gradients in the flame. Obviously, many metals will possess monoxide dissociation energies such that some free atoms will

be formed when the aerosol decomposes and some will be formed by reduction of the monoxide in the interconal zone. The degree to which the emission of such elements is aided by the fuel-rich phenomenon depends upon the extent of free atom production in the interconal zone. Upon production of free atoms normal thermal excitation will occur in most cases. The fact that some metals emit via chemiluminescence has been well established (117) and it cannot be said that there is no metallic chemiluminescence in the fuel-rich flame. However, to date there has been no evidence to indicate that the enhancements found in the fuel-rich flame are due to chemiluminescence.

IV. THE EFFECTS OF NITROGEN AND ETHANOL

A. Introduction

Analytical flame spectroscopy necessitates the addition of materials to the flame. Commonly, there are two types of additives that must be considered, gases and solutions. Solution type additives can be broken down into solvents, anions and cations. Cation additives are generally either the metals being analyzed or other metal species. In addition to interacting with the flame to produce atomic emission, cations can yield continuous radiation through ion recombination (118, 119). The effects of anions have been discussed in some detail by Dean (20, p. 105), Herrmann and Alkemade (1, p. 66), and Mavrodineanu (68, p. 166). By and large, anion effects are produced from interactions with cations rather than interactions with the flame. Anion-cation interactions and cation-cation interactions are the principal concern in the study of interferences in flames. Since this work did not encompass interference effects, attempts were made to maintain consistency by always using perchlorate salts to provide both the cation and anion.

In analytical studies the largest constituent of the solution is of course the solvent. One would naturally suspect that the solvent would play a major role in altering the natural flame processes and as a consequence there have been a considerable number of studies of the effects of solvents (48, 59, 61, 120-126). The overall conclusion that can be drawn from these studies is that solvents affect flame analysis in two ways, by altering the flame itself and by altering the nebulization characteristics of the system. In recent years the use of organic solvents has become widespread (20, p. 51-64). Gilbert (19) lists 20 organic solvents which have found application in analytical situations. The attraction of organic solvents is an enhancement in emission. A number of reasons for the enhancement have been suggested. These are: increased flame size (126); smaller aerosol particle size (127, 128); increased aspiration rates (20, p. 59); higher heats of combustion (20, p. 59); and removal of the cooling effects of water (129). All of these processes may contribute to the enhancement, however, it is doubtful that they all contribute to the same extent in every system. A possible relationship between enhancement from organic solvents and the fuel-rich phenomenon will be discussed subsequently.

The principal gas additive in flames is air. Air enters most flames, via diffusion from the surrounding atmosphere. The oxygen content of the air alters the stoichiometry of the combustible gases while the atmospheric nitrogen tends to dilute the flame gases. The presence of nitrogen, as a diluent, produces a number of changes in the properties of the flame gases. Qualitatively, the principal effects can be determined by comparing the properties of the oxyacetylene flame with the air-acetylene flame. Thus, nitrogen tends to: raise the ignition temperature; lower the burning velocity; decreases the limits of inflamability; and lower the flame temperature (62).

In the Kniseley flame, as used for this study, the two principal additives are nitrogen and ethanol. Ethanol is introduced to the flame system through the Beckman burner which provides the aerosol droplets. The droplets are carried into the flame by the premixed gases. However, visual observation of the Kniseley burner in operation indicates that not all of the alcohol enters the flame. A considerable quantity floods over the premixing tube and presumably some ethanol flows back down on the inside of the tube. While the overflow of ethanol prevents backflash, by cooling the tip of the

premixing tube, the loss of solution presents a problem in determining the exact amount of solution actually reaching the flame. Consequently, an important part of the study of the effect of ethanol was to devise a means of measuring the rate at which solution reaches the flame.

The second additive, nitrogen, gains entrance to the flame in three ways. The first, air diffusion, introduces atmospheric nitrogen to the flame after ignition has occurred. Air diffusion is a particularly important source of both oxygen and nitrogen in the upper portions of the flame. The second, air entrainment, provides nitrogen through the ports at the base of the premixing channel. Air entering through these ports becomes an integral part of the premixed gases prior to the combustion process. Since oxygen entering the flame prior to ignition alters the initial stoichiometry of the flame gases, a means of measuring such oxygen had to be devised. Obviously, the measurement of entrained oxygen also provides measurement of the entrained nitrogen. Finally, nitrogen may be introduced as an impurity in the oxygen.

The most important flame parameter is the temperature (20, p. 16). Temperature is of fundamental importance because of its direct relationship to the emission of atomic radiation.

Other flame parameters affect the production of atomic lines by either changing the flame temperature or by affecting the production of free atoms. Consequently, a study of additives must include the measurement of temperature if meaningful results are to be obtained. Unfortunately, there are some serious problems involved in the determination of flame temperatures.

The theory and methodology of flame temperature measurements have been discussed in some detail by Gaydon and Wolfhard (36, p. 234-301) and Mavrodineanu (62, 68, p. 513-532). From a thermodynamic standpoint, the term temperature has physical significance only for those systems that are in thermal equilibrium. Thus, we must first examine the possibility of thermal equilibrium in the Kniseley flame. Petrie (130) states that thermal equilibrium exists in an assemblage of atoms, ions, and molecules if both radiational and collisional equilibria are obtained. Since radiative equilibrium implies that the energy levels are populated by absorption and depopulated by emission at the same rate, no spectral lines can result from a source in radiative equilibrium. Obviously, radiative equilibrium does not exist in the Kniseley flame nor, consequently, can thermal equilibrium.

Thus, temperature, in a true thermodynamic sense, does not exist in the Kniseley flame.

In the absence of the possibility of a thermodynamic temperature the flame spectroscopist must turn to an arbitrary temperature system that will produce temperature values that have physical significance. The assumptions and conditions necessary for the creation of such a system are discussed in considerable detail by Mavrodineanu and Boiteux (68, pp. 495-512). In essence, their approach is to redefine the term "thermal equilibrium" so that radiative equilibrium is not required. Thus, the achievement of collisional equilibrium will permit the measurement of a "flame temperature" that will closely approximate a thermodynamic temperature. The lack of collisional equilibrium in the primary reaction zone has been well established (36, pp. 228-230). However, the arguments of Mavrodineanu and Boiteux (68, p. 509) justify the assumption that collisional equilibrium exists in all parts of the flame except the primary reaction zone and the region lying within a few millimeters of the primary reaction zone.

With acceptance of the possibility of determining a meaningful temperature, in at least parts of the flame, attention must be turned toward the selection of a method

for doing so. In general, there are three types of temperature measurements: rotational temperature measurements; line reversal measurements; and electronic temperature measurements. The literature reveals several studies of rotational flame temperatures (88, 131-133), however, the method did not seem suitable for the Kniseley flame because no molecular species was found that exhibited emission in all three flame zones. Line reversal methods are apparently the most popular temperature measuring techniques. Gaydon and Wolfhard (36), Gaydon (74) and Penner (134) all describe the method in detail. The method is based on the direct application of Kirchhoff's law. Continuous radiation is allowed to pass through a flame containing an emitting metal vapor. Metal lines will appear either in emission or absorption depending upon whether the flame temperature is greater or less than the brightness temperature of the primary source. Variation of the intensity of the continuum to the point where the metal line appears in neither emission or absorption establishes the condition wherein both the flame and source temperatures are equal. Measurement of the brightness temperature of the primary source, via optical pyrometry, permits calculation of the flame temperature. Attempts were made to make reversal

measurements on the Kniseley flame but these attempts were not successful. The principal problem was that the tungsten lamps, employed as primary sources, would burn out before the reversal point was reached. Thus, electronic temperature measurements became the "method of choice" for determining temperature variation in the Kniseley flame.

Electronic temperature measurements are based on the equation,

$$I_{nm} = C\, g_n\, A_{nm}\, \nu_{nm}\, e^{-E_n/kT} \qquad (A)$$

when I_{nm} is the emission intensity of a transition from state n to m, A_{nm} is the Einstein coefficient for spontaneous emission, g_n is the statistical weight of the upper state (n), ν_{nm} is the frequency of the transition, E_n is the excitation energy, and k is the Boltzman constant. C is the constant for a particular system and is difficult to determine. Consequently, C is removed from the expression by considering the relative intensities of two spectral lines such that

$$\frac{I_1}{I_2} = \frac{g_1 A_1 \nu_1}{g_2 A_2 \nu_2}\, e^{\frac{-(E_1-E_2)}{kT}} \qquad (B)$$

The above expression is valid for the transitions in any element, but Broida and Shuler (135) have presented a good case for the use of iron lines for making temperature determinations. Consequently, iron was the element selected for making temperature determinations on the Kniseley flame. Since the values for E, g, A, and ν are tabulated for most of the lines of iron, measurement of the intensity ratio between two lines permits the direct calculation of temperature via expression B.

The temperature values, obtained with the two-line method, must be evaluated in the light of several complications. First, a thermal gradient exists across any horizontal cross section of the flame. Thus, a temperature based on emission from the entire depth of a cross section will represent an average rather than a unique flame temperature. Second, the direct application of equation B requires that the intensities of the two lines used are not affected by such processes as self-absorption or chemiluminescence. While some care went into the selection of a line pair, there are no guarantees that the observed intensity variation is solely a function of temperature. Third, the temperature value, as computed from equation B, is highly dependent upon the literature

values for gA_{ij}. Unfortunately, there is considerable disagreement among the various references as to the numerical value of these terms. Table 10 shows the changes produced in the calculated temperature due to differences in the selected gA_{ij} value. As is easily seen, error due merely to an unfortunate choice of gA_{ij} values can be quite severe. Finally, there is a question as to how reproducible temperature measurements must be to retain a sufficient degree of physical significance. Throughout this work, replicate temperature determinations produced variations of about 50°K. This represents an error of about 2%. On the surface this seems like good agreement. However, from the standpoint of utility, the intensity variation produced by a 2% change in temperature should be examined. Table 11 is an attempt to do this. The percent intensity variation due to a 2% temperature change, at both 2,000°K and 3,000°K, is shown for several iron lines. Obviously the intensity variations are too large to be reasonably ascribed to experimental error. Thus, it must be concluded that temperature determinations will have to be more reproducible than 2% before their use in a quantitative fashion will be warranted.

Table 10. Temperature values calculated for three line pairs with three sets of gA_{ν} values. Intensity ratio arbitrarily selected to place value in range of flame temperatures

Fe line pair (Å)	Arbitrary intensity ratio	Temperature calculated using gA_{ν} values of NBS[a] (°K)	CW[b] (°K)	DC[c] (°K)
$\frac{3705.57\ Å}{3709.25\ Å}$	6.22	2583	2620	2647
$\frac{3748.26\ Å}{3749.49\ Å}$	1.618	2768	2685	2649
$\frac{3734.87\ Å}{3737.13\ Å}$	3.060	2531	2671	2625

[a]Source: (136).
[b]Source: (137).
[c]Source: (138).

Table 11. Variation in calculated[a] relative intensity as a result of a 2% change in temperature at both 3000 K° and 2000 K°

Fe line (Å)	Relative intensity at 3000°K	Relative intensity at 3060°K	Variation produced by 2% change in temperature at 3000°K	Relative intensity at 2000°K	Relative intensity at 2040°K	Variation produced by 2% change in temperature at 2000°K
3440.61	0.095	0.124	30.6	0.00010	0.00016	60.0
3709.25	0.0055	0.0077	20.0	0.0000015	0.0000024	60.0
3737.13	0.089	0.114	28.1	0.00013	0.00019	46.1
3748.26	0.035	0.045	28.6	0.000046	0.000069	50.0
3930.30	0.025	0.032	28.0	0.000047	0.000068	44.7

[a]Source of gA_{ν} values: (136).

Since the temperature determinations made on the Kniseley burner were no more precise than 2% and since there was reason to question their accuracy, the quantitative use of the temperature values was not attempted. However, it was felt that the values obtained had at least qualitative merit and that their use as an indication of temperature changes in the flame was fully justified.

B. Experimental

The work described in this section consists of a number of studies, each of which required a slightly different experimental arrangement. Those components and parameters that remained unchanged throughout this section are listed in Table 12.

Figure 29 shows, schematically, the arrangement used to add varying proportions of gas to the flame. The fuel and primary oxidant supply were monitored by flow meters B and A respectively. The arrangement of the other three flow meters varied somewhat from one experiment to another depending on which burner was employed. When the sleeved Kniseley burner (Figure 6) was used the auxiliary gas supply was connected to the burner through the single port in the sleeve.

Table 12. Experimental conditions which remained constant

Component	Description
Monochromator	1.0 meter Czerny-Turner
Slits	0.025 mm for both entrance and exit slits; entrance slit diaphragmed to 1, 2, or 5 mm depending on experiment.
Detector	EMI 6255B photomultiplier. Applied voltage 1250 volts.
Amplifier	Leeds and Northrup 9836-B micro-microammeter.
Amplifier gain	Variable, adjusted to provide the most convenient scale for each experiment.
Recorder	Leeds and Northrup Speedomax G, Model S millivolt recorder.
Infusion pump	Infusion/Withdrawal Pump, Model 600-900, Harvard Apparatus Co., Inc.
Scan Rate	5 Å/min; except for scans of total region 3000-6000 Å for which a 125 Å/min scan rate was employed.
Solutions	Concentration varied depending on experiment; all solutions made with ethanol as solvent.

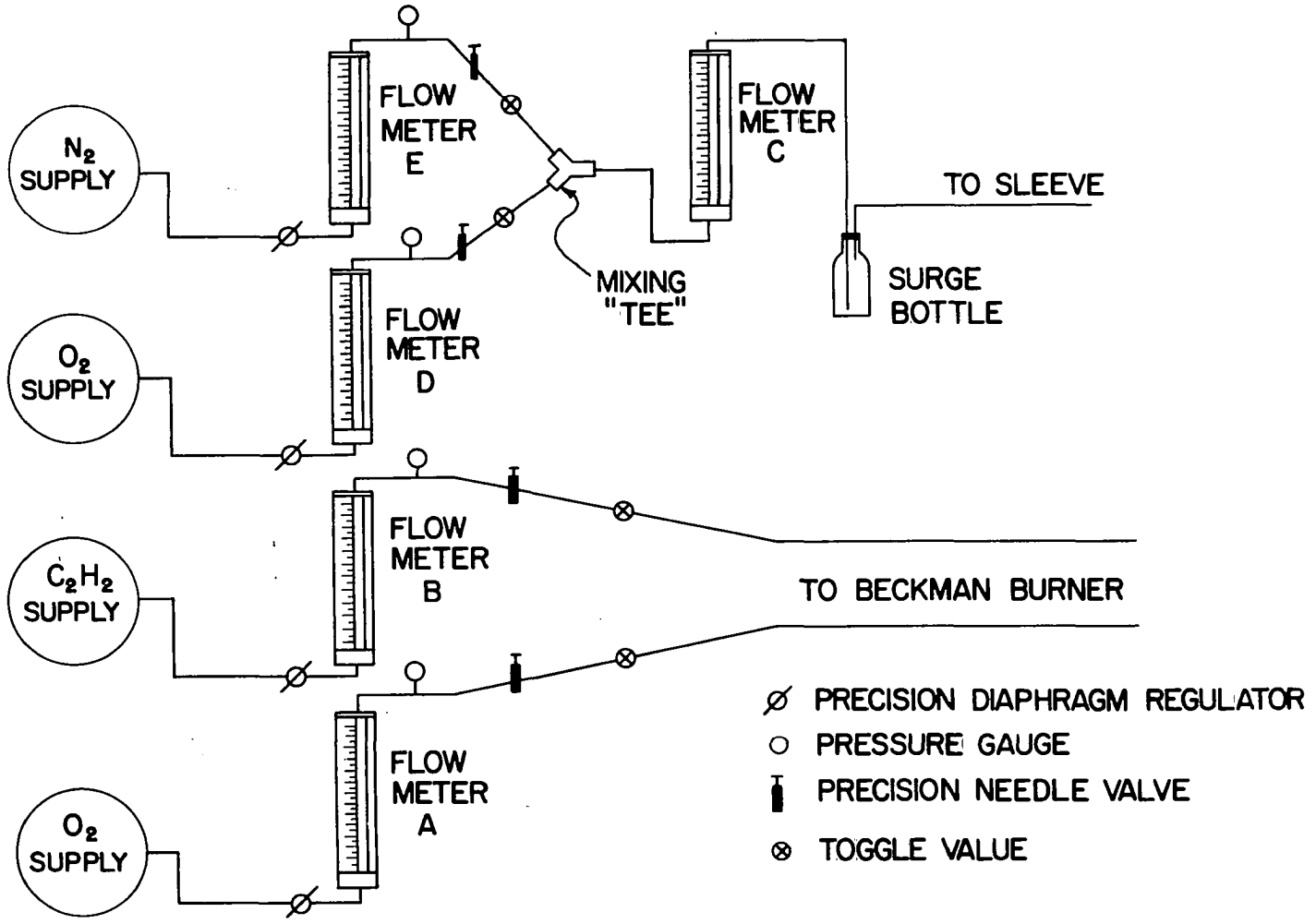

Figure 29. Schematic diagram of gas delivery system

A surge bottle was placed between flow meter C and the burner to smooth out any fluctuations in the auxiliary gas stream. In the absence of this bottle the flame tended to become unstable. A mixture of oxygen and nitrogen was formed in the mixing-"tee" with the relative proportions of each gas being monitored by flow meters D and E. Flow meter C monitored the total flow of the auxiliary gas. When the tapered chimney boron nitride burner (Figure 7) was employed the system was altered. The fuel and oxidant were admitted to the Beckman burner as before. However, flow meters D and E were not necessary since the auxiliary gas was monitored directly by meter C and all of the oxygen added through the Beckman burner. The auxiliary gas was admitted to the tapered chimney type burner by inserting four #18 surgical needles through the holes provided for this purpose. The needles were connected to the surge bottle with Tygon tubing. Thus, the surge bottle provided both uniform gas flow and a manifold for dividing the gas stream.

Meter C was also employed to measure the volume of air that was naturally drawn into the flame through the ports at the base of the premixing channel. The system shown in Figure 29 was opened to the atmosphere between the mixing chamber

and meter C. Thus air drawn into the flame would first be drawn through meter C. Calibration of meter C, with air, was accomplished by using a wet-test meter. Since the calibration is performed by forcing air through the flow meter, while the determination is made by drawing the air through, there is some question as to whether a given reading on the flow meter reflects the same volume flow in both cases. The possible error in flow rate was checked, by measuring the pressure drop across the rotameter with a differential manometer. The drop was found to be about 2 millimeters of mercury. Variation in volume measurement due to such a small pressure drop is well within the limits of experimental error.

The variation in detection limits as a function of the volume of nitrogen internally introduced into the flame by the burner was studied for the elements La, V, U, Ce, and Lu. A sleeved Kniseley burner was employed with a boron nitride premixing channel (Figure 5). The study covered the range 8 to 33 volume percent nitrogen in the total gas flow. The range was limited by the burner. At nitrogen contents under about 8% the burner tip became overheated. The upper limit, 33%, occurred when only nitrogen was introduced through the sleeve. The total gas flow through the sleeve was maintained

constant for all volumes of nitrogen. Thus, the oxygen flow through the sleeve varied from one nitrogen flow to the next. The flame stoichiometry was adjusted for each nitrogen flow setting by varying the acetylene flow until optimum line emission occurred.

A more detailed study was made of the effect of nitrogen on the detection limit of lanthanum. For this study, the tapered chimney type burner was used. The burner was operated within the range from no nitrogen addition to an upper limit of 33% (by volume). The oxygen and acetylene flows were maintained constant throughout the work. Thus, the total gas flow increased as the nitrogen content increased. Since the nebulization characteristics of the burner changed with varying total gas flow, an infusion pump was employed to keep the rate of sample introduction constant. Three parameters were measured for each setting of the nitrogen flow. These were the lanthanum line height, the noise level, and the background level.

The same experimental system was used to determine the effect of replacing the nitrogen with either helium or argon. For each of the three gases, scans were made, from 3000 Å to 6000 Å, of the emission from the interconal zone. In addition

detection limits were obtained for the metals, Cr, V, and La with each of the gases. The change in the apparent flame temperature produced by the addition of each of the gases was also determined.

Measurement of the volume of sample solution reaching the flame was accomplished through the following method. An ethanolic solution containing 1000 μg/ml of strontium was prepared. This solution was nebulized into the Kniseley burner in the normal way. A 5 ml beaker that had been filled with glass-wool was inverted a few millimeters above the burner tip. In this way the emergent stream of aerosol was completely trapped in the glass wool. The strontium was leached from the glass wool with alcohol and the resulting solution diluted to 100 ml. The strontium concentration was then determined by flame analysis.

The analytical method was carefully checked to insure that the results obtained were accurate. A series of studies revealed that the results were not dependent upon the trapping time. However, trapping times of 2 to 10 minutes were found to be the most desirable. Below 2 minutes the concentration of the solutions were low and resulted in large relative errors while trapping times above 10 minutes were

unnecessarily long. The leaching procedure was also checked and found to be essentially complete after 20 ml of alcohol had been passed through the glass wool.

In a number of experiments, sample was introduced into the burner with the aid of an infusion pump. Curves were constructed that related the volume of sample reaching the flame to the infusion rate. From these curves and a series of solutions containing varying concentrations of lanthanum, an experiment was designed that provided for the introduction into the flame of varying volumes of alcohol but the same number of lanthanum atoms. Thus, the effect of the alcohol upon lanthanum emission could be studied. During the same experiment, the emission of LaO, C_2, CN, and OH as a function of the alcohol concentration was also studied. Apparent temperature measurements were made as a function of the alcohol content of the flame.

C. Results and Discussion

The determination of the rate at which air entered the burner through the air-ports produced some surprising results. The total volume entrained is considerably in excess of what might be expected. A typical set of flow rates would be:

O_2 flow, 4.52 l/min; C_2H_2 flow, 5.69 l/min; and air flow, 4.07 l/min. Thus, air entrainment accounts for about 28 percent of the total gas volume rising through the premixing channel. Since air is about 80 percent nitrogen (by volume), the nitrogen content of the premixed gases then is about 21 percent (by volume) of the total flow. Consequently, nitrogen must be expected to significantly alter such flame parameters as temperature, burning velocity and ignition temperature. The inability to operate the Kniseley burner in the absence of the air holes may now be explained on the basis of the removal of the 21 percent nitrogen from the premixed gases. The resulting increase in burning velocity coupled with a lower ignition temperature will tend to cause flash-back. The oxygen entering the flame due to air entrainment is also of significance. The principal effect will be to change the stoichiometry. Thus, the calculated fuel-ratio, for the above gas flows, will be 0.79 or 0.98 depending upon whether or not the entrained oxygen is taken into account.

Of the several factors which influence the rate at which air is entrained through the lower ports, the most marked is the rapid decrease in entrainment with increasing acetylene flow. The magnitude of this effect can be seen in Figure 30.

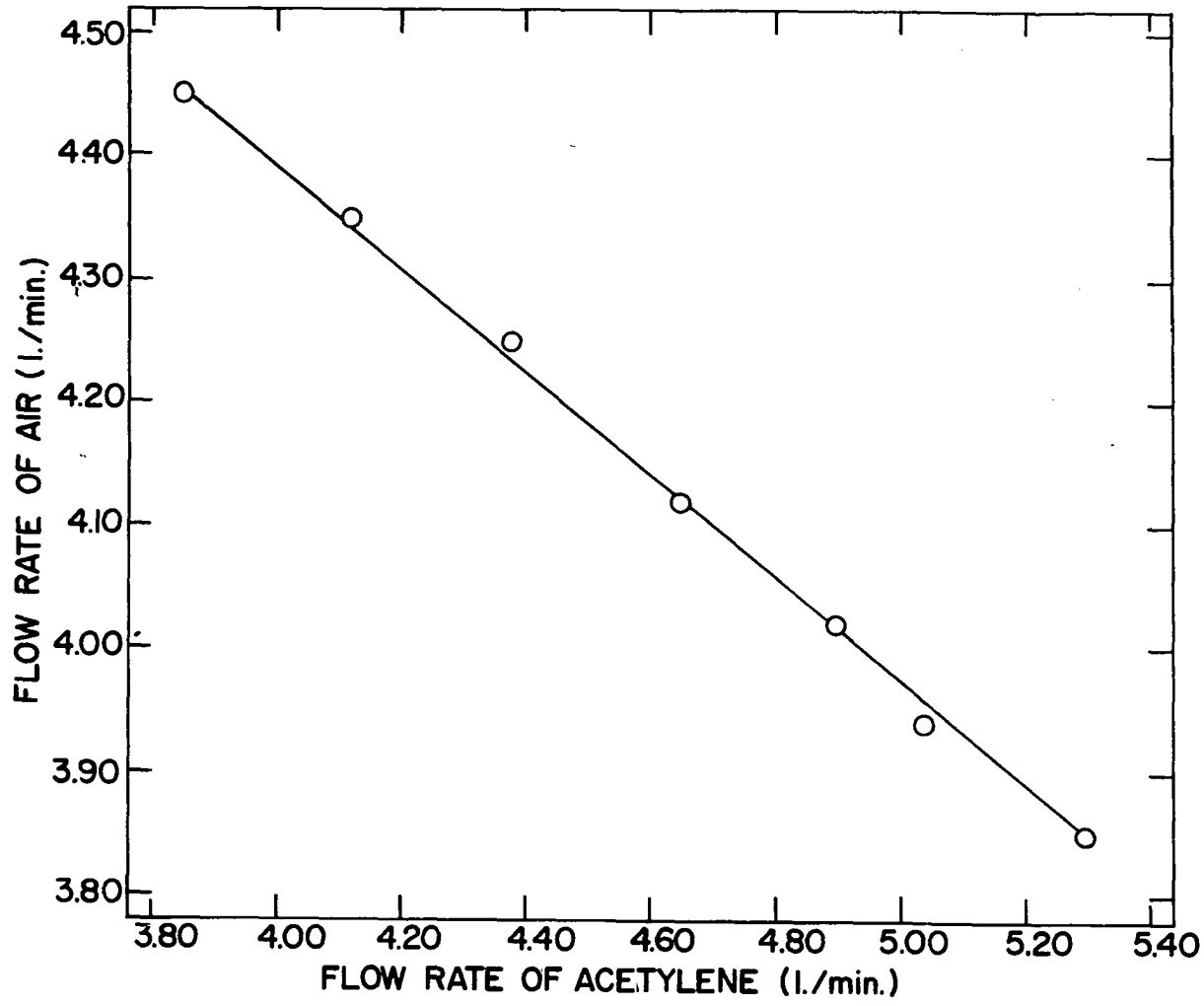

Figure 30. Effect of acetylene flow on the rate at which air enters the lower ports of the Kniseley burner

Decreased oxygen flow also produces a decrease in the entrainment rate. However, since in most studies the oxygen flow is maintained constant the variation produced by oxygen is not significant. Changes in geometrical factors, such as the clearance between the tip of the Beckman burner and the base of the premixing channel, the diameter of the premixing channel, and the taper leading into the premixing channel will also alter the entrainment. Further, since the flow characteristics of each Beckman burner are different, wide variation in entrainment rate will be produced if one Beckman burner is substituted for another.

The entrainment rate is dependent to a large extent upon the Venturi effect produced by the oxygen exiting the Beckman burner. Thus, the decrease in entrainment due to acetylene flow can be attributed to the acetylene flow shielding the air from a region of reduced pressure. At higher acetylene flows the shielding is more effective and the entrainment rate reduced.

Unfortunately, the entrainment rate cannot be predicted a priori for a given burner. Therefore, if knowledge of the volume of air entrained is desired, measurements must be made for each set of conditions and for every burner.

In order to compare different sets of flame conditions, some standard parameter must be selected. Commonly this standard is a value known as the detection limit (1, pp. 255-276, 21, 139-141). The definition and measurement of detection limits have been discussed by Herrmann and Alkemade (1, pp. 255-276). Many of the factors included in the definition of detection limits are related to instrumental parameters. However, if one excludes the influence of instrumental conditions, the detection limit can be defined in terms of the background noise-to-signal ratio as follows

$$\frac{X}{[M]} = \frac{\text{noise variation}}{\text{signal intensity}} \qquad (C)$$

where X is the detection limit and [M] is the concentration of the metal being studied. The value of X varies as a function of [M], therefore the detection limits for a given element should not be compared unless they are determined using the same metal concentration. Further, since the purpose of the detection limit studies was the comparison of flame conditions rather than the establishment of absolute detection limits, the values of X for a given series of conditions were normalized. The values thus obtained are referred to as relative detection limits. For the data in Table 13, the

detection limits were adjusted to the value found at a nitrogen content of 24%.

The determination of the noise level provides the greatest source of error in detection limit measurements. In most cases a subjective estimate of the noise is necessary and frequently the error found in a series of replicate determinations exceeds 20%. This, of course, produces a significant error in the detection limit found. Variation is also produced when different instrumental systems are employed since a portion of the noise arises from the system itself. In addition the signal can vary since different burners will have different gas flow rates and different nebulization rates. For these reasons, variation in detection limit values cannot be considered significant until the changes approach an order of magnitude. For the purposes of this work, variations up to a factor of five were considered insignificant.

Table 13 reveals the fact that changes in the nitrogen content of a flame does not change the detection limit. In no case does the relative detection limit reach a factor of five. Also, there seems to be no trends toward higher or lower values as a function of the nitrogen content. Thus, the scatter seen in the values may be attributed to random variation.

Table 13. Variation in the relative detection limits for La, V, U, Ce, and Lu as a function of the nitrogen content of the premixed gases

Element	Line (Å)	Solution Conc. (μg/ml)	Relative detection limit (μg/ml) at nitrogen (volume %) contents of 10%	19%	24%	29%	33%
La	5791	100	1.74	0.58	1.00	1.18	-
V	4408	2	1.13	2.26	1.00	0.87	0.83
U	5915	100	1.21	0.79	1.00	0.86	1.43
Ce	5697	100	2.49	2.02	1.00	2.81	2.66
Lu	4518	10	1.69	1.10	1.00	1.69	1.82

Since decreased nitrogen content should result in higher temperatures, there should be an increase in the line intensity with decreasing nitrogen content. The increased intensity is observed. This may cause some question as to why a corresponding increase in detection limit is not seen. A study of Figure 31 reveals the reason. Figure 31 shows the variation in the background, noise, and line intensity for lanthanum as a function of the nitrogen content. The expected increase in line emission is seen but accompanying the increase is a similar increase in both the background and the noise levels. Since the noise increases at about the same rate as does the line emission, the ratio of the two remains unchanged. The increase in both background and noise would be expected on the basis of a temperature increase. However, the important factor is the relative rate of increase. For the example shown in Figure 31 the rates are the same and nitrogen does not affect the detection limits. However, since lanthanum shows no line emission in the air-acetylene flame, there must be some region through which the signal decreases faster than does the noise. The change in the slope of the lanthanum curve between 20% and 34% N_2 apparently marks the beginning of this decrease. Presumably, in a region that has

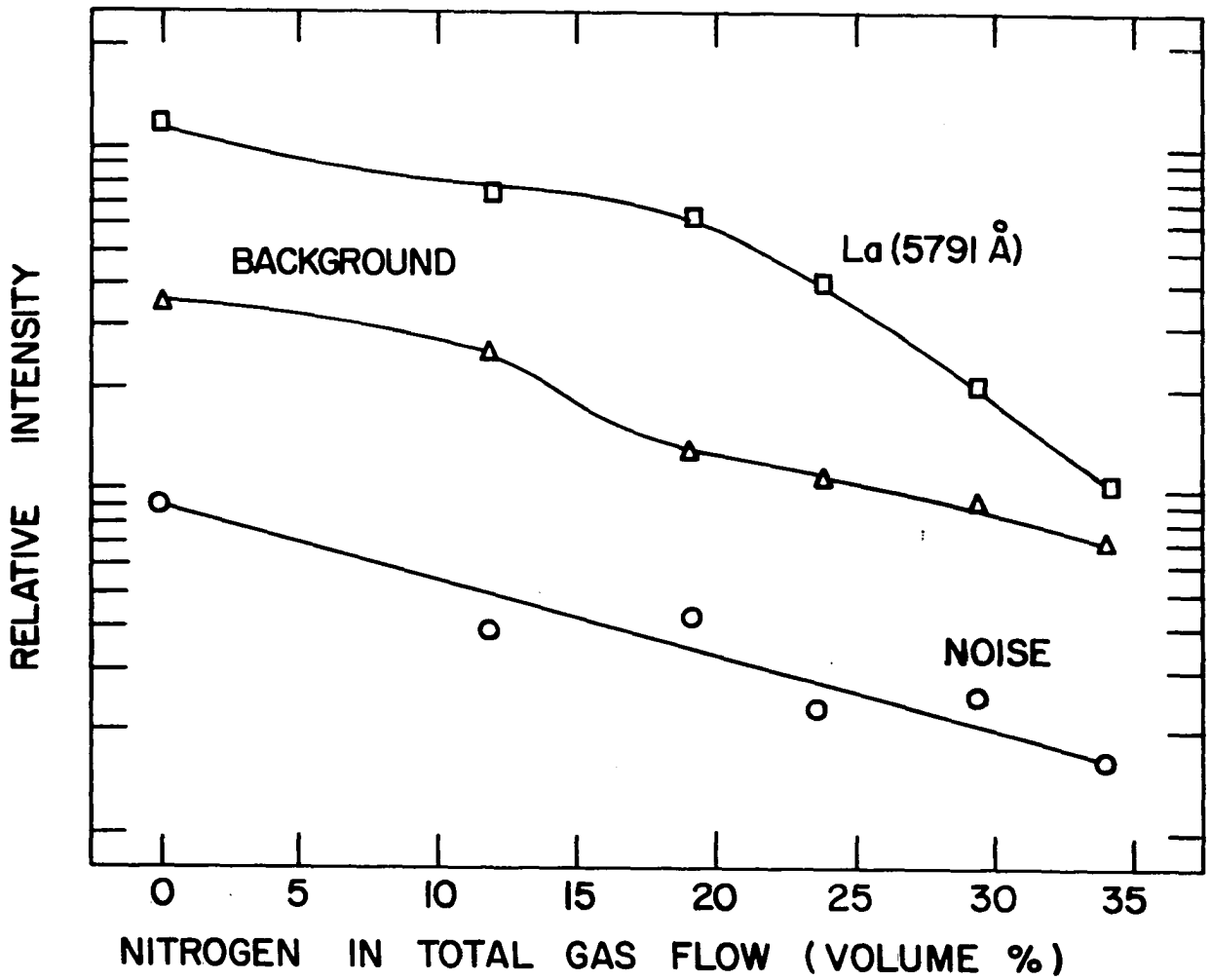

Figure 31. Effect of nitrogen content on the background, noise and La line emission from the interconal zone of a tapered chimney type burner

less background, such as the region between 3100 Å and 4000 Å, some gains could be made by decreasing the nitrogen content. However, gains of at least an order of magnitude would be necessary before the difficulties involved in adapting the burner would be worth the trouble.

The apparent temperature variation as a function of the nitrogen content is shown in Figure 32. The points plotted are average values from four determinations made on four separate days. As discussed previously, the actual temperature values should be ignored. However, the 200 degree temperature decrease found in going from 0 to 34% nitrogen is significant. This change is reflected in the intensity variations shown in Figure 31.

The changes in the background emission from the interconal zone produced when nitrogen is replaced with a monatomic gas are shown in Figure 33. The two monatomic gases used as substitutes were argon and helium. Both of these gases produce more intense background than does nitrogen. The exception is CN which shows considerably more intensity in the flame with nitrogen. This observation is consistent with the conclusion, discussed in the preceding section, that a major portion of the CN is formed from atmospheric nitrogen that is

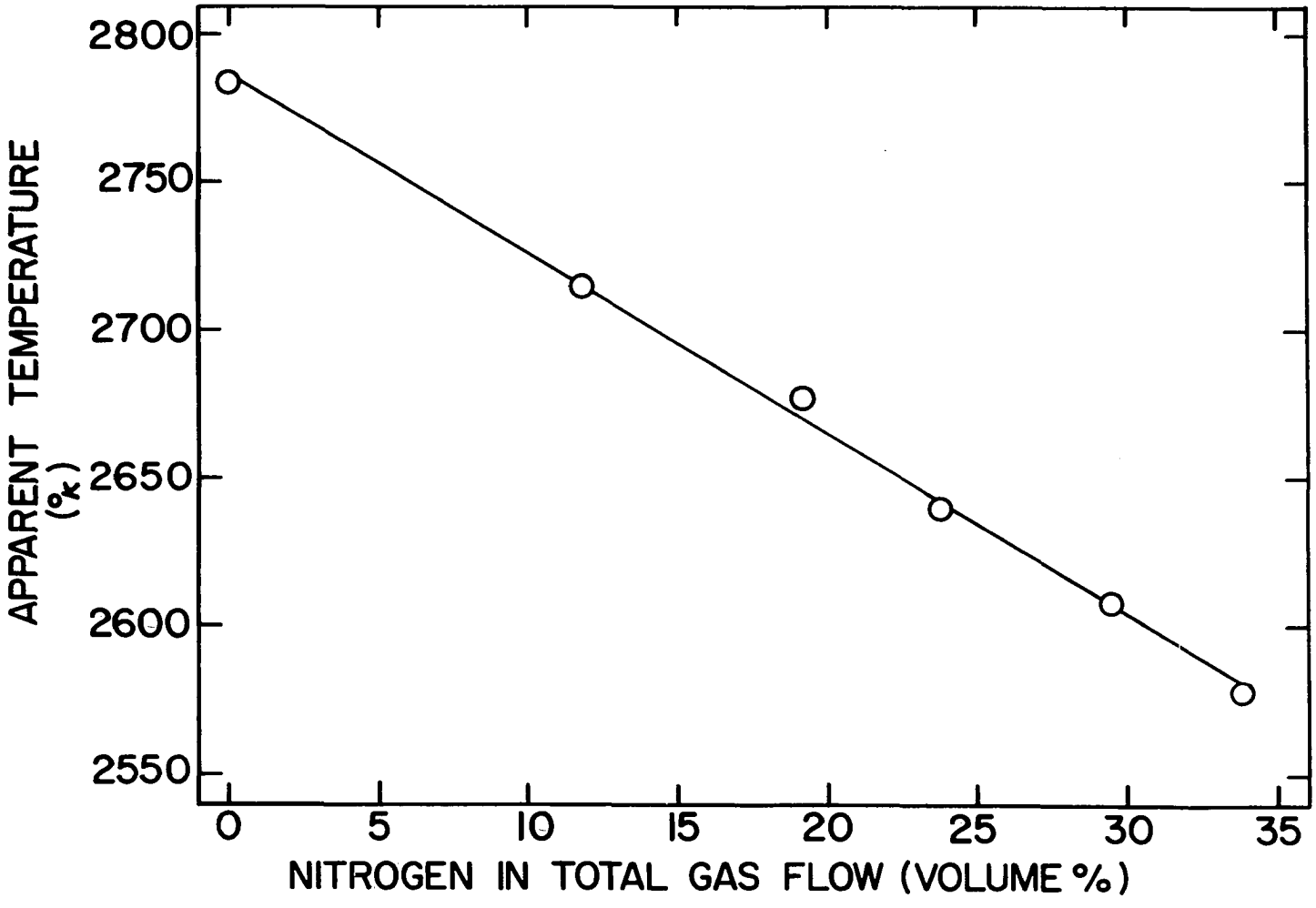

Figure 32. Effect of nitrogen flow through a tapered chimney type burner on the apparent temperature of the interconal zone

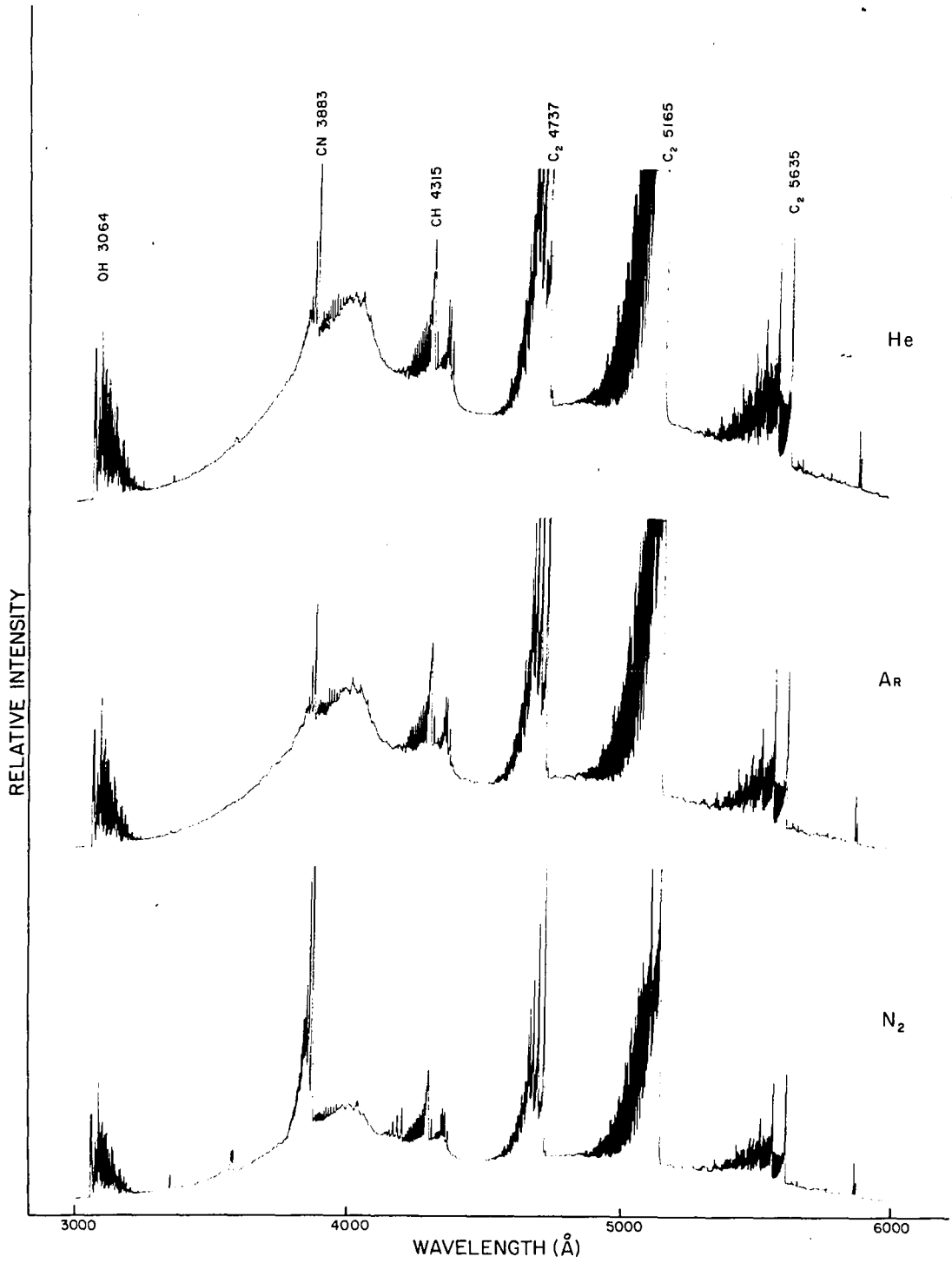

Figure 33. Effect of various diluent gases on the background emission from the interconal zone of the fuel-rich Kniseley flame

drawn through the air ports. When air is excluded from the burner at the air ports, little nitrogen is available to the premixed gases prior to ignition. The CN emission seen with argon and helium must be formed from the nitrogen which enters the flame via the atmospheric diffusion or as an impurity in the oxygen. Thus, the formation of CN observed here is analogous to that observed by Marr (66).

Since the increase in background emission was apparently a temperature phenomenona, the apparent flame temperature was measured for each of the three gases. The results are listed in Table 14. Again, emphasis must be placed on the fact that only the differences between the measured temperatures should be considered significant. The flame shows an increase of 45 degrees when nitrogen is replaced with argon and an increase of 100 degrees when helium is used. The increase experienced when the diatomic N_2 is replaced with a monatomic gas is easily explained. Nitrogen possesses numerous electronic, vibrational, and rotational modes which raise the net heat capacity by partitioning the available energy. The two monatomic gases have no internal modes and since their lowest electronic excited states lie well above the energy available in the flame, the net heat capacities for the two

Table 14. Effect of N_2, Ar, and He on the apparent temperature of the interconal zone of the Kniseley flame

Gas entering burner through air ports	Apparent temperature (°K)
Nitrogen	2735
Argon	2780
Helium	2835

molecules must be attributed to the translational modes. Thus, the lower heat capacities of the monatomic gases permit more of the energy from the combustion to go toward raising the flame temperature. The observation of higher flame temperatures with helium than with argon is more difficult to explain. According to classical thermodynamics the heat capacities of all monatomic gases will be the same at normal pressures. Consequently, differences in heat capacities cannot explain the observation. Since little information is available on the high temperature characteristics of the two gases the reasons for the higher temperature must lie in the realm of speculation. However, at temperatures up to about

100°C, the thermal conductivity of helium is an order of magnitude higher than that of argon (142). If this difference is maintained at elevated temperatures, then helium would be more efficient in heat transfer processes and thereby produce a higher apparent flame temperature.

The relative detection limits for three elements in each of the three flames are shown in Table 15. The values for helium and argon containing flames are relative to the values obtained with nitrogen. As was seen in the case of varying the nitrogen content, the replacement of nitrogen

Table 15. Effect of N_2, Ar, and He on the detection limits of La, V, and Cr.

Element	Conc. (μg/ml)	Line (Å)	Relative detection limit with auxiliary gas being N_2	Ar	He
La	100	5791.34	1.00	0.49	0.50
V	10	4379.24	1.00	1.15	1.45
Cr	0.5	3605.33	1.00	0.85	0.38

with a monatomic gas does not appear to have a significant effect upon the detection limit values at the levels studied here. Thus, for practical purposes little is to be gained by going to the extra trouble of replacing nitrogen with another gas.

The results of the study on the effects of nitrogen then indicate that the principal function of nitrogen in the Kniseley flame is to act as a diluent. The fact that the Kniseley flame cannot be operated without air entrainment through the lower ports gives evidence that a diluent is necessary. However, the replacement experiments show that nitrogen is not the only gas that can act in this manner. Further, variation in the volume of the diluting gas can produce changes in the flame temperature, but no gains are experienced in detection limit values due to the temperature increase in the cases studied.

Nitrogen, when added to the fuel-rich Kniseley flame, does not appear to play a significant role in the fuel-rich phenomenon. However, the second additive, ethanol, is a combustible material and must contribute to the flame chemistry in some manner. Thus, ethanol may have considerable importance in the production of line enhancement.

Table 16 shows the data from a typical experiment involving the determination of the volume of solution reaching the flame. In this experiment the burner was operated over the range of gas flows commonly used for routine analytical studies. The most significant observation is that only 20 percent of the sample that enters the Kniseley burner actually reaches the flame. Changes in the flow of oxygen and acetylene do not appear to affect the actual volume entering the flame to any great extent. However, the aspiration rate (see column headed "volume aspirated") does show some sensitivity to the oxygen flow. Thus, while the amount of solution reaching the flame remains nearly constant, the percentage reaching the flame does change somewhat.

The findings illustrated in Table 16 were substantiated by similar studies with other burners and while the volume reaching the flame varied from one Kniseley burner to the next, the change was not severe. Of some five separate burners tested, the highest value found was 24% and the lowest 13%. For all five burners, the volume of solution reaching the flame showed little sensitivity to the oxygen and acetylene flow rates providing the gas flows were kept within the normal operating range of the specific burner. The factor

Table 16. Tabulation of typical data from a study of the effect of O_2 and C_2H_2 flow on the volume of solution reaching the Kniseley flame

Run #	O_2 flow (l/min)	C_2H_2 flow (l/min)	Normal aspiration rate (ml/min)	Trapping time (min)	Rate of solution input (ml/min)
1	3.76	5.30	1.16	6.0	0.23
2	3.76	5.02	1.15	5.0	0.22
3	3.76	4.76	1.15	5.5	0.22
4	3.76	4.50	1.12	7.5	0.21
5	3.45	4.50	1.11	6.0	0.22
6	3.45	4.76	1.08	6.0	0.23
7	3.45	5.02	1.10	6.0	0.22
8	3.45	5.30	1.08	6.0	0.22

most affecting the volume of alcohol reaching the flame was the burner alignment. If the burner was only slightly misaligned, reductions to as low as 5% were experienced.

Of particular interest is the comparison of the amount of alcohol reaching the Kniseley flame with the amount reaching the Beckman flame. With the Beckman burner, the entire "volume aspirated" enters the flame, yet the Kniseley burner produces enhancements in the emission of many elements (35) while only about one-fifth of the solution reaches the flame. Much of the enhancement can be attributed to a marked decrease in background emission from the Kniseley flame. However, of possible importance is the difference in the manner with which the two burners use the aerosol. Aerosol exiting the Beckman burner contains a number of large droplets. Gibson et al. (61) report that these larger droplets can be detected well up into the secondary reaction zone. In the Kniseley burner, however, the larger droplets are removed either through condensation on the walls of the premixing channel or by the action of the rising gases. Thus, the emergent stream from the Kniseley burner consists of very small droplets. No evidence has been found to indicate that these smaller droplets exist beyond the primary reaction zone. The Kniseley

burner then makes use of all of the solution reaching the flame almost immediately whereas the Beckman burner gradually evaporates off the solvent and thus distributes the sample throughout the flame.

Studies similar to those described above were made using the tapered chimney type burner and analogous results obtained. In addition, a study was made with the tapered chimney burner to determine the effect of nitrogen flow, through the lower access ports, on the rate at which sample entered the flame. The results are shown in Figure 34. An infusion pump was used to insure a constant sample input rate of 0.51 ml per minute and the oxygen and acetylene flow were maintained constant at 3.76 l/min and 4.76 l/min respectively. Since changes in the oxygen and acetylene flows produce little change in the rate of sample introduction, the continuous increase in the rate, seen in Figure 34, may be attributed to the increase in total gas flow in the premixing channel rather than some form of a shielding effect. The larger gas volume apparently results in a more efficient breakup of the larger droplets and thereby provides a larger percentage of relatively light particles. Further, the larger gas volumes

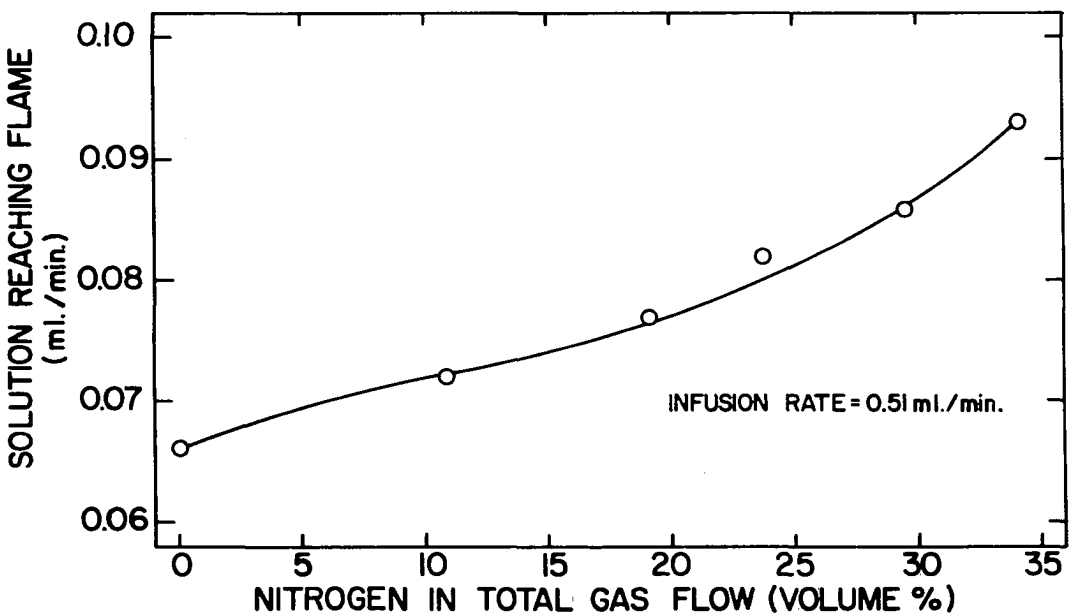

Figure 34. Effect of the introduction of nitrogen on the rate of sample introduction to the tapered chimney type burner

would be more effective in preventing the condensation of the smaller droplets.

Gibson, Grossman, and Cooke (61) point out that control of the sample input rate is essential to serious study of flame phenomenon. In their work the control was accomplished by using an infusion pump. For total consumption burners such an approach is satisfactory. However, the Kniseley burner is not in reality a total consumption burner. Therefore, a study was made to determine whether or not an infusion pump would provide the desired control. The results are shown in Figures 35 and 36. Figure 35 shows the actual volume of solution reaching the flame as a function of the infusion rate. The continuous, if not regular, increase would be expected. However, the percentage of solution reaching the flame (Figure 36) goes through a maximum at a point below the normal aspiration rate of the burner. The normal aspiration rate is that rate at which sample is drawn into the burner when no infusion pump is employed. For the specific burner and gas flow rates used to prepare Figures 35 and 36, the normal aspiration rate was 1.05 ml/min. The shape of Figure 36 is difficult to explain in the absence of detailed knowledge of the physical phenomena occurring both at the tip of

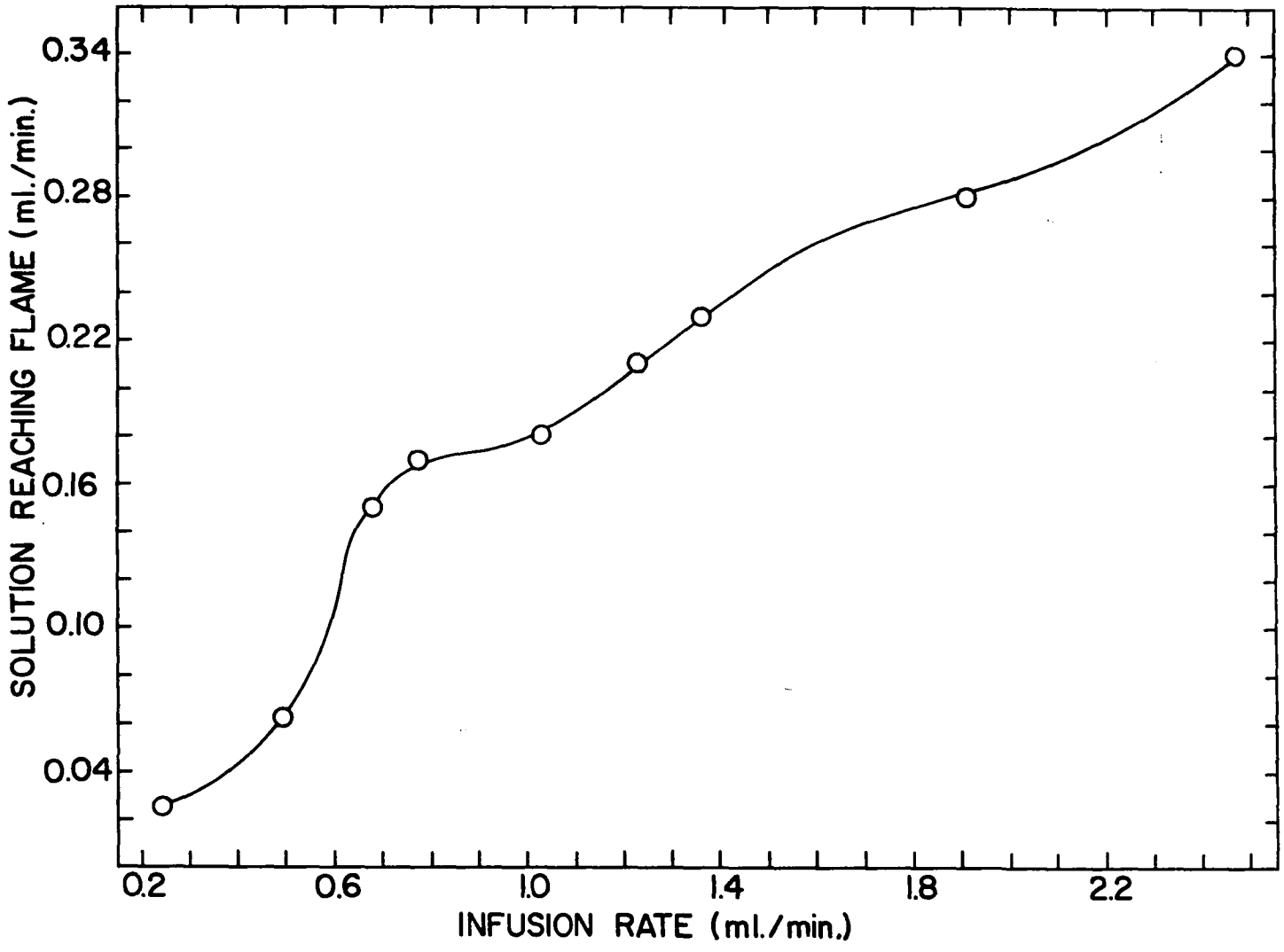

Figure 35. Effect of infusion rate on the amount of sample reaching the flame

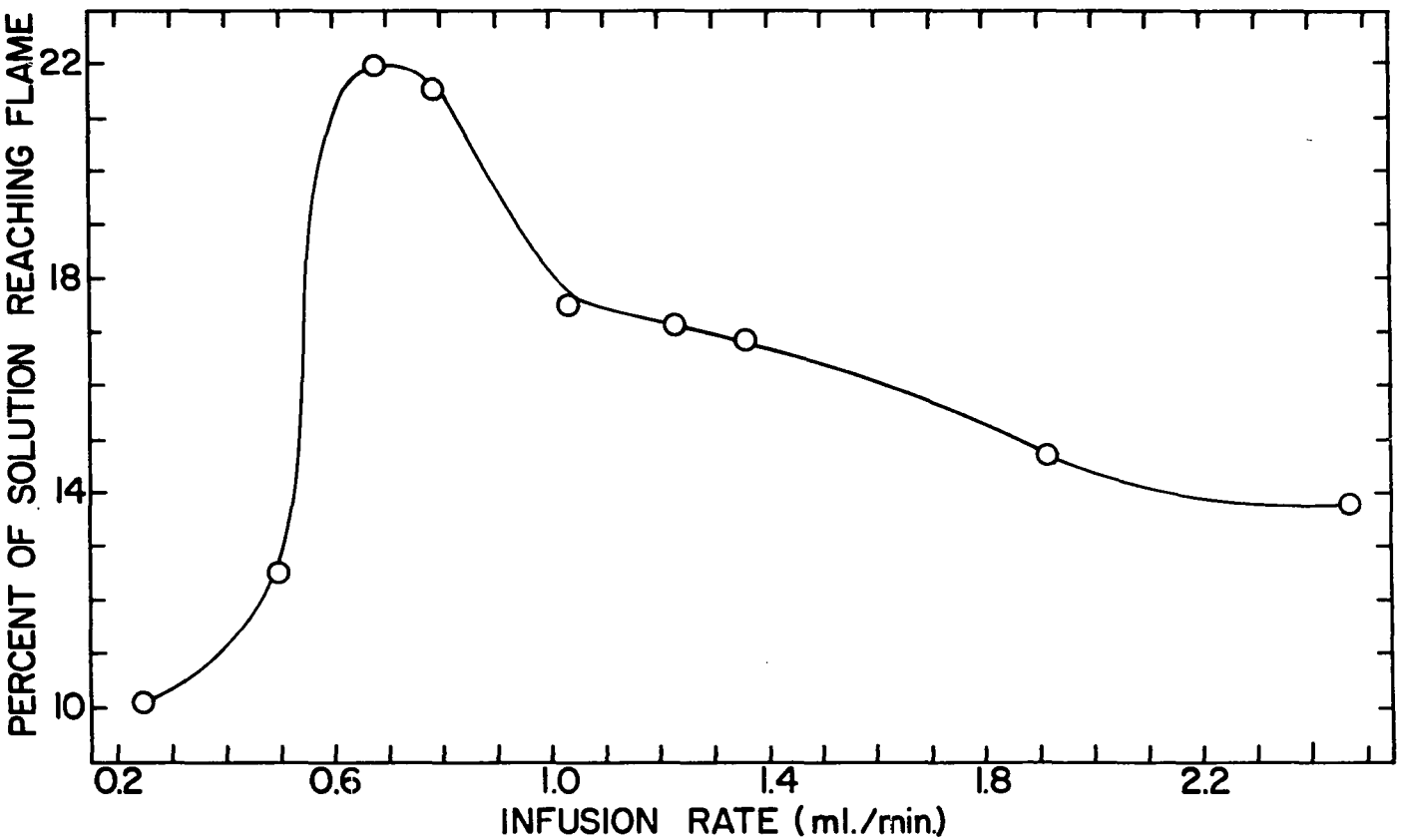

Figure 36. Effect of infusion rate on the percentage of sample reaching the flame

the Beckman burner and within the premixing channel. Unfortunately, these processes are not clearly understood. Certainly the extreme turbulence observed when the Beckman burner is operated normally gives evidence of the complexity of the problem. Despite the lack of an explanation, some inferences can be drawn from Figure 36. Obviously, the most efficient nebulization occurs not at the normal aspiration rate, but rather at a rate slightly below that of normal aspiration. Further, since only small droplets are observed exiting the tip of the Kniseley burner, the reduction in nebulization efficiency at rates above the normal aspiration rate must reflect a change in the droplet size distribution. Any successful explanation of th shape of Figure 36 must provide for this change as well as the location of the maximum.

The relationship between infusion rate and the volume of solution reaching the flame varies from one burner to the next. Further, variations occur from day to day even with the same burner. Generally, day to day variations are minor. However, if a knowledge of the rate at which solution reaches the flame is desired, measurements must be made both before and after a particular experiment is run in order to insure that the rate has not changed during the experiment.

Figure 35 was used to determine the combination of solution concentration and infusion rates that would provide a constant 20 mg per minute of lanthanum entering the flame irrespective of the volume of alcohol entering. A Kniseley burner with a stainless steel premixing channel was employed and the range 0.16 to 0.31 ml of solution per minute studied. The range over which the alcohol volume may be varied is limited. Below 0.16 ml per minute there is too little alcohol to provide adequate cooling of the burner tip; above 0.31 ml per minute the burner floods and causes distortion of the flame. Actually in this experiment considerable flooding did occur even at 0.31 ml per minute. The range of alcohol flows over which a burner may be operated varies slightly from burner to burner. The values listed above pertain only to the burner actually used for this experiment.

The change in the apparent temperature as a function of the alcohol content of the flame is shown in Figure 37 while Figure 38 shows the effect of the solvent on the emission of lanthanum and lanthanum oxide. The only significant variations in the intensity of the two lanthanum specie occurs near the end of the range studied. These may be explained, as well as the shape of Figure 37, simply as manifestations of a

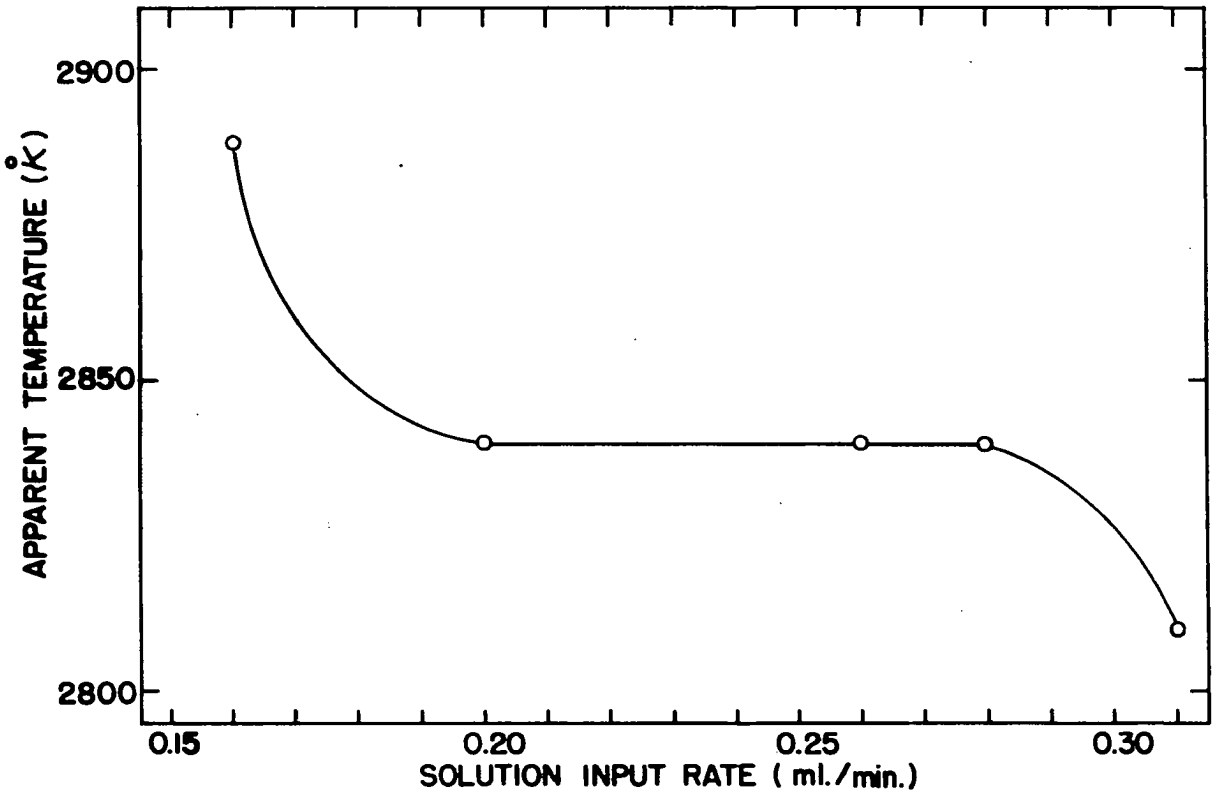

Figure 37. Variation in the apparent temperature in the interconal zone of the Kniseley flame as a function of the solution input rate

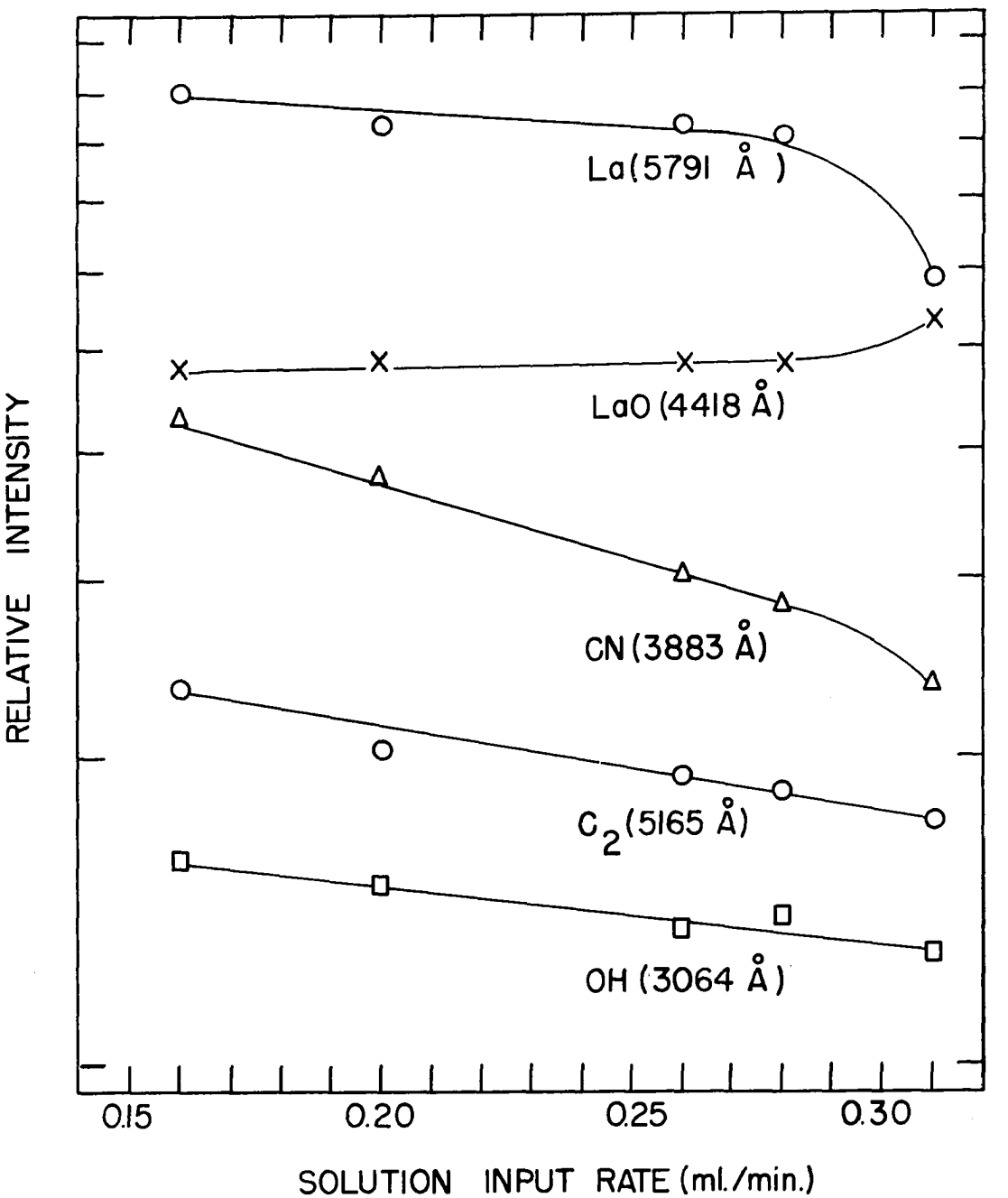

Figure 38. Effect of sample input rate on the emission of various species from the interconal zone of the Kniseley burner

cooling effect produced by the replacement of acetylene with ethanol. Thus, at low alcohol flow rates the cooling effect of the alcohol is reduced and the flame achieves a slightly higher temperature. This temperature increase is reflected both in Figure 38 and in the increase in lanthanum line emission. Lanthanum oxide emission occurs primarily from the secondary reaction zone and would thus not be expected to show the same sensitivity to temperature change as would lanthanum. Further, higher temperatures would tend to favor the decomposition of lanthanum oxide. At the highest alcohol flow rate, flooding occurs. This greatly distorts the flame and thereby invalidates the emission intensities found at an alcohol input rate of 0.31 ml per minute. However, the rapid decrease in line emission and the corresponding increase in band emission can be explained on the basis of cooling by the large amount of alcohol that floods into the flame. This cooling effect will favor the formation of lanthanum monoxide at the expense of free atoms.

The change in apparent temperature at each end of the range is quite small. However, as discussed previously the values shown represent the average temperature through a cross section of the flame. Thus, the temperature near the flame

center will experience a greater variation than will be detected by the measurements. Further, since the aerosol is directed into the central portions of the flame, the effects of the alcohol should be greater at the flame center than near the edges.

At each alcohol flow setting, the acetylene flow was readjusted so that optimum lanthanum line emission occurred. Thus, both the acetylene and alcohol flow rates changed at each setting. Since the acetylene flow was changed, the volume of air entrained changed and thus the net oxygen content of the premixed gases varied from one setting to the next. Table 17 shows a tabulation of the various flow data and the results of a series of calculations of the flame stoichiometry. The fuel equivalent of the alcohol is calculated assuming the following reaction:

$$C_2H_5OH + 2O_2 \rightarrow 2\ CO + 3\ H_2O \qquad \text{(ff)}$$

Thus, one mole of ethanol is equivalent to 4/3 of a mole of acetylene if both are burned to CO and H_2O. Table 17 reveals that the adjustment of the acetylene flow in order to compensate for changes in the alcohol flow rate are small. These produce correspondingly small changes in the air

Table 17. Tabulation of flow data from a study of the effect of ethanol on the atomic and molecular emission from the Kniseley flame

Ethanol input rate (ml/min)	O_2 flow (l/min)	C_2H_2 flow (l/min)	Air entrained (l/min)	O_2 from air (l/min)	C_2H_2 equivalent of ethanol (l/min)	Total O_2 (l/min)	Total C_2H_2 (l/min)	Fuel-ratio (uncorrected)	Fuel-ratio (corrected)
0.16	3.76	4.75	4.08	0.82	0.08	4.58	4.83	0.79	0.95
0.20	3.76	4.72	4.08	0.82	0.10	4.58	4.82	0.80	0.95
0.26	3.76	4.71	4.08	0.82	0.13	4.58	4.84	0.80	0.95
0.28	3.76	4.68	4.10	0.82	0.14	4.58	4.82	0.80	0.95
0.31	3.76	4.60	4.12	0.83	0.16	4.59	4.76	0.82	0.96

entrainment rate. However, since an adjustment had to be made to gain optimum emission, the indication is that the alcohol is capable of supplying some of the carbon species essential to the fuel-rich phenomenon. This conclusion is further born out by the observation that when alcohol is added to a premixed flame the interconal zone grows in size. Further, if the acetylene flow is reduced to the point where no interconal zone is present the addition of alcohol will produce an intercone which cannot be distinguished from the zone produced with acetylene alone. The most significant observation to be made from Table 17 is the difference between the corrected and uncorrected fuel-ratios. In the case shown in Table 17, failure to correct the fuel-ratio for both the solvent and air entrainment will result in an error of about 18 percent. Thus, the fuel-rich oxyacetylene flame is considerably leaner than was originally supposed by Curry (57) who apparently did not attempt to measure the air entrainment rate of the Beckman burner. Entrainment rate measurements on the Beckman burner are quite difficult and to date have not been accomplished. However, since entrainment in the Kniseley burner is produced by a Beckman burner, a good first approximation would be that both entrain air at about the same rate.

Also of interest is the fact that optimum line emission occurs at the same corrected fuel-ratio in all cases except for the 0.31 ml per minute value. Since burner flooding occurred at this level of alcohol flow, the exception should not be considered significant.

The behavior of C_2, CN and OH as a function of the alcohol content of the flame is also shown in Figure 38. These results are easily explained on the basis of the observed apparent temperature variation. Thus, CN and C_2 show continuously decreasing emission with decreasing temperature. This observation is expected and does not indicate that the concentration of these species changes as a function of the alcohol concentration. The relatively flat behavior of OH is also expected. Since OH emits primarily from the secondary reaction zone, the species would not be strongly affected by small temperature changes near the flame center. Further, since the flame normally produces very large quantities of OH, the changes produced by minor variations in the alcohol content would be too small to be detected by emission techniques.

The study of the effect of alcohol on the Kniseley flame has produced several significant observations. First, the Kniseley burner when operated normally makes use of only about

one-fifth of the total solution aspirated. Further, the range of solution flow over which the burner can be successfully operated is apparently restricted to between 0.1 and 0.3 ml per minute. However, the potential for extending this range has not been investigated. Second, the alcohol seems to produce two effects in the flame; the flame temperature is lowered by increased alcohol flow and the flame stoichiometry is altered. Variation in emission as a function of alcohol content seems to stem directly from temperature changes. From the evidence presented for lanthanum, there is no reason to believe that alcohol plays a direct role in the enhancement process.

The literature contains several attempts to attribute the enhancement effects of organic solvents on atomic emission, to chemiluminescence (48-50, 61, 117). As was discussed previously the term chemiluminescence is frequently misused in this connection. However, since the above work indicates that the solvent plays no direct role in the excitation process, the possibility of explaining the enhancement with organic solvents without involving chemiluminescence should be examined. The various physical changes that occur when water is replaced with an organic solvent have been listed previously.

Of these, the factor most closely allied to excitation is the increase in temperature. From the intensity expressions A and B, the fact that increased temperature can cause increased emission intensity is obvious. In addition, increased temperature will increase reaction rates and cause shifts in the equilibrium points of many reactions. With the possibility that some of the reactions are capable of producing free atoms, temperature effects alone can be the cause of some of the observed enhancements. Further, since the mechanisms proposed for the fuel-rich phenomenon depend to a large extent upon the presence of carbon-containing species, the production of such species from the organic solvent should be considered. For the most part, the studies on enhancements due to organic solvents have been performed with total consumption burners (117). Thus, the aerosol droplets will tend to vary in size and will distribute throughout the flame more or less as a function of their volume, with the larger droplets decomposing higher in the flame. Upon decomposition of the aerosol, either by evaporation or combustion the individual atoms within each droplet will find themselves in an environment relatively rich in carbon-containing species. Thus, a condition is created that might be termed "local fuel-richness".

The metal-containing species could then go through a series of reactions analogous to those postulated for the fuel-rich oxyacetylene flame.

The foregoing is not intended as an indictment of the possibility of chemiluminescence. The work described by Gilbert (117) clearly demonstrates that many metals do show chemiluminescence in the presence of organic solvents. However, the possibility that all enhancements with organic solvents are due to chemiluminescence is unlikely. The above discussion is intended as an alternate explanation.

V. SUGGESTIONS FOR FUTURE WORK

The work described in this thesis offers numerous starting points for future investigations of both the fundamental and practical aspects of the Kniseley flame. The most pressing need is for accurate temperature data, without which theoretical considerations of flame processes are not possible. As previously discussed, the existing spectroscopic methods for determining flame temperature suffer from some serious disadvantages. Therefore, the development of non-spectroscopic techniques may prove valuable. Gaydon and Wolfhard (36, p. 273-282) suggest several possibilities that should be examined critically.

A second area which should be investigated is the study of both the kinetics and mechanisms of flame reactions. Two serious difficulties block work in this direction. First, exactly what reactions are occurring has not been established and second, the speed with which flame reactions occur prevent study via normal spectroscopic techniques. However, in recent years the highly sophisticated technology of time resolved spectroscopy has profitted from advances in modern electronics. Thus, the application of time resolution to

flame spectroscopy may well yield a wealth of information essential to the understanding of flame reaction processes.

The use of both atomic and molecular absorption techniques in the study of flames holds great promise. Atomic absorption has enjoyed considerable popularity in recent years and therefore many of the techniques are known and may be applied directly to flame studies. Molecular absorption, on the other hand, is still in the embryonic stage and needs attention of its potential is to be brought into fruition. The value of absorption techniques to flame studies lies in the fact that the data obtained are directly related to the ground state concentration. Knowledge of the absolute concentrations of the various flame specie is essential to the evaluation of the possible flame equilibria.

An area having more immediate practical application is the study of various chemical interferences in the Kniseley flame. In numerous cases chemical interferences have been reported to limit the application of flame spectroscopy to some types of material. Since the same processes that produce the fuel-rich phenomenon may also inhibit the formation of the compounds allegedly responsible for these interferences, the Kniseley flame holds the possibility of permitting the

flame analysis of systems not previously susceptible to the technique. Studies of interferences may also provide information pertinent to some fundamental considerations. As discussed previously, knowledge of the specie designated MX is limited and since interference-causing compounds constitute a form of MX, studies of the variation in interferences as a function of the spatial properties of the flame should add valuable information on the behavior of the metallic species in the Kniseley flame.

Some of the important species known to be present in hydrocarbon flames, were not included in this study. Among these are C, CO, CO_2, and H_2O. Their exclusion was primarily due to the limitations of the instrumental system employed. Both C and CO emit in the ultraviolet, while CO_2 and H_2O are best studied in the infrared portion of the spectrum. These regions are inaccessible to the system previously described. However, proper instrumentation does exist and should permit the extension of the profile studies to these specie Further, most of the techniques used in this study should be directly applicable to both ultraviolet and infrared instrumentation.

Since the fuel-rich phenomenon appears to be a product of environmental control, studies of other controlled environments should be made. The various combinations of fuel, oxident, auxillary gas, and solvent appears limited only by the imagination and ingenuity of the investigator.

Finally, there is considerable need for improvement in burner design. The use of pneumatic nebulization systems, which are affected in one way or another by the gas flow, seem to be an unnecessary limitation to flame spectroscopy. One good possibility for eliminating the pneumatic system appears to be ultrasonic generation of the aerosol. While some study has been done in this area, much development work is still needed.

VI. SUMMARY

The recent development of the premixed fuel-rich oxy-acetylene flame has significantly extended the scope of analytical flame spectroscopy. While the practical applications of such flames have received much attention, the explanation of the so-called fuel-rich phenomenon has hithertofore been vested in speculation rather than experimental evidence.

Studies of the emission spectra from each of the three zones of the premixed flame have led to a better understanding of the fuel-rich phenomenon. The vertical and horizontal variation in the emission of both the natural flame species and some metallic species have been measured. The resulting profiles have been compared and possible relationships between them discussed.

Evidence has been found to support the conclusion that the interconal zone is a region relatively rich in carbon containing species but deficient in oxygen. The possibilities of producing free atoms through either chemical reduction of the monoxide, by carbon bearing species, or a favorable shift in the monoxide dissociation equilibrium, due to the low oxygen

concentration, have been examined with respect to this evidence.

In addition, studies have been made to determine the effects of nitrogen and ethanol on the fuel-rich phenomenon. Nitrogen has been found to act primarily as a diluent which may be replaced by any of a number of other gases. Ethanol has been shown to contribute to the flame stoichiometry but to play no direct role in the production of free atoms. The possibility of producing further analytical enhancement through control of the amount of nitrogen and ethanol entering the flame has been examined. In the cases studied, no significant improvements were obtained.

VII. LITERATURE CITED

1. Herrmann, R. and C. T. J. Alkemade. Chemical Analysis by Flame Photometry. 2nd ed. New York, N.Y., Interscience Publishers. 1963.

2. Talbot, W. H. F. Brewster's J. Sci. 5, 77 (1826).

3. Kirchhoff, G. and R. Bunsen Phil. Mag. 20, 89 (1860).

4. Kirchhoff, G. and R. Bunsen Pogg. Ann. d. Physik 110, 161 (1860).

5. Kirchhoff, G. and R. Bunsen Ann. Chim. Phys. 62, 452 (1861).

6. Kirchhoff, G. and R. Bunsen Pogg. Ann. d. Physik 113, 337 (1861).

7. Janssen, J. Compt. Rend. 71, 626 (1870).

8. Champion, P., H. Pellet, and M. Grenier Compt. Rend. 76, 707 (1873).

9. Lundegardh, H. Svensk Kem. Tidskr. 42, 51 (1930).

10. Lundegardh, H. Z. Physik 66, 109 (1930).

11. Lundegardh, H. Kgl. Lantbruks-Akad. Handl. Tidskr. 75, 241 (1936).

12. Lundegardh, H. Lantbruks-Högskol. Ann. 3, 49 (1936).

13. Lundegardh, H. Soil Sci. 45, 447 (1938).

14. Lundegardh, H. Svensk Kem. Tidsks. 50, 135 (1938).

15. Lundegardh, H. and T. Philipson Lantbruks-Högskol. Ann. 5, 249 (1938).

16. Lundegardh, H. Metallwirtschaft 17, 1222 (1938).

17. Lundegardh, H. Die Quantitative Spectralanalyse der Elemente. Vol. 1. Jena, Germany, G. Fischer Verlagsbuchhandlung. 1929.

18. Lundegardh, H. Die Quantitative Spectralanalyse der Elemente. Vol. 2. Jena, Germany, G. Fischer Verlagsbuchhandlung. 1934.

19. Gilbert, P. T., Jr. Advances in Emission Flame Photometry. In Analysis Instrumentation. pp. 193-233. New York, N.Y., Plenum Press. 1964.

20. Dean, J. A. Flame Photometry. New York, N.Y., McGraw-Hill Book Company, Inc. 1960.

21. Gilbert, P. T., Jr. Beckman Instruments, Inc. (Fullerton, California) Bulletin 753, (1959).

22. Piette, M. Acetylene J. 30, 115 (1928).

23. Alekseeva, V. G. and S. L. Mandel'shtam Zhur. Tekm. Fiz. 17, 765 (1947).

24. Mavrodineanu, R. and H. Boiteux. L'Analyse Spectrale Quantitative Par La Flamme. Paris, France, Masson et Cie. 1954.

25. Knutson, K. E. Analyst 82, 241 (1957).

26. Allan, J. E. Analyst 83, 466 (1958).

27. Allan, J. E. Spectrochim. Acta 18, 259 (1962).

28. David, D. J. Nature 187, 1109 (1960).

29. Gatehouse, B. M. and J. B. Willis Spectrochim. Acta 17, 710 (1961).

30. Fassel, V. A., R. H. Curry, and R. N. Kniseley Spectrochim. Acta 18, 1127 (1962).

31. Fassel, V. A., R. B. Myers, and R. N. Kniseley Spectrochim. Acta 19, 1187 (1963).

32. Fassel, V. A. and V. G. Mossotti Anal. Chem. 35, 252 (1963).

33. Mossotti, V. G. and V. A. Fassel Spectrochim. Acta 20, 1117 (1963).

34. Kniseley, R. N., A. P. D'Silva, and V. A. Fassel Anal. Chem. 35, 911 (1963).

35. D'Silva, A. P., R. N. Kniseley, and V. A. Fassel Anal. Chem. 36, 1287 (1964).

36. Gaydon, A. G. and H. G. Wolfhard. Flames, Their Structure, Radiation, and Temperature. 2nd ed. London, England, Chapman and Hall, Ltd. 1960.

37. Fristrom, R. M. and A. A. Westenberg. Flame Structure. New York, N.Y., McGraw-Hill Book Company, Inc. 1965.

38. Gilbert, P. T., Jr., R. C. Hawes, and A. O. Beckman Anal. Chem. 22, 772 (1950).

39. Golightly, D. W. Spectral Detection Sensitivities of the Elements in the Premixed, Fuel-Rich, Oxyacetylene Flame. Unpublished M.S. thesis. Ames, Iowa, Library, Iowa State University of Science and Technology. 1965.

40. Mossotti, V. G. The Atomic Absorption Spectra of the Lanthanide Elements. Unpublished Ph.D. thesis. Ames, Iowa, Library, Iowa State University of Science and Technology. 1964.

41. Cotton, F. A. and G. Wilkinson. Advanced Inorganic Chemistry. New York, N.Y., Interscience Publishers. 1962.

42. Fiorino, J. A. The Design and Performance of a Long-Path Oxy-acetylene Burner for Atomic Absorption Spectroscopy. Unpublished M.S. thesis. Ames, Iowa, Library, Iowa State University of Science and Technology. 1965.

43. Fastie, W. G. J. Opt. Soc. Am. 42, 641 (1952).

44. Czerny, M. and A. F. Turner Z. Physik 61, 792 (1930).

45. Jones, H. C., D. J. Fisher, and M. T. Kelley U.S. Atomic Energy Commission Report TID-7629 (Division of Technical Information Extension, AEC), 31 (1962).

46. Rains, T. C., H. P. House, and O. Menis Anal. Chim. Acta 22, 315 (1960).

47. Beck, B. L. Rev. Sci. Instr. 33, 756 (1962).

48. Buell, B. E. Anal. Chem. 34, 635 (1962).

49. Buell, B. E. Anal. Chem. 35, 372 (1963).

50. Carnes, W. J. and J. A. Dean Analyst 87, 748 (1962).

51. Dean, J. A. and W. J. Carnes Analyst 87, 743 (1962).

52. Dean, J. A. and J. A. Simms Anal. Chem. 35, 699 (1963).

53. Winefordner, J. D. and C. Veillon Anal. Chem. 36, 943 (1964).

54. Kahn, H. L. J. Chem. Ed. 43, A7 (1966).

55. Princeton Applied Research Corporation. Instruction Manual, Precision Lock-in Amplifier, Model HR-8. Princeton, New Jersey, author. 1965.

56. Princeton Applied Research Corporation. Instruction Manual, Mechanical Light Chopper, Model BZ-1. Princeton, New Jersey, author. 1965.

57. Curry, R. H. Flame Spectroscopy of the Rare Earth Elements. Unpublished Ph.D. thesis. Ames, Iowa, Library, Iowa State University of Science and Technology. 1962.

58. Smith, G. F. Anal. Chim. Acta 8, 397 (1953).

59. Eckhard, S. and A. Püschel Z. Anal. Chem. 172, 334 (1960).

60. Fukushima, S. Mikrochim. Acta, 332 (1960).

61. Gibson, J. H., W. E. L. Grossman, and W. D. Cooke Anal. Chem. 35, 266 (1963).

62. Mavrodineanu, R. Spectrochim. Acta 17, 1016 (1961).

63. Simon, L. Optik 19, 621 (1962).

64. Rann, C. S. and A. N. Hambly Anal. Chem. 37, 879 (1965).

65. Marr, C. V. Air Force Research Center Report AD-101208 (Defense Documentation Center, Arlington, Va.), 1 (1956).

66. Marr, C. V. Air Force Research Center Report AD-152611 (Defense Documentation Center, Arlington, Va.), 1 (1957).

67. Meggers, W. F., C. H. Corliss, and B. F. Scribner National Bureau of Standards Monograph 32, Part 1 (1961).

68. Mavrodineanu, R. and H. Boiteux. Flame Spectroscopy. New York, N.Y., John Wiley and Sons, Inc. 1965.

69. Pearse, R. W. B. and A. G. Gaydon. The Identification of Molecular Spectra. 3rd ed. New York, N.Y., John Wiley and Sons, Inc. 1963.

70. Lewis, B. and G. von Elbe. Combustion, Flames, and Explosions of Gases. 2nd ed. New York, N.Y., Academic Press, Inc. 1961.

71. Henning, F. and C. Tingwald Z. Physik 48, 805 (1928).

72. Behmenburg, W., H. Kohn, and M. Mailänder J. Quant. Spectry. Radiative Transfer 4, 149 (1964).

73. Avni, R. and C. T. J. Alkemade Mikrochim. Acta, 460 (1960).

74. Gaydon, A. G. Spectroscopy of Flames. New York, N.Y., John Wiley and Sons, Inc. 1957.

75. Hornbeck, G. A. and R. C. Herman Ind. Eng. Chem. 43, 2739 (1951).

76. Phillips, J. G. Astrophys. J. 107, 389 (1942).

77. Deslandres, H. A. and A. D'Azambuja Compt. Rend. 140, 917 (1905).

78. Landsverk, O. G. Phys. Rev. 56, 769 (1939).

79. Mulliken, R. S. Z. Electrochem. 36, 603 (1930).

80. Freymark, H. Ann. Physik 8, 221 (1951).

81. Ballik, E. A. and D. A. Ramsey Astrophys. J. 137, 61 (1963).

82. Johnson, R. C. Phil. Trans. Roy. Soc. A226, 157 (1927).

83. Mulliken, R. S. Phys. Rev. 29, 637 (1927).

84. Pretty, W. E. Proc. Phys. Soc. London 40, 71 (1928).

85. Shea, J. D. Phys. Rev. 30, 825 (1927).

86. Fox, J. G. and G. Hertzberg Phys. Rev. 52, 638 (1937).

87. Moore, C. E. and H. P. Broida J. Res. Natl. Bur. Std. 63A, 19 (1959).

88. Dieke, G. H. and H. M. Crosswhite John Hopkins University Bumblebee Series Report 87, (1948).

89. Schüler, H. and A. Woeldike Physik Z. 44, 335 (1943).

90. Schüler, H. and A. Michel Z. Naturforsch. 11a, 403 (1956).

91. Benedict, W. S. and E. K. Plyler Phys. Rev. 83, 2454 (1951).

92. Carroll, P. K. Can. J. Phys. 34, 83 (1956).

93. Hsieh, R. C. and D. T. A. Townsend J. Chem. Soc., 332 (1939).

94. Ferguson, R. E. J. Chem. Phys. 23, 2085 (1955).

95. Goldfinger, P. Mém. Soc. Roy. Sci. Liége 15, 378 (1955).

96. Herman, R. C., G. A. Hornbeck, and K. J. Laidler Science 112, 497 (1950).

97. Herzberg, G. Spectra of Diatomic Molecules. 2nd ed. New York, N.Y., Van Nostrand Co., Inc. 1950.

98. Barrow, R. F. Arkiv Fysik 11, 281 (1956).

99. Herzberg, G. Mém. Soc. Roy. Sci. Liége 18, 397 (1957).

100. Knight, H. T. and J. P. Rink J. Chem. Phys. 35, 199 (1961).

101. Brewer, L., W. T. Hicks, and O. H. Krikorian J. Chem. Phys. 36, 182 (1962).

102. Ackermann, R. J., E. G. Rauh, and R. J. Thorn J. Chem. Phys. 40, 883 (1964).

103. Goldstein, H. W., P. N. Walsh, and D. White J. Phys. Chem. 65, 1400 (1961).

104. Inghram, M. G., W. A. Chupka, and J. Berkowitz Mém. Soc. Roy. Sci. Liége 18, 513 (1957).

105. Berkowitz, J., W. A. Chupka, and M. G. Inghram J. Chem. Phys. 27, 87 (1957).

106. Grimley, R. T., R. P. Burns, and M. G. Inghram J. Chem. Phys. 34, 664 (1961).

107. Behrens, H. Flame Instabilities and Combustion Mechanism. In Forth Symposium on Combustion. pp. 538-545. Baltimore, Md., Williams and Wilkins Co. 1953.

108. Kiess, N. H. and A. M. Bass J. Chem. Phys. 22, 569 (1954).

109. Marr, C. V. and R. W. Nicholls Can. J. Phys. 33, 394 (1955).

110. Durie, R. A. Proc. Phys. Soc. A35, 125 (1952).

111. Dieke, G. H. and H. M. Crosswhite J. Quant. Spectry. Radiative Transfer 2, 97 (1962).

112. Broida, H. P. and K. E. Shuler J. Chem. Phys. 20, 168 (1952).

113. Broida, H. P. and A. G. Gaydon Proc. Roy. Soc. A218, 60 (1953).

114. Gaydon, A. G. Spectroscopy and Combustion Theory. London, England, Chapman and Hall, Ltd. 1948.

115. Phillips, J. G. and L. Brewer Mém. Soc. Roy. Sci. Liége 15, 314 (1955).

116. Chapman, W. R. J. Chem. Soc. London 119, 1677 (1921).

117. Gilbert, P. T., Jr. Chemiluminescent Flame Spectrophotometry. In Proceedings of the Xth Colloquium Spectroscopicum Internationale. pp. 171-215. Washington, D.C., Spartan Books. 1963.

118. Hartley, W. N. Phil. Trans. Roy. Soc. 185A, 161 (1894).

119. Hartley, W. N. Proc. Roy. Soc. 79, 242 (1907).

120. Dean, J. A. and W. J. Carnes Anal. Chem. 34, 192 (1962).

121. Neeb, K. H. Z. Anal. Chem. 184, 414 (1961).

122. Robinson, J. W. and R. J. Harris Anal. Chem. Acta 26, 439 (1962).

123. Fink, A. Mikrochim. Acta, 314 (1955).

124. Pungor, E., A. Hegedus, I. Konkoly-Thege, and E. E. Zapp Mikrochim. Acta, 1247 (1956).

125. Kingsley, G. R. and R. R. Schaffert J. Biol. Chem. 206, 807 (1954).

126. Lady, J. H. Applications of Solvent Extraction to Flame Spectrophotometry. Unpublished Ph.D. thesis. Knoxville, Tenn., Library, University of Tennessee. 1955.

127. Caton, R. O. and R. W. Bremmer Anal. Chem. 26, 805 (1954).

128. Eggertson, F. T., G. Wyld, and L. Lykken Am. Soc. Testing Materials Spec. Tech. Publ. 116, 52 (1951).

129. Dean, J. A. and H. L. Beverly. The Role of Organic Solvents in Flame Photometry. Unpublished paper presented at Pittsburgh Conference on Analytical Chemistry and Applied Spectroscopy. Pittsburgh, Pa., March 1959. Knoxville, Tenn., Chemistry Department, University of Tennessee. 1959.

130. Petrie, W. Am. J. Phys. 16, 378 (1948).

131. Shuler, K. E. J. Chem. Phys. 18, 1466 (1950).

132. Broida, H. P. J. Chem. Phys. 21, 340 (1953).

133. Gaydon, A. G. and H. G. Wolfhard Proc. Roy. Soc. Series A 199, 89 (1949).

134. Penner, S. S. Quantitative Molecular Spectroscopy and Gas Emissivities. Reading, Mass., Addison-Westly Publishing Co. 1959.

135. Broida, H. P. and K. E. Shuler J. Chem. Phys. 27, 933 (1957).

136. Corliss, C. H. and W. R. Bozman National Bureau of Standards Monograph 53, (1962).

137. Corliss, C. H. and B. Warner Astrophy. J. Suppl. Series 8 (83), 395 (1964).

138. Dieke, G. H. The Iron Thermometer. Unpublished Quarterly Report, Oct. 1-Dec. 31, of the Department of Physics, John Hopkins University. Baltimore, Md., 1950. Xerox copy. Ames, Iowa, Spectrochemistry Group I, Ames Laboratory. ca. 1959.

139. Winefordner, J. D. and T. J. Vickers Anal. Chem. 36, 1939 (1964).

140. Alkemade, C. T. J. Contribution to the Development and Understanding of Flame Photometry. Unpublished Ph.D. thesis. Utrecht, Holland, Library, University of Utrecht. 1954.

141. Whisman, M. and B. H. Eccleston Anal. Chem. 27, 1861 (1955).

142. Lange, H. H. Handbook of Chemistry. 6th ed. Handbook Publishers, Inc. Sandusky, Ohio. 1946.

VIII. ACKNOWLEDGMENTS

The author considers himself fortunate to have worked under the guidance of Dr. Velmer A. Fassel and wishes to thank him for the advice and encouragement which were freely given throughout the course of this investigation.

Thanks are also extended to Mr. Richard N. Kniseley who offered many valuable suggestions and frequently surrendered his time to assist the author in overcoming the many practical problems that were encountered.

The capable assistance of Mr. James Rasmuson in obtaining some of the data is gratefully acknowledged.

Finally, a great deal of credit is due to the author's wife, Rosemarie, whose tolerance and ability to filter family responsibility have made possible the completion of this work.